WETTABILITY AND FLOATABILITY OF COAL MACERALS AS DERIVED FROM FLOTATIONS IN METHANOL SOLUTIONS.

BY
MARIA EWELINA HOLUSZKO

B.A.Sc., Technical University of Silesia, Mining and Mineral Process Engineering, Poland, 1979

A THESIS SUBMITTED IN PARTIAL FULFILLMENT OF THE REQUIREMENTS FOR THE DEGREE OF MASTER OF APPLIED SCIENCE

in
THE FACULTY OF GRADUATE STUDIES
(Department of Mining and Mineral Process Engineering)

We accept this thesis as conforming
to the required standard

THE UNIVERSITY OF BRITISH COLUMBIA
June 1991

In presenting this thesis in partial fulfilment of the requirements for an advanced degree at the University of British Columbia, I agree that the Library shall make it freely available for reference and study. I further agree that permission for extensive copying of this thesis for scholarly purposes may be granted by the head of my department or by his or her representatives. It is understood that copying or publication of this thesis for financial gain shall not be allowed without my written permission.

Department of MINING AND MINERAL PROCESS ENGINEERING

The University of British Columbia
Vancouver, Canada

Date AUG. 26, 1991

ABSTRACT

In this study wettability and floatability of coal petrographic components were examined using the concept of critical surface tension. Two techniques were studied; film flotation and small-scale flotation tests. Both tests use Zisman's concept of critical surface tension of solids. In these tests particles are separated according to their respective critical surface tension of wettability (film flotation) or critical surface tension of floatability (small-scale flotation).

Surface heterogeneity of coal particles arises from the chemical composition of coal surface. The coal macerals are known to have different chemical composition and surface properties. Surface properties of macerals and their flotation response have usually been evaluated with the contact angle or direct flotation tests. In this study, the estimation of surface properties of coal macerals was accomplished by studying their critical surface tension of wettability and floatability.

The wettability distributions of coal samples of various petrographic composition were obtained from film flotation. Wettability of petrographic components was evaluated in terms of an average critical surface tension of wettability.

In small-scale flotation experiments, coal particles were separated according to their critical surface tension of floatability. Differences in floatability and wettability distributions of coal lithotypes and maceral concentrates are discussed. Microscopic examination of the products from film and small-scale flotations was used to further study the effect of coal petrographic composition on the wettability and floatability.

TABLE OF CONTENTS

LIST OF FIGURES

LIST OF TABLES

AKNOWLEDGEMENT

The author wishes to express her sincere gratitude to her research supervisor Dr. Janusz S. Laskowski for his guidance and support over the course of her graduate study.

Thanks are also extended to the technical staff of the Mining and Mineral Process Engineering for their assistance, especially to Mrs. S. Finora and Mr. F. Schmidiger.

The author wishes to express her appreciation to Professors A.L Mular, G. W. Poling and M.R. Bustin for teaching interesting courses. Special thanks are extended to Professor J. Leja for many valuable discussions, and to all fellow students in Department of Mining and Mineral Process Engineering (UBC), with whom the author had a pleasure to work and cooperate.

A special gratitude is due to Michelle Lamberson of the Department of Geological Sciences for providing lithotype samples and very helpful comments and suggestions regarding petrographic analysis.

In particular, the author wishes to express her thanks to Dr. Dave Lefebure of Ministry of Energy, Mines and Petroleum Resources for significant support in the final stages of thesis preparation, and all collegues from Coal Section for their moral

support.

Mr. Dave A. Grieve and John Cunningham read an early draft of this thesis and contributed to the improvement of the text for which the author is the most grateful.

A very special thanks are given to my mother, for her enduring support, to my loving husband and wonderful daughter for their understanding, and sharing hardship of the past years.

CHAPTER 1

INTRODUCTION

Coal is by far the world's largest source of energy. The economic deposits may however be exhausted sooner than anticipated if they are not properly exploited and processed. The saying, that "tailings of today may be the plant feed of tomorrow", suggests that we might be constrained to process significantly lower grade coals in the future. In that case, the understanding of the full potential of coal may become imperative.

In the processing of any ore it is critical to understand the mineralogy of ore at the earliest possible opportunity, whereas with coal, the mineralogy and petrography are usually considered as a supplementary evaluation. Traditionally, coal quality has been assessed through parameters such as ash content, volatile matter, size and suite of physico-chemical properties, with significant neglect of the petrographic composition of coal. The only area where petrography has gained appreciation is in the prediction of coking properties of coals, since a certain ratio of reactive petrographic components to the inert ones is required to produce acceptable quality coke (Ammosov et al., 1957; Shapiro et al., 1964; Benedict et al.,1973; Gray et al., 1978).

A more diverse use of coal dictates increasingly complex specifications for the coal quality. These uses include: coal as a

primary energy source for power generation; conversion of coal to gaseous liquids or solid fuels; metallurgical uses in production of steel; and, finally, coal as a source of hydrocarbons in the production of a variety of chemical products. It is becoming apparent that most of these technological uses require coal with specific properties, and, in many instances coals enriched in certain petrographic components are needed. From the pollution control point of view, some of the processes require strict limits on the quantity of mineral matter and other deleterious elements in coal.

To meet these specifications more efficient and more refined coal cleaning techniques are necessary. For more effective cleaning, the liberation of combustible components of coal from mineral matter and liberation of macerals from each other must result. This will involve a greater degree of comminution of coal, followed by very efficient treatment of fines.

The processing of fine coal has always been more problematic than the cleaning of coarse coal, and therefore more expensive. Presently, only fines produced from metallurgical coals receive adequate treatment, because only for these coals, can the cleaning cost be justified. For the processing of fine coal, froth flotation remains the most effective method, although other methods relying on the surface properties of coal, such as oil agglomeration, have received attention in recent years.

In British Columbia the production of metallurgical coal in 1991 exceeded 22 million metric tones. This comprises more than

85 % of the total coal production in the province (Mineral Statistics, EMPR, 1991). Due to the geological conditions, the intensive mechanization and non-selective mining, the amount of fines (material below .50 mm in size) in the run-of-mine coal in majority of seams exceeds 35 %, and for some reaches 60 %. On average, 15 to 20 % of the total clean coal product comes from the cleaning by froth flotation.

The effectiveness of flotation relies on the natural hydrophobicity of coal particles. The hydrophobicity of coal changes with the rank, petrographic composition, degree of oxidation and the amount of mineral matter associated with the coal. For each grain subjected to the flotation, the average surface properties determine its floatability. The separation of an assembly of particles into fractions of equal critical surface tensions of wettability and floatability, as developed in recent years (Hornsby and Leja, 1980; Hornsby, 1981; Fuerstenau et al., 1985), is an elegant way of obtaining the distribution of particles according to their surface properties.

The wettability and floatability of petrographic components have been a subject of a number of studies. Two approaches were usually used: testing floatability of petrographic components under real flotation conditions (Horsley and Smith, 1951; Klassen, 1966; Hower et al., 1984; Sarkar et al., 1984; Bujnowska, 1985) or relating wettability parameters such as contact angle of various macerals to the flotation (Brown, 1961; Klassen, 1966; Parekh and Aplan, 1978; Sobieraj and Myrcha, 1980; Arnold and

Aplan, 1989).

It is of special interest, however, to examine natural surface properties of coal grains of various petrographic composition in terms of their critical surface tension of wettability and floatability. Consequently, this will show the influence of the petrographic composition of individual particles on their average surface properties, and perhaps help in understanding the nature of surface heterogeneity of coal. The possibility of selective separation of petrographic components is important in both the laboratory and the industrial applications. It is not necessary to obtain complete separation of petrographic components, as long as the proportion of certain components in concentrate is achieved.

The first three chapters consist of a literature review of wettability and floatability, the relationship between hydrophobicity and floatability, followed by an analysis of coal surface properties. The experimental testing and discussion of wettability and floatability of coal particles of different petrographic composition, as derived from two methods: film flotation and small-scale flotation are discussed in the following chapters.

CHAPTER 2

HYDROPHOBICITY AND FLOATABILITY

2.1 Wettability of solids

2.1.1 Theory of the wettability of solids by liquids

When a drop of liquid is placed on a solid, the liquid either spreads to form a thin, more or less uniform film or remains on the surface as a discrete drop. The former behavior is generally described as a complete wetting, the latter as incomplete or partial wetting. A solid can be classified as lyophilic if the liquid completely wets it, or lyophobic if it is only partially wetted. Hydrophobic and hydrophilic are the terms which specifically apply to wetting by aqueous solutions.

Thomas Young (1805) in his equation described wetting conditions in terms of surface tensions. He viewed surface tensions as the forces acting along the perimeter of a drop of liquid placed on an ideally smooth solid surface. Both phases were considered to be in equilibrium with the surrounding vapor phase. He derived the following equation known as Young's equation:

$$\gamma_{sv} - \gamma_{sl} = \gamma_{lv} \cos\theta \qquad 2.1.1$$

γ_{sv}, γ_{sl}, γ_{lv} are the solid/vapor, solid/liquid, liquid/vapor

interfacial surface tensions and θ is the angle of contact measured across the liquid phase (Figure 2.1.1). This equation may also be derived from thermodynamic conditions (Gibbs, 1928; Johnson, 1959).

Young's equation provides a precise thermodynamic definition of the contact angle, but suffers from the lack of direct measurement of solid surface tensions. Hence, it cannot be experimentally verified.

There are a number of other objections to Young's equation. The most obvious one is the assumption that the surface of the solid is an ideal one. Real solid surfaces are usually characterized by imperfections such as roughness, and heterogeneity. If the surface is rough, a correction factor has to be introduced as a weighing factor for $\cos\theta$ to compensate for the roughness (Wenzel, 1936),the heterogeneity can to be corrected in a similar way (Cassie and Baxter, 1944; Cassie, 1948).

Using thermodynamics, Dupre (1869) defined the work of adhesion, W_a, as the reversible work necessary to separate unit area of the interface between two immiscible liquids in equilibrium, into two unit areas of liquid/vapor interfaces of these liquids. This was further extended to the liquid/solid interfaces. Work of cohesion, W_c, is the work necessary to form two unit area surfaces from one liquid.

The cohesion of the given liquid and its adhesion to the given solid, are the two parameters that determine wetting or non-wetting conditions. Harkins (1952) defined the phenomenon of wetting as the difference between the work of adhesion (W_a) of the

liquid to the solid (or other substrate) and the work of cohesion W_c of the liquid. If the difference (S) is greater than zero the liquid should spread (or wet) the solid (substrate), if S is less than zero the non-wetting should occur.

Since

$$W_a = \gamma_{sv} + \gamma_{lv} - \gamma_{sl} \quad \text{and using Young's equation} \qquad 2.1.2$$

$$W_a = \gamma_{lv} (1+\cos\theta) \qquad 2.1.3$$

$$W_c = 2\gamma_{lv} \qquad 2.1.4$$

$$S = W_a - W_c \qquad 2.1.5$$

Hence $S = \gamma_{sv} - \gamma_{lv} - \gamma_{sl} > 0$ denotes wetting 2.1.6

and $S = \gamma_{sv} - \gamma_{lv} - \gamma_{sl} < 0$ denotes non-wetting 2.1.7

For $S = \gamma_{lv} \cos\theta - \gamma_{lv} < 0$ then $\gamma_{lv} \cos\theta < \gamma_{lv}$ 2.1.8

In these expressions only the interfacial tensions pertaining to fluid phases can be reliably determined. The interfacial tensions of solid phases cannot be measured, only their difference is measurable, by $\gamma_{lv} \cos\theta$. This quantity is called the adhesion tension. For the non-wetting conditions, the adhesion tension should be less than γ_{lv}.

Also, $W_a/W_c = \gamma_{lv} (1 + \cos\theta)/2\ \gamma_{lv}$ 2.1.9

and then $\cos\theta = 2\ W_a/W_c - 1$ 2.1.10

For particle-to-bubble contact to be possible, the free energy change (ΔG) during the attachment has to be negative $\Delta G < 0$ (Laskowski, 1974; 1986a; 1989) and is given by equation 2.1.11

$$\Delta G = \gamma_{lv} (\cos\theta - 1) \quad 2.1.11$$

as a result the attachment is possible only when $\theta > 0$ ($\cos\theta < 1$). Further, for $\cos\theta$ to be smaller than 1, (equation 2.1.10) W_a must be smaller than W_c, $W_a < W_c$ and $S < 0$. Young's equation and the spreading coefficient equation are of great importance in froth flotation, because they describe the thermodynamic conditions for wettability and floatability of a solid.

One of the measurable thermodynamic parameters in flotation systems is contact angle, θ. The contact angle measured at equilibrium is a unique function of the three interfacial tensions. Whenever a particle is attached to an air bubble, there is always a definite angle formed at the border of interfaces. This angle is assumed to be directly related to the flotation of a particle. The major problem with interrelating floatability with contact angle lies in the fact that, it does not reflect the kinetic conditions of the flotation process (Laskowski, 1974; Laskowski, 1989). Despite all the drawbacks caused by heterogeneity

(Wenzel, 1949; Neuman and Good, 1972) and roughness of the measured surface (Good, 1973) and resulting hysteresis, the contact angle is still an extremely useful indicator of the wettability of solids.

2.1.2 Critical surface tension of wetting

Young's equation provides semi-empirical estimates of the surface tension of hydrophobic solids, by using the contact angle and liquid surface tension data. An experimental method for evaluating the surface tension of hydrophobic solids was developed by Zisman (1964). He found that the contact angle, measured by sessile drop on a hydrophobic solid, is a function of γ_{lv} and decreases eventually to zero, when γ_{lv} is reduced. The value of γ_{lv} at which the contact angle just reaches zero was defined as the critical surface tension of wetting, γ_c. In other words, γ_c is that value of γ_{lv} below which liquid spreads on a particular surface and wets it completely.

From an extensive study of the contact angles of a homologous series of organic liquids (later studies by Zisman showed that it was not essential to use homologous liquids) on a hydrophobic solid, $\cos\theta$ was found to be a linear function of γ_{lv} (Fox and Zisman, 1950). Extrapolation to $\cos\theta = 1$ gives the value of γ_c. Mathematically, $\cos\theta$ is related to γ_{lv} by:

$$\cos\theta = 1 + b\,(\gamma_c - \gamma_{lv}) \qquad 2.1.12$$

This plot is frequently referred to as the Zisman plot. The constant b was shown to be related to the degree of the hydrophobicity of the solid surface, and found to be a function of γ_c, $b = 1/\gamma_c$ (Good and Girifalco, 1960). Parekh and Aplan (1974; 1978) tested γ_c of a number of minerals and coal, and found that the increasing slope of the line was associated either with higher adsorption of surfactant onto the mineral surface (increased hydrophobicity), or with increasing rank in the case of coal. The slope correlates with the rank in a very similar manner as does the contact angle.

To some extent, the value of γ_c depends on the set of liquids used to measure it. This is particularly true if there are polar interactions. Zisman described γ_c as a useful empirical parameter whose relative value acts as one would expect of surface tension of solid, γ_s, (γ_s represents the value of γ in a vacuum, without any adsorption of vapor), an indicator of specific energy of the solid. Many attempts have been made to identify γ_c with γ_s or γ_s^d (γ_s^d, critical surface tension arisen from the dispersive forces).

Good and Girifalco (1960) implied that for nonpolar liquids and solids, the critical surface tension of wettability is equal to the surface tension of the solid $\gamma_c = \gamma_s$. Similarly, Fowkes (1963) showed that $\gamma_c = \gamma_s^d$. Their experimental results appear to support these predictions. One might therefore expect that for non-polar solids, $\gamma_c = \gamma_s$, provided there is no significant adsorption at the solid /air or solid/liquid interface

($\pi_e = 0$).

Another common way of expressing the wettability of inherently hydrophobic minerals in solutions of changing surface tensions is through the adhesion tension diagram, $\gamma_{lv} \cos\theta$ versus γ_{lv}, (Figure 2.1.3), on such a diagram the contact angles plot gives a straight line, and is represented by the equation:

$$\gamma_{lv} \cos\theta = A\ \gamma_{lv} + (1-A)\ \gamma_c \qquad 2.1.13$$

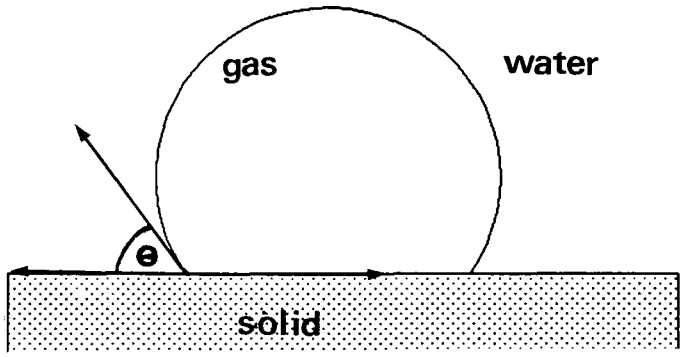

Figure 2.1.1 Contact angle formed by water, vapor (gas), and solid phases.

The maximum slope occurs when A=1, and therefore $\cos\theta = 1$ (θ=0), and represents the maximum polarity (hydrophilicity) of the solid. A gradual decrease in the magnitude of A below unity is interpreted as an increase in nonpolarity. Once the wettability line becomes parallel to the $\cos(180^o)$ line, there is practically no adhesion of

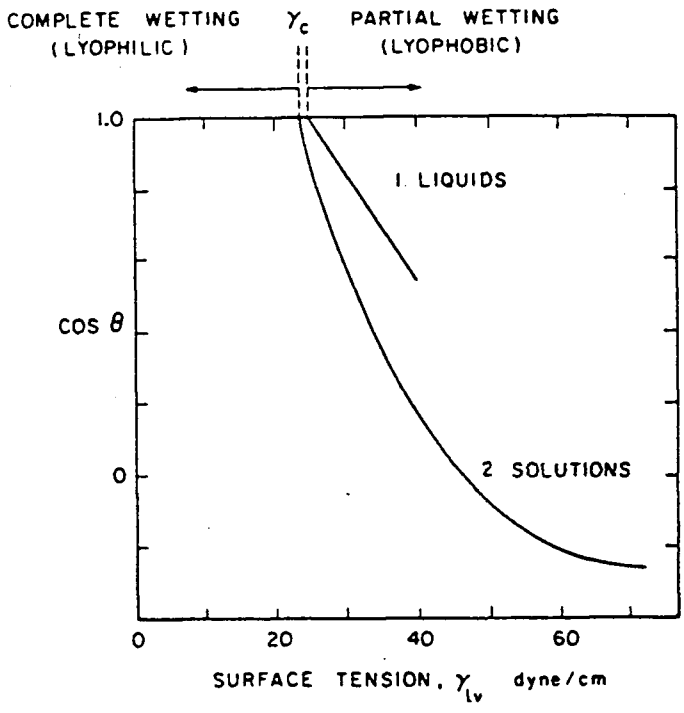

Figure 2.1.2. Zisman diagram for liquids and aqueous solutions on hydrophobic solids (Hornsby and Leja, 1983).

liquid to the solid. This represents a highly non-polar solid surface (maximum hydrophobicity), (Kelebek, 1987). Further, the polarity was found to be related to the slope of the adhesion tension line, by the expression

$$A = 1.7\ X_{hl} - 0.7 \qquad 2.1.14$$

where X_{hl} is the fraction of the hydrophilic portion of the mineral surface as calculated from Cassie's equation (Cassie, 1948). Figure 2.1.3 from Kelebek (1987) shows that the increase in polarity is accompanied by a regular increase in the slope of the adhesion tension line of these solids. Paraffin is shown to be completely non-polar, while stibnite has the highest polarity, since the slope of its adhesion line is almost positive. For non-

polar solids, the parameter which reflects the difference in wettability properties is γ_c. However, when the solid becomes more polar, the slope of the adhesion tension line becomes a more sensitive parameter of wettability.

For two solids with significantly different values of γ_c (determined in solutions of the same alcohol) a selective wetting region will exist if $\gamma_c^a < \gamma_{lv} < \gamma_c^b$, as indicated in Figure 2.1.4 by the shaded area. In this case, solid B will be wetted, while solid A will be only partially wetted. The wettability region for solid B and D will be the same, even though their polarity is different.

The concept of critical surface tension of wettability, irrespective of its many limitations, is still a useful parameter in the characterization of the relative wettability of a solid surface. Wettability of a number of low-energy (inherently hydrophobic) solids was tested using this method (Fox and Zisman,1950; Hornsby, 1981). The first values of the critical surface tension of wettability for coals of different ranks and lithotypes were reported by Eissler and Van Holde (1962). They found the critical surface tension, γ_c, for anthracite equal to 39.8 dyne/cm, for fusain to 54 dyne/cm, and for vitrain from coals of various ranks, were estimated to range from 41 to 56 dyne/cm. The highest value of γ_c corresponded to the vitrain of the high volatile and the lowest to the low volatile rank of coal. Parekh and Aplan (1978) found critical surface tension of wetting γ_c for graphite and coal to be at 45 dyne/cm (irrespective of rank).

The most common way of assessing critical surface tensions has been based on obtaining reliable contact angle values and then plotting the adhesion tension diagram such as the one in Figure 2.1.4. The value of critical surface tension is obtained as the intercept of $\gamma_{lv}\cos\theta$ with the $\theta=0$, line and represented by γ_{lv}. Because many problems are usually associated with contact angle measurements especially of powder samples, other alternative methods of critical surface tension estimation have become more attractive.

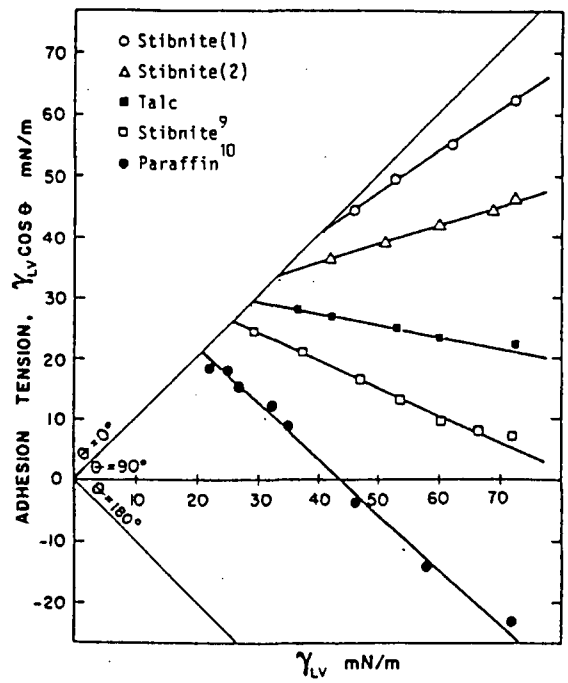

Figure 2.1.3 Wettability diagram illustrating adhesion tension of various specimens; stibnite, talc and paraffin wax as a function of surface tension (Kelebek, 1987).

Garshva et al., (1976) used a modified Walker (1952) procedure to measure immersion time of the disappearance of powder into solutions of decreasing surface tension to define γ_c. In another procedure (Yarar, 1985), small-scale flotation tests were

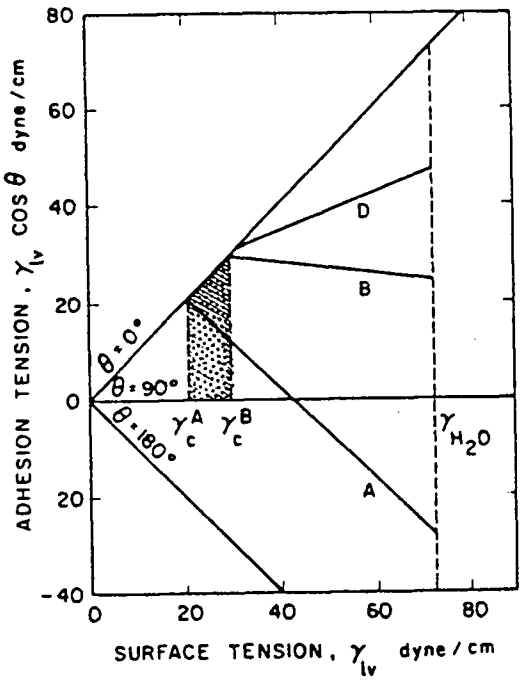

Figure 2.1.4 Adhesion tension diagram illustrating wettability lines for three hydrophobic solids in aqueous solutions of a short-chain n-alcohol, and selective wetting region (shaded area) between solids A and B, (Hornsby and Leja, 1983).

performed on a number of hydrophobic solids, using methanol solutions to vary surface tension. The weight percent of recovery of the hydrophobic fraction versus surface tension yielded a floatability tension distribution with a minimum and maximum. The value of γ_c of wetting was determined by extrapolation to zero flotation recovery. In the same study it was shown that there is a very good agreement with critical surface tension of wettability of three different solids estimated by this technique and contact angle method (Figure 2.1.7). For the heterogeneous solids the recovery of floating fraction versus surface tension of solution was represented by a wider cumulative distribution curve, with a more obvious minimum and maximum. Homogeneous solids form an almost straight line, indicating only one value of γ_c for all particles

within the sample.

Marmur et al., (1986) called the highest surface tension at which all particles were imbibed "total floating concentration", TFC, and the lowest methanol concentration at which all particles are wetted, the "total sinking concentration" (TSC). He argued that one should not use the term critical surface tension, because the measurement of γ_c depends on the relative adsorption of solutes to the solid-liquid and liquid-vapor interfaces. Reported γ_c values should be supplemented by some estimate of the relative adsorption of the solute to the various interfaces. He used the term "critical spreading concentration" to characterize the lowest concentration of the least polar components (methanol and ethanol) in a binary solution leading to complete spreading. On the other hand he concluded that γ_s calculated at TSC is in good agreement with the γ_c calculated from the contact angle. The difference between TFC and TSC is due to either a variation in surface energies of particles or contact angle hysteresis. The latter is associated with possible roughness and chemical heterogeneity of the particle.

Similarly, a modified Walker test was used by Fuerstenau et al., (1985; 1986; 1987a; 1988b) to test surface properties of an assembly of coal particles. Fuerstenau used the term film flotation to describe this technique. Coal particles were placed onto the surface of solutions of decreasing surface tension, forming a monolayer identified as the film. Three parameters were defined: $\gamma_c$min, the surface tension of the solution that wets all particles, $\bar{\gamma}_c$, the mean critical wetting surface tension of particles in the

distribution; and $\gamma_c max$, the surface tension of the solution above which none of the particles are wetted, (Figure 2.1.5). An average wetting surface tension was proposed as an index for correlating the wetting behavior of coals with their composition and degree of surface oxidation. It was shown that an average wetting surface tension of coals increases upon surface oxidation. The increase in $\bar{\gamma}_c$, a quantitive measure of the coal surface energy, was found to be caused by the increase in oxygen functional groups. A marked change in γ_c with oxidation is mainly a result of an increase in the value of $\gamma_c max$, since the $\gamma_c min$ did not shift appreciably.

The competence of film flotation for characterizing the hydrophobic/hydrophilic nature of solid particles was established through tests with particles of different densities and shapes that have homogeneous hydrophobic surfaces (Fuerstenau et al., 1988a). Materials such as sulphur, silanated glass beads and quartz, and paraffin coated coal, graphite, calcite, magnesite and pyrite particles were floated using the film flotation technique. It was concluded that the technique is nearly independent of particle shape, size, and density over fairly wide range. These results confirmed that the process involved in film flotation is predominantly controlled by interfacial forces. Another important conclusion was reached in regard to the effects of preferential adsorption on involved interfaces. It was shown that the value of $\bar{\gamma}_c$, determined from film flotation using different polar reagents (to vary surface tension), of the graphite particles was the same. A more comprehensive study on the wetting behavior and related

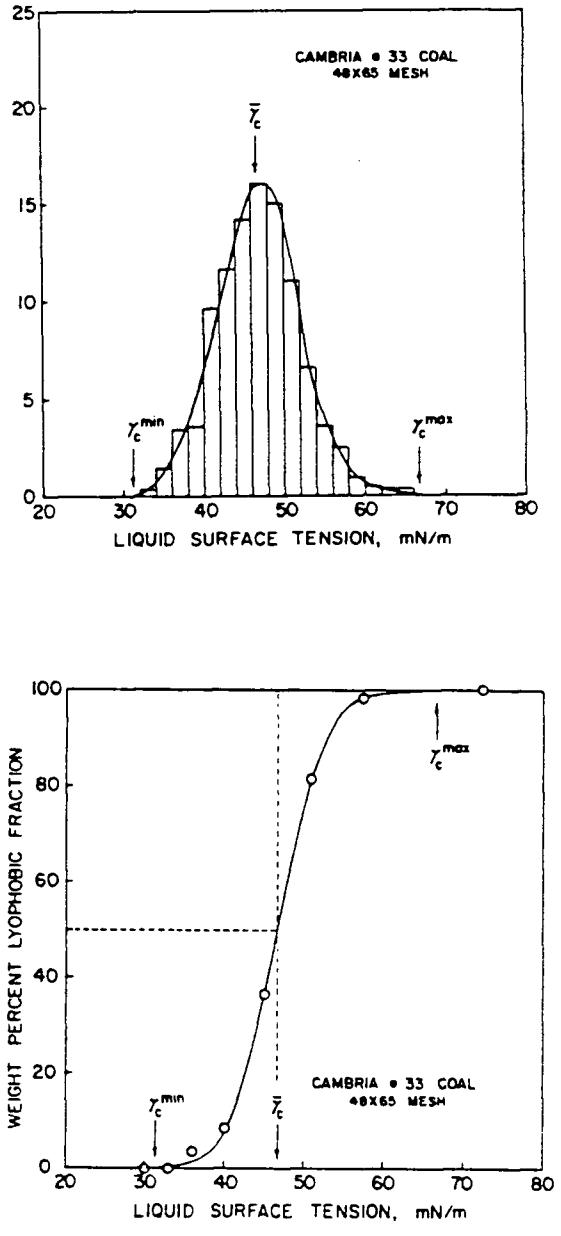

Figure 2.1.5 Film flotation wettability distribution curve for Cambria No. 33 bituminous coal (a) frequency histogram for lyophobicity of Cambria No. 33 coal (b) partition curve, (Fuerstenau et al., 1988b).

properties of methanol solutions was reported by Kelebek (1987). He showed that the relative adsorption density of methanol at the aqueous solution-gas interface reaches a maximum value when the surface tension is between 40 and 30 dyne/cm (35 and 65 methanol concentration). Complete wetting due to adsorption of methanol at solid surface may occur when the adsorption of methanol at the solution-gas and/or solid-solution interfaces reach a maximum value.

Hornsby and Leja (1980) showed that the selective separation of two solids of different γ_c was achieved by simple manipulation of the surface tension of the wetting solution. In their method, they used a mixture of two solids, each with known γ_c, and carried out separation in test tubes with varying methanol solutions. Similar results were reported by others (Kelebek and Smith, 1985; Finch and Smith, 1975).

Separation of two solids by flotation depends on the relative wettability of particles. The selective separation of two hydrophobic solids with different γ_c of wettability, fulfilling the selective wettability conditions, was found possible and quite practical. In view of this relation between flotation and selective wettability, the concept of critical surface tension is directly relevant to flotation.

2.1.3 Critical surface tension of floatability

In section 2.1.2 it was shown that a selective wetting region exists between solids with different γ_c values. The γ_c determined from wettability represents, however, only the static wetting behavior of particles. It is obvious that, under the actual flotation conditions, particles are subjected to dynamic non-equilibrium conditions. Therefore it may be expected that floatability cannot be unambiguously predicted from wettability analyses.

The development of the concept of a critical surface tension of floatability, as proposed by Hornsby (Hornsby, 1980; Hornsby and Leja, 1983), indicated that a significant difference in critical surface tension of floatability, γ_{cf}, values may exist between two solids, even though there may be little or no difference in their γ_c values. Such a difference would provide a selective floatability region, where separation of the two solids should be possible.

The differences in the critical surface tension of floatability between particles of the same γ_c arise from the differences in critical surface tension of adhesion, γ_{ca} ($\gamma_{ca} > \gamma_c$), below which adhesion of a bubble to the particle is not possible, and critical surface tension of particle-bubble stability, below which a particle-bubble aggregate becomes unstable. These two parameters, and the hydrodynamic conditions in the flotation cell, decide whether a particle will successfully attach to an air bubble and separate from the flotation slurry. For flotation to occur, the collision between a particle and a bubble

in the flotation system is necessary. This condition is usually fulfilled by adequate hydrodynamic flotation criteria, and was shown to be independent of a particles hydrophobicity.

The adhesion of a bubble to a particle increases as the induction time decreases (Laskowski, 1974). Induction time was also found to decrease as the particle size and the viscosity of the solution in the disjoining film decreases (Laskowski, 1974). As the γ_{lv} approaches the limit of γ_c, the induction time increases at some point and it becomes larger than the time of contact between bubble and particle. This indicates the proximity of critical surface tension of adhesion, γ_{ca}. The contact angle associated with this value is referred to as θ_{ca}. The critical contact angle of adhesion is always larger than zero. Figure 2.1.6 illustrates the concept of the critical surface tension of adhesion for hypothetical solid B.

Assuming collision and adhesion have taken place, there will be limiting values of γ_{lv} and θ below which a particle of a given size and density will not float due to unstable particle-bubble aggregate, even though θ has a finite value. The particle-bubble aggregate stability depends on the size, density and wettability of floated particles. For particles with identical surface properties (same wettability characteristics, γ_c and slope b of line B), but different sizes, the floatability will be different. The latter would be described by different values of critical surface tension of particle-bubble stability, γ_{cs} or different values of corresponding contact angle, θ_{cs}, as shown in

Figure 2.1.6. Two particles of different sizes, where $d' < d''$ would have the relevant $\theta'_{cs} < \theta''_{cs}$ and $\gamma'_{cs} < \gamma''_{cs}$. Therefore, if the γ_{lv} were such that $\gamma'_{cs} < \gamma_{lv} < \gamma''_{cs}$, the smaller particle would be floated, whereas the larger particle would be non-floatable, due to insufficient particle-bubble aggregate in solution of γ_{lv}.

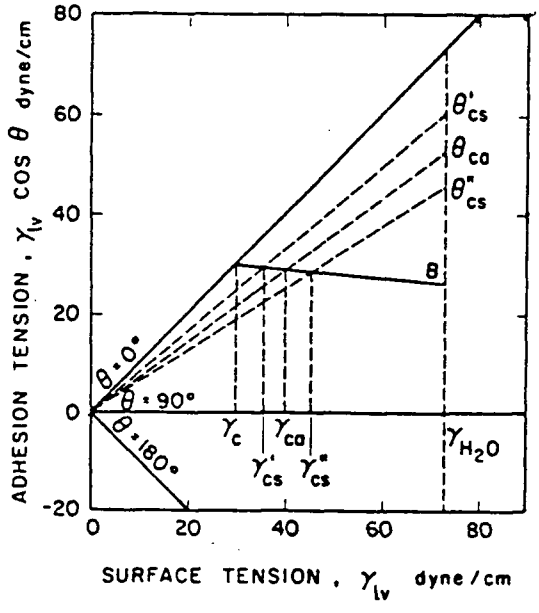

Figure 2.1.6 Adhesion tension diagram; the concept of critical surface tension of adhesion, γ_{ca}, for a hydrophobic solid with wettability line B, (Hornsby and Leja, 1983).

The values γ_{cs} or γ_{ca} could be the limiting floatability parameters for particles, depending on which is greater. For example, for the two particles of solid B in Figure 2.1.6, the γ''_{cs} value is the limiting value for flotation of the larger particle, whereas γ_{ca} becomes the critical value in the floatability of the smaller one. In general, a particle will be floatable if $\gamma_{lv} > \gamma_{cf}$, where γ_{cf} represents either γ_{cs} or γ_{ca}

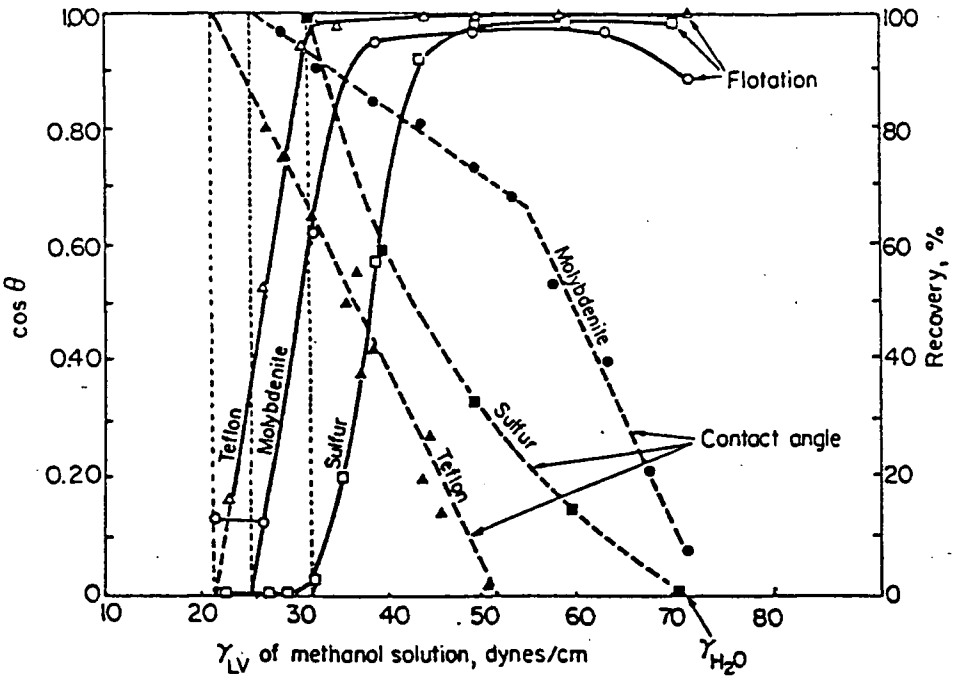

Figure 2.1.7 Effect of the surface tension of methanol/water solutions on floatability and wettability of molybdenite, sulphur and teflon, (Yarar and Kaoma, 1984).

(whichever is larger), and is the critical surface tension of floatability. If the two solids to be separated have a wide variety of particle size distributions, there may be a range of γ_{cf} values instead of one discrete value. The same may be true for the systems with the heterogeneous particles, where broad bands of wettability represents their surface properties.

2.2. Hydrophobicity and floatability

2.2.1 Hydrophobicity theories

The hydrophobic solids are those which display partial or incomplete wettability by water. A number of solids exhibit varying degrees of hydrophobicity when their surfaces are freshly formed (Leja, 1983). These solids may be either organic, such as hydrocarbons, waxes, graphite, tars, bitumen and coals, or inorganic, such as sulphur, talc and molybdenite.

Hydrophobicity is of paramount importance in many surface based processes. The success of froth flotation primarily depends on the hydrophobicity of the floated particles. The hydrophobicity controls not only the thermodynamics of flotation but also the kinetics of the process.

To explain hydrophobicity, Gaudin (1957) showed that during the process of surface formation solids remain naturally hydrophobic only if their fracture or cleavage occurs without rupture of interatomic bonds other than residual ones. These surfaces can only interact with the aqueous environment through dispersion forces. Breakage of covalent or ionic bonds leads to hydroxylation or ionization of the surface, which in turn renders the solid surface hydrophilic. The hydrophobicity of a solid (water rejection) decreases with an increase in the amount of polar sites (hydroxyl or ionic) on the mineral surface. Through these polar sites water becomes attracted to the surface.

According to Frumkin and Dieriagin (in Klassen, 1966) hydrophobicity can be explained using a water hydration layer concept. Low hydration of a mineral surface indicates strong hydrophobicity, whereas high hydration indicates hydrophilicity. In view of this theory, three types of films, disjoining particle and bubble, may be created as a result of surface hydration: stable, metastable and unstable. A stable wetting film is characteristic of a strongly hydrated surface, while an unstable film is typical of a hydrophobic solid. A metastable wetting film becomes unstable below a critical thickness of the disjoining film; this is typical for flotation with collector systems. An instability of water films on hydrophobic solids is due to the lack of hydrogen bonding in these films as compared to the bulk water. In other words, the proximity of a nonpolar surface imposes on the neighboring water molecule an unfavorable configuration (Laskowski and Kitchener, 1969).

Laskowski and Kitchener (1969) used Fowkes concept of interfacial energies to explain the hydrophobic-hydrophilic transition of the solid surface. They concluded that the work of adhesion of water to a solid depends on dispersion forces, hydration of non-ionic polar sites, and electrical charge. Hydrophobicity arises whenever the two latter terms are small, because dispersion energies are always smaller (except for fluorocarbons) than the (exceptionally large) work of cohesion of water. The solid is hydrophobic whenever it interacts with water through dispersion forces only. Hydrophobicity arises essentially

from the weakness of adhesion of water to the solid (Fowkes, 1963; Laskowski and Kitchener, 1969).

2.2.2 Floatability

As discussed in section 2.1.3, for a particle to be floatable, not only dewetting of the particle surface have to be thermodynamically favorable, by fulfilling $\theta > 0$ or $\gamma_{lv} > \gamma_c$ conditions, but several other criteria also have to be satisfied (Laskowski, 1974; Trahar and Warren, 1976; Laskowski, 1986; Laskowski, 1989):

a) the particle must collide with a bubble;

b) the disjoining film separating the particle and bubble must thin, rupture and recede within the collision time;

c) the particle-bubble aggregate formed must be of sufficient strength to withstand disruptive forces in the flotation cell.

The criteria described above can be expressed in terms of probabilities as proposed by Tomlinson and Fleming, (1963;) and later discussed by Laskowski (1974)

$$P_f = P_c * P_a * P_s \qquad 2.2.1$$

where P_c, P_a, P_s are the probabilities of collision, attachment, and particle-bubble aggregate stability, respectively.

The probability of collision as discussed by many (Tomlinson and Fleming, 1963; Reay and Ratcliff, 1973; Anfrus and Kithchener, 1977; Jameson et al., 1977, Yoon and Luttrell, 1989) was found to be independent of particle hydrophobicity. It mainly depends on the hydrodynamic conditions of flotation, and particle as well as bubble size.

The probability of adhesion, or probability of attachment is difficult to quantify in terms of solid hydrophobicity, because the contact angle does not characterize the kinetic effects during flotation contributing to resistance to the attachment. For a particle to be attached successfully to a bubble, not only a finite contact angle has to be formed, but also the induction time, the time required for thinning, rupture and recession of the disjoining film, has to be smaller than the contact time. A small induction time has generally been found for solids which form large contact angles. The adhesion depends, as discussed in section 2.1.3, on the magnitude of the contact angle related to the critical surface tension of adhesion.

The stability of the particle-bubble aggregate is directly related to the contact angle. The larger the contact angle, the stronger the particle-bubble aggregate, and, as a result, the larger the value of P_s.

CHAPTER 3

COAL

Coal is an organic sedimentary rock composed of two basic materials: inorganic crystalline minerals and organic carbonaceous components recognized as macerals.

The organic part of coal is formed from peat deposits produced in swamps through the accumulation of plant material, and has undergone further biochemical and metamorphic changes, referred to as coalification. Coalification is the progressive enrichment of the coal matrix in organically bound carbon. In general, higher carbon content indicates higher rank of coal. Many physical and chemical properties of coal vary with rank.

Macerals form the organic part of coal and are divided into three groups - vitrinite, liptinite and inertinite. There are three important compositional properties which determine coal quality: rank, type and grade. While rank and type reflect properties of the organic part of coal, the grade refers to the content of mineral matter associated with coal.

3.1 Coal properties

3.1.1 Chemical composition of coal

In a chemical sense, coal is a substance of high molecular weight and non-uniform structure. Coal as a whole is

strongly aromatic; its aromaticity increases more or less steadily with rank, reaching its maximum at about 94% carbon in vitrinites. Coal has a polymeric structure. The average structural unit in coals from lignite to the low-volatile bituminous stage contains about 20 C atoms and about 4-5 aromatic rings. In the anthracite stage the size of clusters and number of rings per cluster increases rapidly (van Krevelen, 1961; Lowry, 1963; Ignasiak, 1975; Ignasiak, 1977; Larsen, 1978; Given, 1984). The distribution of carbon into different hydrocarbon forms as a function of rank is shown in Figure 3.1.1

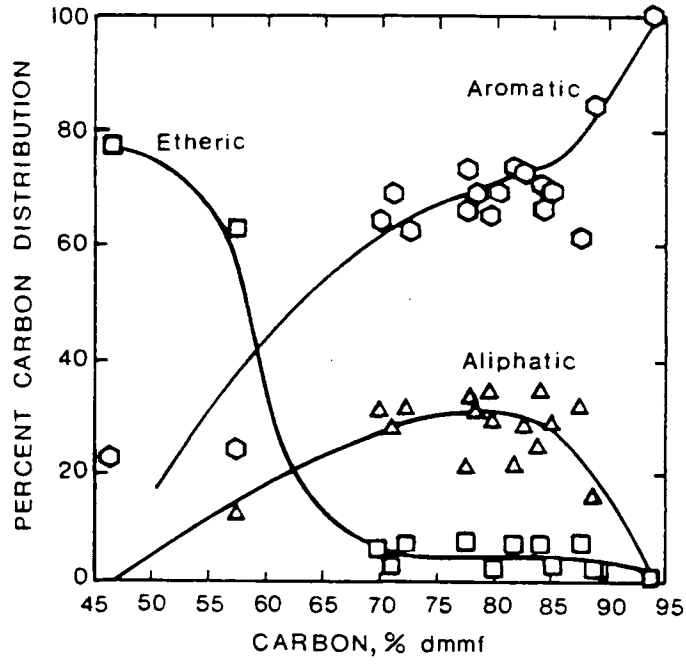

Figure 3.1.1 Carbon distribution in coals of different ranks, (Whitehurst et al., 1980).

One of the earliest proposed coal structures was that of van Krevelen in 1954. Another model of coal structure was suggested by Given (1960). The most commonly referred to is the model proposed by Wiser (1975). In his model hydroaromatic structure is predominant, with weak bonding between aromatic units (Figure 3.1.2). Oxygen functional groups are incorporated in the carbon skeleton. Coal compositional properties change with the changing chemical structure of coal associated with the rank.

3.1.2 Rank

Rank of coal is not a directly measurable quantity. To define it, it is necessary to refer to a specific physical or chemical property which exhibits adequate change in the course of coalification. Rank represents the degree of chemical and physical changes which occur in the organic part of coal as a result of coalification. Coalification is the progressive transformation of peat through lignite, subbituminous, bituminous, anthracite to meta-anthracite coal, associated with the progressive enrichment in organic carbon.

Rank of coal can be estimated by chemical parameters, for example, moisture content, calorific value, volatile matter content (ASTM D 388-77) or carbon, oxygen and hydrogen (ISO, Seyler). An International Committee on Coal Petrology (ICCP) uses optical properties, e.g. vitrinite reflectance. The new classification proposed by Alpern (1983), incorporates all parameters within their

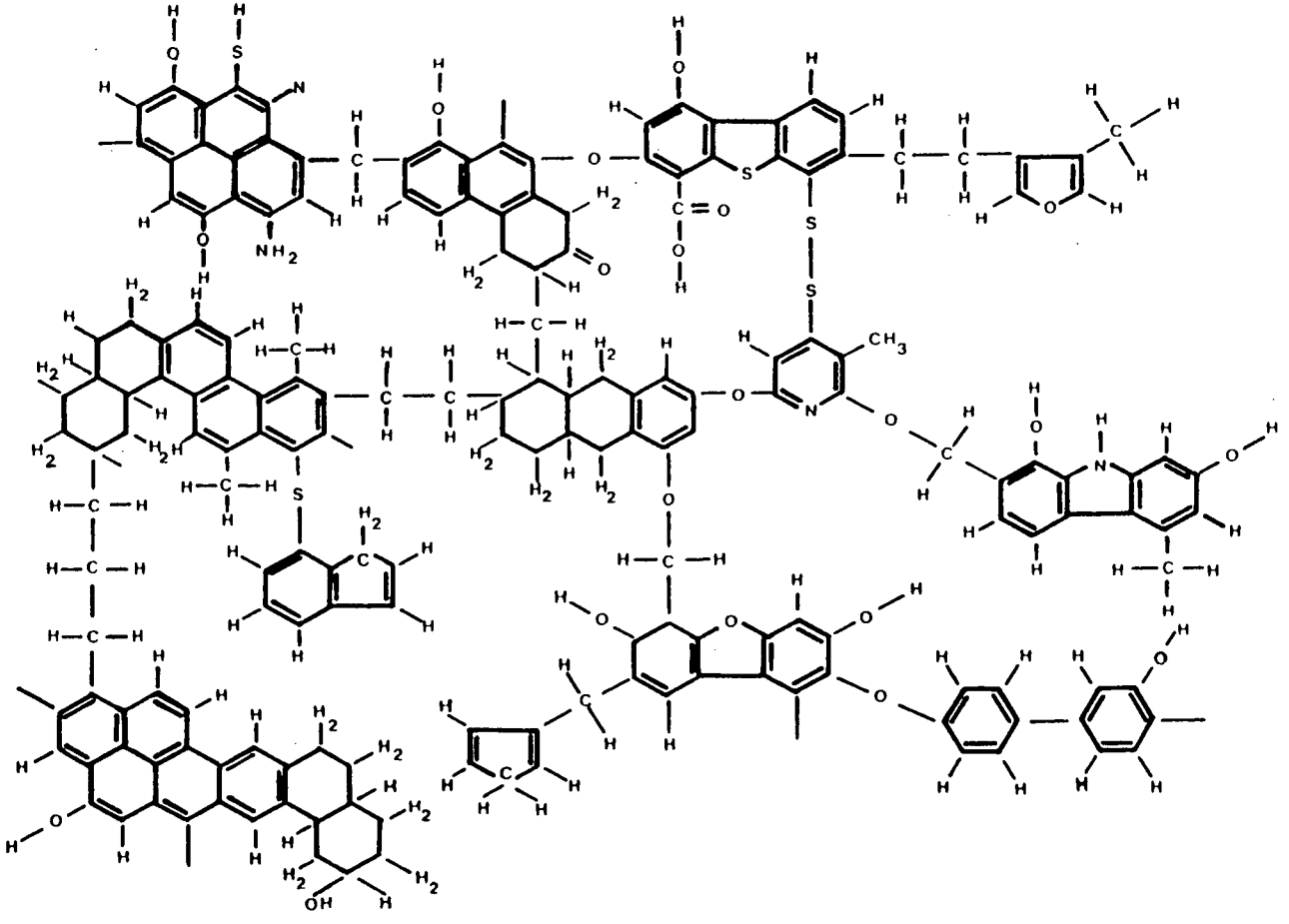

Figure 3.1.2 The Wiser model of structural groups and connecting bridges in bituminous coals (Wiser, 1975).

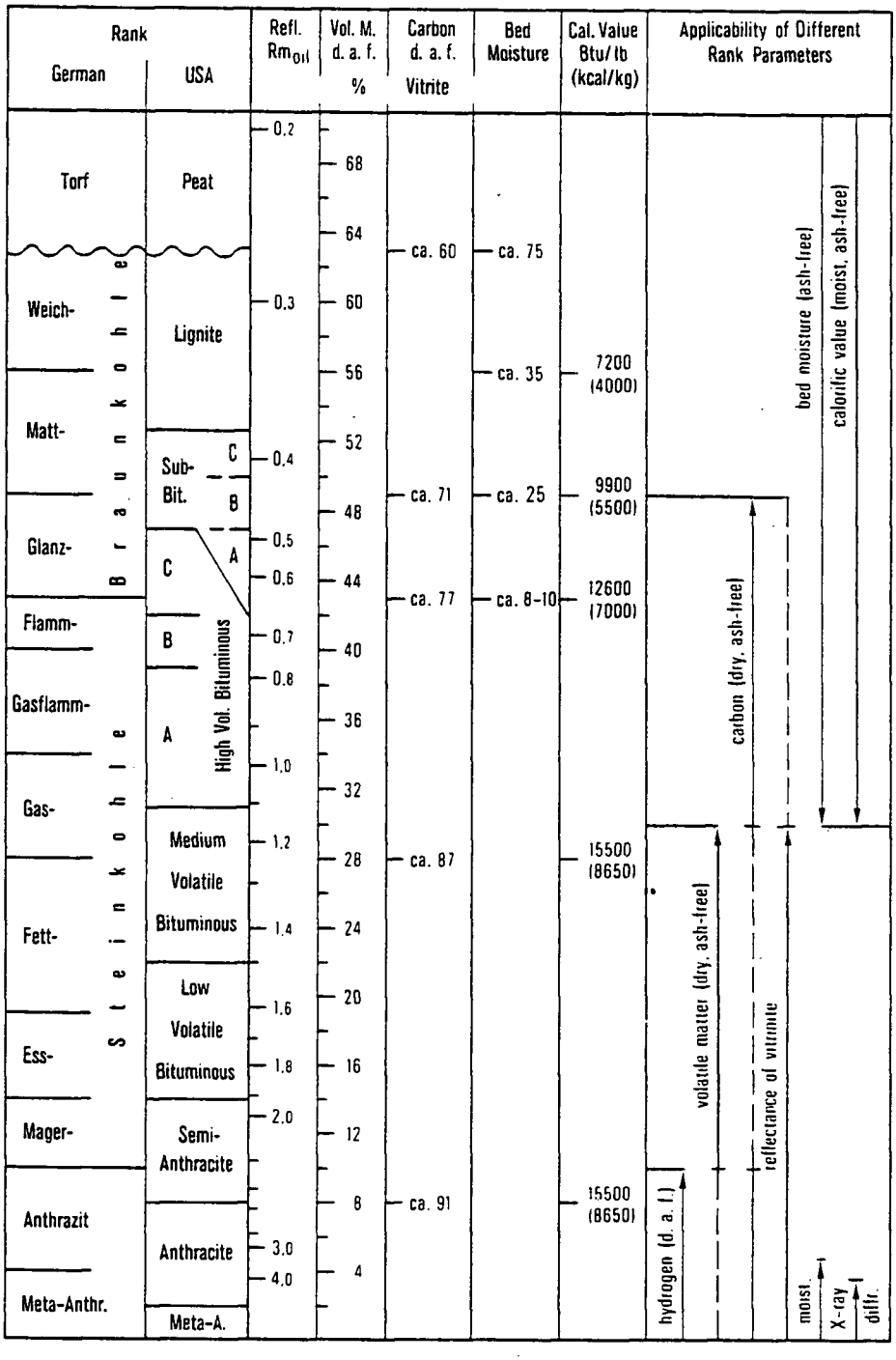

Table 3.1.1 Different physical and chemical rank parameters and their applicability to the different coalification stages (adapted from Stach, 1982).

range of applicability and recognizes petrographic composition as the important element in coal classification.

The chemical changes of coal structure vary during different stages of coalification, and therefore some rank indicators are more appropriate than others in particular rank stages. Table 3.1.1 compares different physical and chemical rank parameters and shows their applicability to the different coalification stages.

For the coals from peat to medium-volatile bituminous, moisture and calorific values (dry, ash-free basis) are very good indicators of rank. Vitrinite reflectance and volatile matter (dry, ash-free basis) are the accepted rank parameters for medium to high-rank coals, with reflectance of vitrinite increasing with coalification, and volatile matter content decreasing as rank increases. Reflectance appears to be the most widely applicable and the most consistent rank parameter, as it is generally independent of petrographic composition, the exception may be coals with high liptinite content, where suppression of reflectance of vitrinite was found to be significant (Raymond and Murchison, 1991).

Different macerals undergo change at different rates during coalification, and therefore comparative rank studies should be determined on vitrinite or a concentrate of this maceral. Vitrinite is the maceral which reflects coalification changes most reliably, irrespective of the fact that it is the most abundant component of humic coals.

Progressive rank increase is closely related to changes

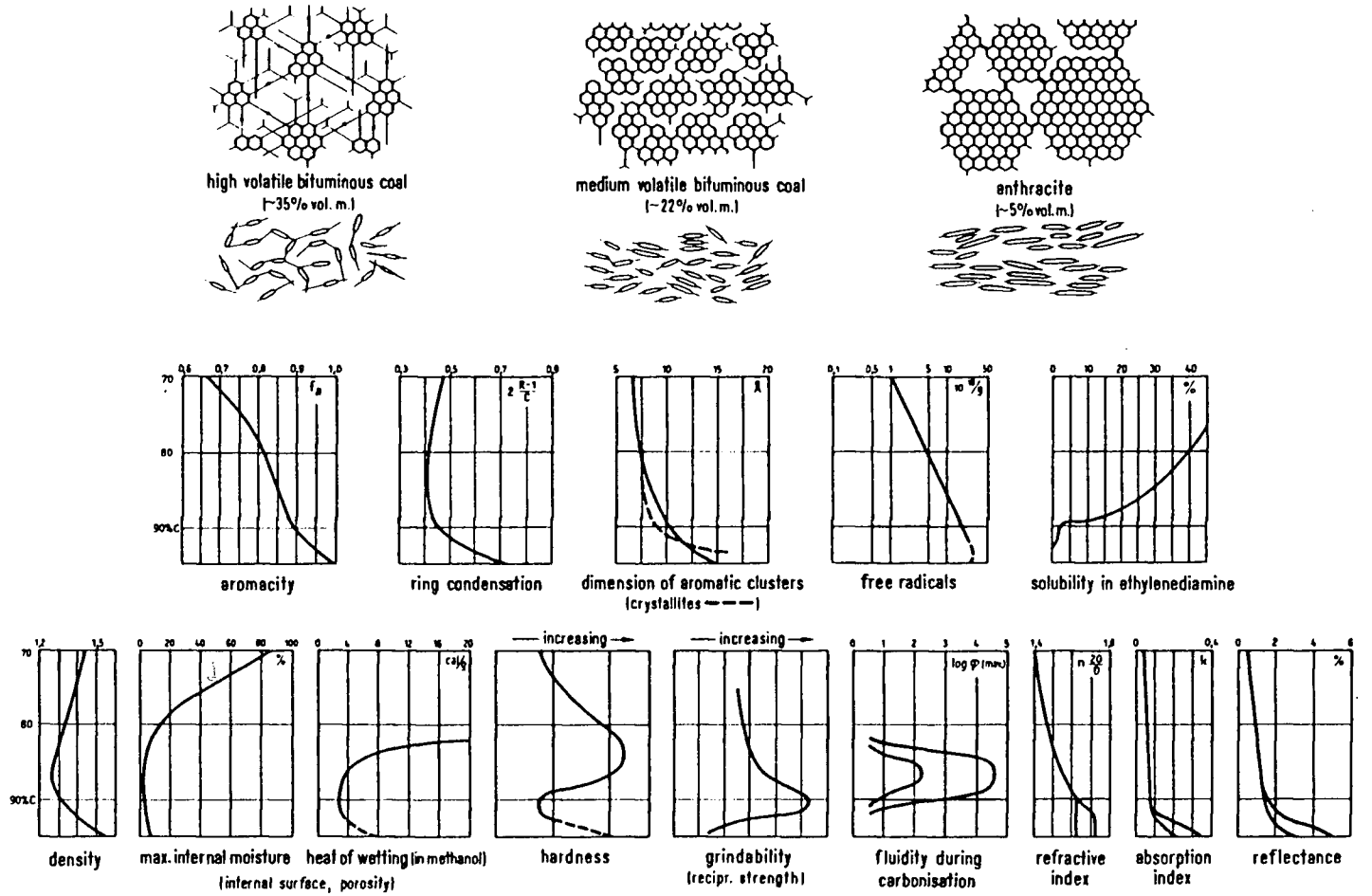

first row: molecular structure
– o – = hydrogen bonding
— = molecular bonding

second row: orientation of molecules perpendicular to the bedding plane
lenses = aromatic clusters
lines = non-aromatic elements

third row: development of chemical properties in relation to carbon content (daf)

fourth row: development of physical properties in relation to carbon content (daf)

Figure 3.1.3 Physical and molecular changes of vitrite during the coalification of bituminous coals and anthracites, (Teichmuller, 1982).

in chemical structure of coal. A steady decrease in moisture content from lignite to high-volatile bituminous coal is due to a decrease in the porosity, and oxygen functional groups. As a result, the carbon content gradually rises. Figure 3.1.3 illustrates physical and chemical changes occurring during the coalification of bituminous coals as adopted from Teichmuller (1982).

As coalification progresses from high-volatile bituminous to medium-volatile coals, there is a continued fall of moisture content and a corresponding rise in the calorific value. In bituminous coals volatile matter falls due to the removal of aliphatic groups and the increase in aromatization of coal. In the anthracite stage there is a rapid fall in the hydrogen content along with an increase in aromaticity and a strong increase in reflectivity (Mackowsky, 1982)

3.1.3 Type of coal

Type of coal reflects different plant and depositional conditions and the extent of the change occurred during the biochemical and geochemical processes of coal formation. Two major types of coal are recognized, humic or banded coals which are formed in situ (autochthonous), and sapropelic or non-banded which are formed from drifted debris of materials such as spores, pollen, and degraded peat, and are deposited in standing waters (allochthonous).

Sapropelic coals differ from humic coals in their uniform

texture, great strength and conchoidal fracture. Sapropelic coals are distinguished chemically by high hydrogen content and a high yield of volatile matter. They can be divided into cannel and boghead coal. Cannel coals are composed of peat degradation products, mainly resistant plant parts such as waxy and resinous substances which were concentrated during the degradation of peat. Cannel coals also contain high amounts of vitrinite, but in very comminuted form. Boghead coals are derived mainly from algal material that grows in situ (Bustin et al., 1983).

Humic coals are predominant. They originate from organic matter which has undergone change by humification, the process of peat formation with restricted oxygen supply. The scheme in the Table 3.1.2 shows the dependency of the transformation of organic substances on oxygen supply (Teichmuller, 1982).

	Process	Product	
aerobic → decrease of O-supply → anaerobic	disintegration	usually no solid residue, possibly liptobioliths	increase of hydrogen and nitrogen in transformation products →
	mouldering	mould	
	peatification	peat	humic coals
			sapropelic coals
	putrefaction	sapropel	sapropelites
			petroleum

Table 3.1.2 The dependency of the transformation of organic substances on oxygen supply, (Teichmuller, 1982)

Humic coals usually consist of macroscopically recognizable bands of coal. These different types of coal within the seam are called "lithotypes". The composition of lithotypes is strongly dependant on the maceral composition and the association of macerals with different proportions of mineral matter (e.g. Diesel, 1985 a,b). Lithotypes and macerals, as well as their definitions, are discussed in section 3.2.

3.1.4 Mineral matter

The mineral matter in coal occurs as inorganic matter from the original plant material, detrital particles and authigenic deposits associated with the first stage of coalification, or as deposits associated with the second stage of coalification, after consolidation of coal (Rao and Gluskoter, 1973; Renton, 1978; Stach et al., 1982; Finkelman, 1982;). Table 3.1.3 shows the common coal minerals and their origin as adapted from Mackowsky (1982). Authigenic and detrital minerals are termed syngenetic, whereas minerals formed later are referred to as epigenetic. The syngenetic minerals tend to be fine and intimately intergrown with the coal organic part, while epigenetic are usually deposited in the cracks and fissures of macerals.

The terms extraneous and inherent mineral matter are also frequently used to describe physically separatable mineral matter from inseparatable. These technical terms may be rather misleading,

Mineral Group	First stage of coalification		Second stage of coalification	
	Syngenetic formation synsedimentary-early diagenetic (intimately intergrown)		Epigenetic formation	
	Transported by water or wind	Newly formed	Deposited in fissures, cleats and cavities (coarsely intergrown)	Transformation of syngenetic minerals (intimately intergrown)
Clay Minerals	Kaolinite, Illite, Sericite, Clay Minerals with mixed-layer structure Montmorillonite, Tonstein			Illite, Chlorite
Carbonates		Siderite-Ankerite concretions, Dolomite, Calcite, Ankerite Siderite, Calcite	Ankerite Calcite Dolomite Ankerite in Fusite	
Sulphides		Pyrite concretions Melnikovite-Pyrite Coarse Pyrite (Marcasite) Concretions of FeS_2—$CuFeS_2$—ZnS	Pyrite Marcasite Zinc Sulphide (Sphalerite) Lead Sulphide (Galena) Copper Sulphide (Chalcopyrite) Pyrite in Fusite	Pyrite from the transformation of syngenetic concretions of $FeCO_3$
Oxides		Hematite	Goethite, Lepidocrocite ('Needle-Iron Ore')	
Quartz	Quartz grains	Chalcedony and Quartz from the weathering of Feldspar and Mica	Quartz	
Phosphates	Apatite	Phosphorite, Apatite		
Heavy minerals and accessory minerals	Zircon, Rutile, Tourmaline, Orthoclase, Biotite		Chlorides, Sulphates and Nitrates	

Table 3.1.3 Common coal minerals and their origin, (adapted from Mackowsky, 1982).

since they are operational rather than genetic.

Typical syngenetic minerals are pyrite and siderite, and in some coals clays and quartz, etc. (Cook, 1981). Syngenetic minerals are usually dispersed through the coal organic part and present a greater cleaning problems, unless in massive occurrences.

Epigenetic minerals form in coal cleats and fractures as the mineral-forming ions migrate into the coal seams. The major epigenetic minerals are pyrite, calcite and other carbonates, and a variety of rare minerals (Cook, 1981). Physical separation of epigenetic minerals is more efficient because of their nature of association in the coal.

The preferential association of mineral matter with coal macerals has been shown in many studies (Gaudin, 1957; Klassen,-1966; O'Gorman, 1971; Jowett, 1980;). Fusinites, due to their cellular structure, are believed to have the highest potential for secondary mineral emplacement, whereas vitrinites are considered to have the lowest mineral matter content. As a result, the association of mineral matter with lithotypes increases in the order vitrain-clarain-durain-fusain (Klassen, 1966)

The minerals associated with coal have significantly different physical and chemical properties than the coal macerals. Therefore, in many cases knowledge of the type and distribution of these minerals in coal has useful application. In a geological sense, presence of some minerals may provide valuable information on the conditions of coal formation, or as in the case of tonsteins, may allow the seam identification and correlation (Bustin et

al., 1983). Many physical and chemical coal utilization processes are greatly influenced by the mineral matter content. The type and occurrence of mineral matter in coal is particularly important to washability characteristics (Mackowsky and Hoffman, 1960; Falcon, 1983) and to the sizing or even crushing of the coal (Hower et al., 1986; Hower et al., 1987) The intergrowth of mineral matter with coal plays a significant role in determining physical properties of coal grains. In thermal coals, mineral matter content affects the heating value of coal, and its ash fusion point, which in turn influences its tendency to form deposits or cause corrosion on surfaces of heating chambers (Bustin et al., 1983). Pyrite in thermal coal is a potential source of sulfur dioxide in the atmosphere. Presence of mineral matter also leads to problems in filtration and catalyst poisoning in liquefaction (Handbook of Coal Petrology, 1963; Tsai, 1982), and affects quality of coke. Despite all the detrimental effects of mineral matter in coal, there are some beneficial effects. For example, pyrite may act as a catalyst (Gorbaty, 1983) in coal conversion processes such as hydroliquefaction. Moreover, some amount of mineral matter is required for optimum coke strength (Davis, 1976; Gray, 1978; Tsai, 1982).

3.2 Petrographic composition of coal

Macerals are the smallest microscopically distinguishable components of coal, and are analogous to minerals in rock. There are three maceral groups in coal, vitrinite, inertinite and

liptinite. The individual macerals are grouped according to their similar petrographic properties, such as morphology, reflectance, relief and color in reflected or transmitted light. The properties of coal macerals change in the course of coalification. Table 3.2.1 presents macerals and groups of macerals in bituminous coals (ICCP handbook).

Detailed nomenclature	Simplified nomenclature (for technical use)	
Maceral	*Group*	*Symbol*
Collinite Telinite	Vitrinite	V
Sporinite Cutinite Alginite Resinite	Exinite or Liptinite	E
Micrinite { fine-grained micrinite massive micrinite Sclerotinite Semifusinite Fusinite	Inertinite	I

Table 3.2.1 Macerals and groups of macerals in bituminous coals (ICCP Handbook, 1963).

The various associations of macerals with each other, as observed under the microscope, are defined as microlithotypes. On a macroscopic scale, the variation in appearance of different bands of coal, due to maceral concentrations, are called lithotypes.

3.2.1 Origin of macerals

Coal macerals originate from coalified plant remains.

	Microlithotype	Maceral-Group composition mineral-free
Monomaceralic	Vitrite	V > 95%
	Liptite	L > 95%
	Inertite	I > 95%
Bimaceralic	Clarite	V + L > 95%
	Vitrinertite	V + I > 95%
	Durite	L + I > 95%
* Trimacerite	Duroclarite	V > L and I
	Clarodurite	I > V and L
	Vitrinertoliptite	E > V and I

V = vitrinite, L = liptinite, I = inertinite.

* in trimacerites at least 5% of each maceral must be present.

Table 3.2.2 Description of microlithotypes according to the ICCP (ICCP Handbook, 1963).

Some of them still have preserved plant structure, while others are products of degradation of plants, in which case plant structure can no longer be recognized.

Vitrinites are coalification products of humic acids which originate from decomposition of lignin and cellulose of wood cells. The humic acids are formed through moldering and peatification. As digenesis proceeds, humic acids lose their acid character and are changed into humins. Further gelification of humins takes place with increasing rank, which leads to vitrinite formation. The precursors of vitrinite in peat and subbitumous stage are referred to as huminite macerals. The initial differences between plant remains gradually disappear as coal rank increases; therefore

huminite macerals outnumber vitrinite macerals.

Liptinites (or exinites) are derived from hydrogen-rich plant remains such as resins, cutins, waxes and fats. Liptinites contain large amounts of aliphatic constituents (paraffins) as compared to the humic macerals. In low-rank coals, liptinite macerals are characterized by lower reflectance than vitrinite. At the higher rank liptinite assumes the chemical and optical properties of vitrinite. Thus, as coal rank increases, the reflectance of liptinite increases to reach that of vitrinite, at the low-volatile bituminous coal stage.

Inertinite macerals are derived from the same original plant material as vitrinite or liptinite, but they are subjected to a different process of primary decomposition (Teichmuller, 1982). Inertinite macerals are produced by charring (forest fires) or moldering of the wood tissues or other original substances. In general, inertinite macerals are characterized by relatively high carbon content, very low hydrogen, and are enriched in oxygen as compared to vitrinite or liptinite. They are also characterized by an increased level of aromatization of hydrocarbons. Inertinite macerals are the ones which experience the least structural changes during the process of coalification. In terms of optical properties, inertinite is characterized by higher reflectance than vitrinite of the same rank.

The coalification tracks of three main maceral groups are shown in Figure 3.2.1. Each maceral undergoes a particular evolution during coalification. Vitrinites changes in the most

uniform way and is the maceral which reflects most predictably the rank of coal.

3.2.2 Chemical and physical properties of macerals.

The three maceral groups are not only petrographically distinct but also are characterized by different physical and chemical properties. These differences in chemical and physical properties are reflected in the technological behavior of coal macerals.

Vitrinite macerals are the most desired components in coking coal, where they contribute to plasticity of coal. The reactivity in low rank coals means they are readily hydrogenated. In coal processing, vitrintes concentrate in fines due to brittleness and fissuring (T. Laskowski, 1948). The range for density of vitrinite is from 1.3 to 1.45 g/cm^3. Density changes with rank, the minimum density occurring in the medium volatile bituminous rank range.

Liptinite macerals are particularly rich in hydrogen, and as a result yield high amounts of gas and tar when carbonized (Falcon, 1978). For the same reason, coals with high liptinite content are the most suitable for hydrogenation. An increased liptinite content increases the strength of coal (Falcon, 1978). The density of liptinite range from 1.0 to 1.25 g/cm^3 (Kroger and Bade, 1961; Dyrkacz et al., 1981; Tsai, 1982; Crelling, 1983; Dyrkacz et al., 1984a and 1984b).

Inertinite macerals are generally very inert in carbonization and hydrogenation processes. The specific gravity of inertinites is in the range of 1.45 to 1.50. Inertinites, especially fusinite, can be very friable and contribute significantly to dust formation (T. Laskowski, 1948; Hower et al., 1987)

Many of these physical properties have been exploited to separate macerals, sometimes quite successfully (Golouskin, 1959, Kroger 1961, Dyrkacz et al., 1981). The early studies on the separated macerals were done by many distinguished scientists (vanKrevelen, 1961; Given, 1984). A significant amount of modern fundamental research into maceral characterization was accomplished after introduction of the density gradient centrifugation method for maceral separation by Gary Dyrkacz in 1981 (Dyrkacz et al., 1981; Winans and Crelling, 1984; Pugmuire et al., 1984; Silbernagel et al., 1984).

3.2.3 Microlithotypes

Macerals do not always occur as discrete or liberated particles. Most often they are in association with each other and varied amounts of mineral matter. Associations of macerals with each other, as observed microscopically, are called microlithotypes. Microlithotypes are arranged into three main groups; monomaceralic, bimaceralic, and trimaceralic, depending on whether they are composed of macerals from one, two or three maceral groups. Description of microlithotypes according to the ICCP

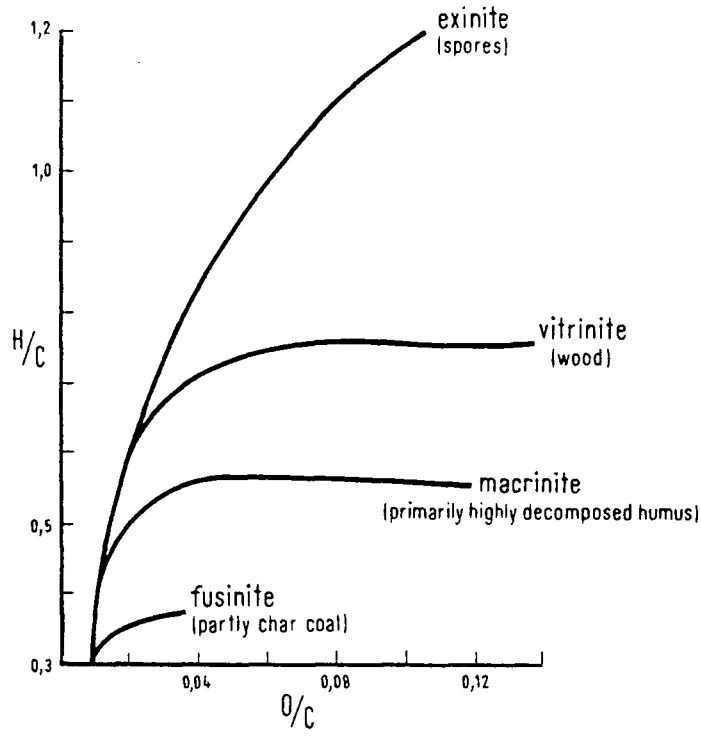

Figure 3.2.1 The coalification tracks of main maceral groups, (Teichmuller, 1982)

Handbook is presented in Table 3.2.2.

According to established procedure (ICCP, 1963; Bustin et al., 1983; Stach et al, 1982; Ward, 1984) minimum band widths are 50 microns, and macerals which account for less than 5% by volume of a particle are disregarded. In practice, a twenty-point reticule is used to count macerals on the examined coal particle.

The association of macerals with mineral matter (20 to 60 % by volume) places a particle into the carbominerite category. When the coal particle is associated with clay minerals it is referred to as carbargillite, and when associated with pyrite, carbopyrite (Stach, 1982).

In many coal utilization processes maceral analysis is

not adequate to predict coal behavior. Microlithotype analysis provides more detailed information on the intimate association of macerals and intergrown minerals. Microlithotype analysis can be very effective in predicting the coal preparation characteristics, for example, grindability of coal (Hower et al., 1987), washability characteristics (Falcon and Falcon, 1983; Hower et al., 1986), and even selectivity in flotation (Cudmore et al., 1986). Another important application of microlithotype analysis is in characterization of coking coals (Brown et al.,1964; Rentel, 1987).

3.2.4 Lithotypes

Lithotypes are macroscopically recognizable bands of coals, and are categorized into four types: vitrain, clarain, durain, and fusain (ICCP, 1963). These four different types of coal are mainly recognized and distinguished from each other on the basis of their luster, texture, stratification and degree of homogeneity.

Lithotypes, as described by Stopes (1919), are preferred associations of macerals in humic coals. Vitrain is considered to be a natural concentrate of vitrinite; fusain is enriched in fusinite and inertinite; clarain has a variable composition of vitrinite, exinite and inertinite; durain is shown to be rich in liptinite and inertinite.

An alternative, simpler method for lithotype classification was developed in Australia (Diessel, 1965a). In this approach coal is regarded as a mixture of two basic components, bright and

dull. Lithotypes are defined according to the proportions of these two components (Bustin et al., 1983). The advantage of this method is that bands of coal are more easily recognized on the basis of varying proportions of two components. In terms of nomenclature, there is no compositional implication as in the ICCP-Stopes system. The comparison between both lithotype classifications is given in Table 3.2.3 (Bustin et al., 1983). A successful attempt was made to correlate microscopic composition of Diessel's lithotype classification by Lamberson and Bustin (1989) using Lower Cretaceous coals of British Columbia. The abundance of vitrinite macerals was shown to decrease from bright to duller lithotypes, while the opposite trend was observed for inertinite.

Stope's Classification	Australian Classification	Description
Vitrain	Bright coal	Subvitrous to vitrous lustre, or conchoidal fracture <10 % dull
Clarain	Banded bright	Bright coal, dull bands 10-40 % dull
	Banded coal	Bright and dull in equal proportions, 40-60 % dull
	Banded dull	Dull coal with some bright bands 10-40 % bright
Durain	Dull coal	Matt lustre, uneven fracture 10 % bright
Fusain	Fibrous coal	Satin lustre, friable

Table 3.2.3 Comparison of two lithotype classifications: Stope's and Australian, (Bustin et al., 1983).

Lithotypes are the petrographic components which are handled on a macroscopic scale. Many of the physical properties of coal have been frequently linked to the lithotype composition (Jeremic, 1980; Stach, 1982; Tsai, 1982; Hower, 1987 and 1988;). Lithotypes can be useful indicators not only of the original environment of coal formation but also of physical and chemical properties of coal.

The density of lithotypes varies quite significantly, with the vitrain having the lowest density, clarain intermediate and the fusain the highest. The porosity of lithotypes differs; in vitrain micropores are predominant, while in fusain mesopores predominate. Mechanical properties such as strength, hardness, and friability are strongly dependant on lithotype composition (Hower et al., 1986; Falcon, and Falcon, 1987; Hower, 1988; Hower and Linberry, 1988; Hower et al., 1990). Apart from physical properties, lithotypes have been shown to have different carbonization responses, due to their distinct plastic characteristics. Coking tests show that stronger cokes were produced from the brighter lithotypes (Gray et al., 1976; Burstlein in Hower et al., 1986).

CHAPTER 4

HYDROPHOBICITY AND FLOATABILITY OF COAL

4.1 Hydrophobic character of coal

Coal is considered to be naturally hydrophobic. This is a result of its hydrocarbon structure. It is the surface of coal which controls the mechanism of water attraction, and therefore the hydrophilic-hydrophobic character of coal. The surface properties of coal may be quite different than the properties of the bulk solid, as in the case of surface oxidation, or selective adsorption.

According to Gaudin (1957), hydrophobicity is only possible for solids in which fracture or cleavage occurs without rupture of interatomic bonds other than residual ones. Whenever rupture occurs in ionic linkages it leads to the hydroxylation or ionization of the surface, and creation of the hydrophilic surface. The thermodynamic condition for hydrophilicity, as discussed in section 2.2.1, implies that the main forces of water attraction to the solid surface are hydrogen bonding (through the surface hydroxyl groups), or the forces arising from the electrical charge of the interface.

In coal, oxygen functional groups such as hydroxyl, carbonyl or carboxyl occur either as a result of oxidation or as a part of the coal structure. The amount and type of these groups

change with the rank of coal, as do many other properties. The oxygen functional groups content, and their type, were frequently used to stress the change of coal surface properties with rank (Ihnatowicz, 1952; Blom, 1957). The hydrophobicity of coal was shown to be a function of rank. For a given rank of coal and controlled level of oxidation, hydrophobicity is primarily dependant on the surface heterogeneity arising from the petrographic composition, as the macerals are known to have varying surface properties.

The important factor in estimation of hydrophobicity of coal is the associated mineral matter. Since coal minerals are hydrophilic, intimate association of mineral matter has a strong effect on the hydrophobicity of coal particles.

4.1.1 Rank

The contact angle has long been the only measure of hydrophobicity of coal. The earliest results on contact angle of different rank of coals were reported by Brady and Gauger (1940) and Elyashevitch (1941). Their results showed that bituminous coals had a higher contact angle than either anthracite or lignite.

In subsequent studies by Horsley and Smith (1951), Sun (1954) very similar results were obtained. The most recent work by Aplan (1983), Gutierrez-Rodriguez et al. (1984), Onlin and Aplan (1984) related hydrophobicity of coal to various rank parameters, such as percent of ultimate carbon content, fixed carbon, oxygen,

OH/carbon ratio, and vitrinite reflectance.

Contact angles are usually determined using either: captive bubble or sessile drop method. In the former technique an air bubble is deposited on the coal surface in solution, whereas in the latter the drop of water is placed on the dry coal surface. In both methods contact angle is measured through the water phase; the higher the contact angle, the more hydrophobic the surface. The results of contact angle values for coals of different ranks are depicted in Figure 4.1.1 after Aplan (1984), Onlin and Aplan (1987) and Arnold and Aplan (1988). According to Onlin and Aplan (1987) and Arnold and Aplan (1988), the captive bubble technique can only characterize the hydrophobicity of higher rank coals, that is when the carbon content is higher than 80%, while the sessile drop technique may be used to assess hydrophobicity over the whole range of coal ranks (Parekh and Aplan, 1978; Guttierez-Rodriguez et al., 1984). The sessile drop results, however, show very significant scatter. It was concluded (Arnold and Aplan, 1988) that a great deal of this scatter is caused by differences in the origin of the studied coals, and further that scatter was reduced when vitrinite reflectance was used as the rank parameter (Figure 4.1.2).

Coal is porous and depending on whether the pores are filled with air or water, the contact angle may display quite different values (Keller, 1987; He and Laskowski, 1991). According to this theory, for lower rank or less hydrophobic coals, the pores are filled with water and therefore the contact angle measured on such a surface may assume very small values, (this is especially true for captive bubble technique).

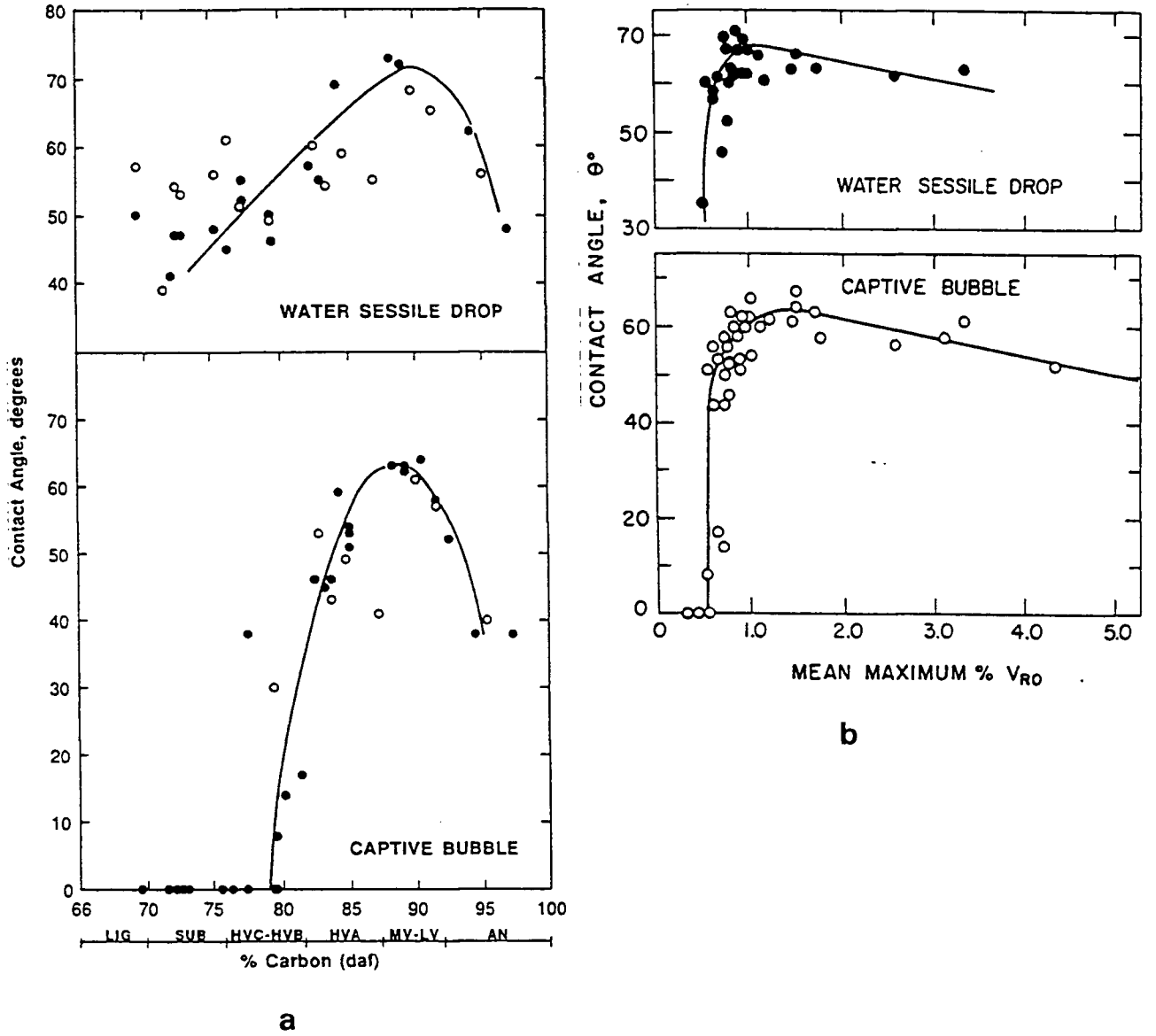

Figure 4.1.1 Contact angle for coals of different ranks measured by captive bubble and sessile drop technique; (a) contact angles versus % Carbon, (b) contact angles versus vitrinite reflectance.

Over the years other indirect techniques of characterizing the hydrophobicity have been successfully applied. These include: rate of disappearance of coal particles deposited on the surfactant solutions (Garshva et al., 1978; Glanville and Wightman; 1980), a measure of immersion time for particles to sink into the liquids of different surface tensions (Fuerstenau, et al., 1986; Fuerstenau, et al., 1987), induction time (time required for particle to attach to an air bubble), (Ye and Miller, 1988). They all have shown a correlation of hydrophobicity of coal to rank, in the same manner as the contact angle.

A decreased hydrophobicity in low rank coals is mainly due to the presence of a high amount of oxygen functional groups in the coal structure. Through those groups water is attracted to the coal surface (Laskowski, 1964; Fuerstenau et al., 1983). In the transition from lignite to higher rank coals (80% C), the coal structure loses a significant portion of the oxygen groups, and at the same time aromatic carbon is increased. The diagram presented by Ihnatowicz (1952), and by Blom (1957), shows the distribution of oxygen groups in coals of different ranks as shown in Figure 4.1.2. The decrease in hydrophobicity as the anthracite rank is reached is often related to its graphite-like structure, aromatic hydrocarbons being less hydrophobic than paraffinic hydrocarbons, (Keller, 1986), (Zismans critical surface tension values for graphite and aromatic hydrocarbons, are higher than for paraffin hydrocarbons indicating lower hydrophobicity).

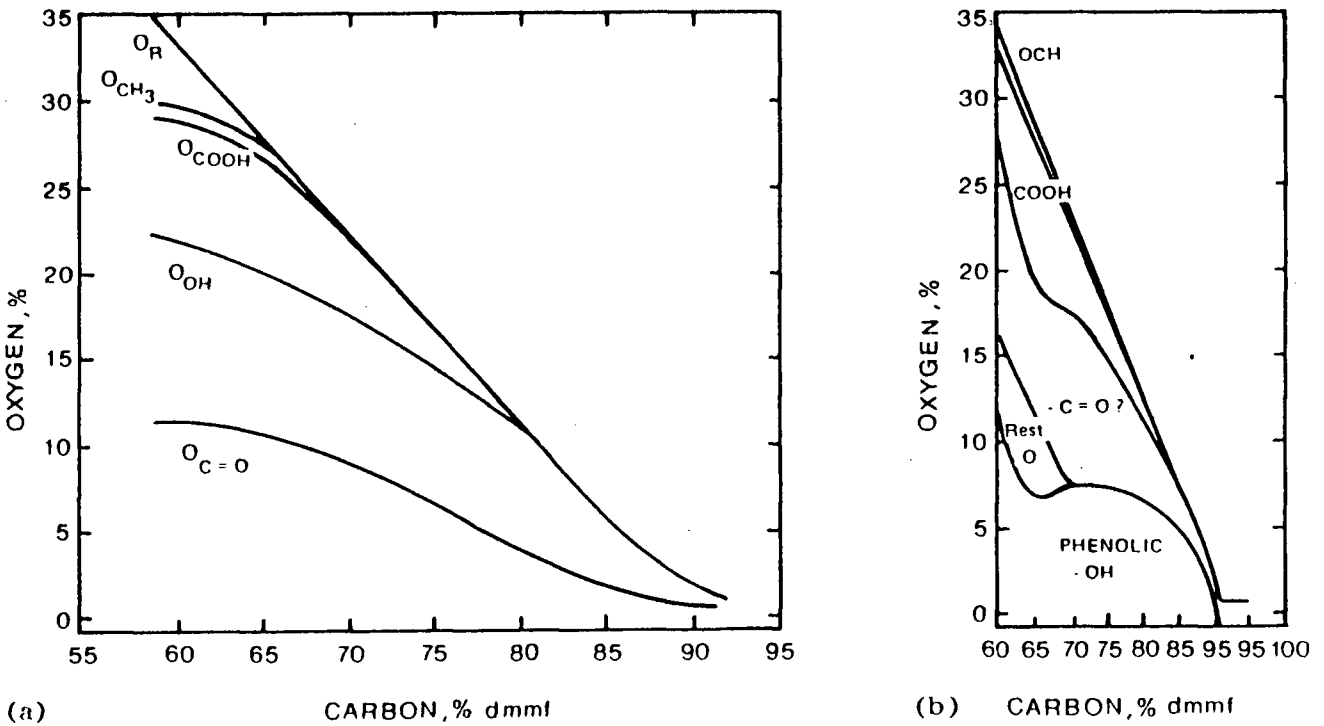

Figure 4.1.2 Distribution of Oxygen groups in coals of different ranks; (a) adapted from Ihnatowicz, (1952); (b) from Blom, (1957).

4.1.2 Oxidation

Oxidation is a chemical process leading to the alteration of many minerals during weathering (Gray and Lowenhaupt, 1989). The oxidation of coal can occur in-situ, during mining and processing, or in the stock-piles. Coal oxidation adversely affects many technological properties of coal. Coking quality and plastic properties of bituminous coals, flotation recovery, and calorific values are all significantly influenced, and, in many cases, some of these properties are lost, when coal is oxidized (Ignasiak et al., 1974; Gray et al., 1976; Berkowitz, 1979; Crelling et al., 1979; Mezularaar et al., 1987).

When coal is exposed to the atmosphere, adsorption of oxygen to the coal surface occurs which is followed by chemical reactions. As a result, oxygen functional groups, such as -OH, -CO, -COOH and -OCH3, are formed on the surface. The low-rank coals are more susceptible to oxidation than higher rank coals (Berkowitz, 1979; Meuzelaar et al., 1987), as their structure already possesses high amounts of oxygen functional groups, which in turn are sites for preferential oxygen adsorption. The higher rank coals are the least susceptible to oxidation.

The oxygen functional groups which are produced on the coal surface as a result of oxidation control coal wettability through the balance of hydrophobic/hydrophilic sites (Fuerstenau et al., 1986), and flotation kinetics by influencing the surface charge (Iskra and Laskowski, 1967; Wen, 1977; Fuerstenau et al.,

1983; Laskowski and Parfitt, 1989; Fuerstenau et al., 1988c). The presence of these polar groups leads to interaction with water molecules, which makes coals hydrophilic. Hydrophobicity of coal will therefore be significantly influenced by the degree of oxidation.

Numerous sophisticated methods and techniques have been employed to study oxidation of coal and its effect on technological behavior. Among these are pyrolysis, mass spectrometry, gas chromatography, thermogravimetry/mass spectroscopy, FTIR technique (Meuzelaar, 1987), along with simpler testing procedures such as chemical titrations of acidic groups (Schafer, 1970; Ignasiak and Ignasiak, 1970), Free Swelling Index, flotation response (Sun, 1954; Yarar and Leja, 1982), salt flotation method flotation of oxidized coals (Iskra and Laskowski, 1967), alkali solubility (Gray et al., 1976), electrostatic charge, petrographic examinations (Chandra, 1962; Marchioni, 1983) and many others (Gray et al., 1976; Gray and Lowenhaupt, 1980). Unfortunately some of these methods fail to detect oxidation on the surface of coal, as they can only measure the change in bulk properties.

The successful methods to test surface oxidation are those which involve direct measurement of hydrophobicity, or behavior of oxidized coal in related processes. Meaningful correlations were found between degree of surface oxidation and the value of contact angle (Horsley and Smith, 1951; Iskra and Laskowski, 1967), immersion time (Garshva et al., 1978; Widyani and Wightman, 1982; Fuerstenau et al., 1986), electrokinetic poten-

tials, and parameters related to the change in the critical surface of wetting and floatability (Fuerstenau et al., 1985; 1987a; Hornsby and Leja, 1980; Hornsby and Leja, 1983).

As natural oxidation proceeds, oxygen reacts with the coal surface and as a result it affects surface properties of coal. It has been shown that the aromatic coal structures are the most resistant to oxidation, because they are free of functional groups. The aliphatic hydrocarbons are more prone to the oxidation as they are characterized by high content of side functional groups. For the same reasons, it was concluded that vitrinite macerals are the most susceptible to oxidation, as compared to inertinite or liptinite macerals (Mackowsky, 1982; Klassen, 1966; Mazeluraar, 1987). Recently, a flotation technique was developed which involves ozone oxidation of coal macerals to selectively float the resin substances from coal (Miller and Ye, 1988). Due to the preferential oxidation of coal macerals, separation of resin from coal was possible to achieve. From a chemical point of view, the resin is considered to have similar composition to some of the liptinite macerals (e.g. resinite), hence this may indicate some resistance to oxidation of liptinite macerals.

4.1.3 Electrical charge

The electrokinetic behavior of coal is difficult to delineate due to coal complex heterogeneity, and its tendency to alter during the exposure to atmosphere (Fuerstenau et al., 1988c;

Laskowski and Parfitt, 1989).

A various heteroatoms and functional groups altogether with mineral matter consist surface of coal. These sites display different electrochemical characteristics, and contribute to the surface charge of individual particles.

The minerals associated with coal can have very different electrokinetic characteristics. For example, aluminosilicates are known to have negative charge at the basal planes and their edges are characterized by isoelectric point (i.e.p) at pH = 9.1, (Al_2O_3). Quartz is negatively charged over entire range of pH, while the carbonates have their i.e.p in the slightly alkaline pH (Laskowski, 1987).

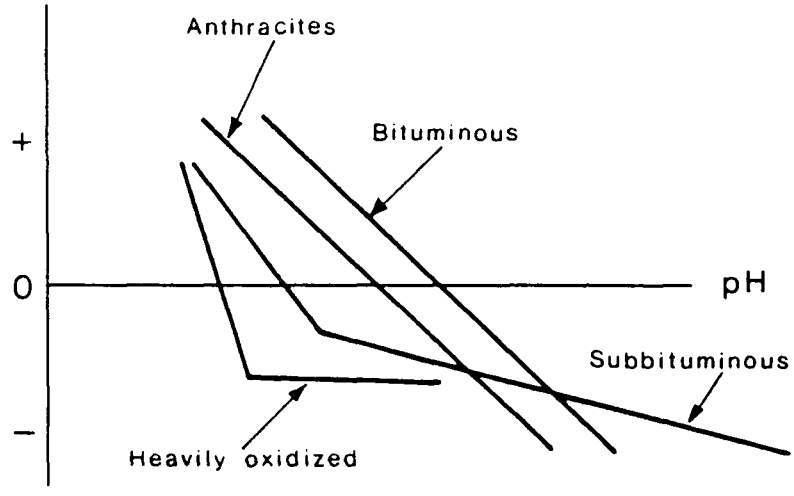

Figure 4.1.3 Generalized zeta-potential versus Ph diagram for coals of various ranks, (Laskowski and Parfitt, 1989).

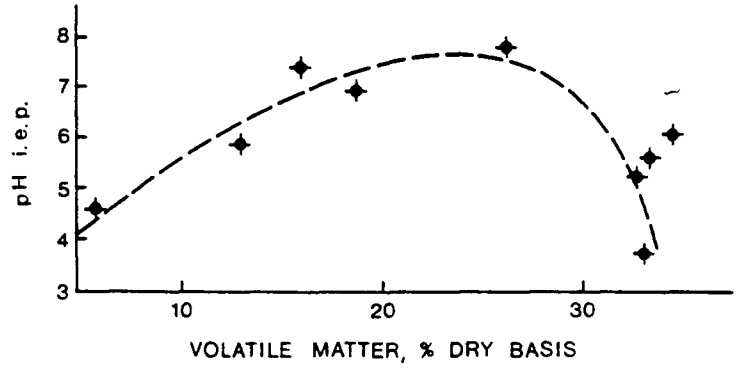

Figure 4.1.4 Isoelectric points for coals of varying rank, (Laskowski, 1968).

Type and varying amounts of mineral matter were shown to significantly alter electrokinetic properties of coal (Fuerstenau, 1988; Laskowski, 1989). A high content of mineral matter was found to change the electrokinetic behavior of coal to resemble that of associated minerals, and usually was reported to move i.e.p towards lower pH values (Fuerstenau et al. 1988c).

The electric charge on coal surface is developed by dissociation of functional groups, such as -COOH and -OH or by adsorption of ions from the solution (Fuerstenau, 1988; Laskowski, 1989). For the carboxylic and phenolic groups, the sign of the charge on the coal surface depends on the pH of the solution, and H+ and OH- are potential determining ions (Campbell and Sun, 1970).

The isoelectric points (i.e.p) for vitrains from anthracite and bituminous coals were found to lie between 4.5 and

7 pH, while for lignite at 2.3 pH. The maximum i.e.p values were found between 6 and 7 for low volatile bituminous coals (Laskowski, 1968; Campbell and Sun, 1970). The data reported by Sobieraj and Myrcha (Sobieraj and Myrcha, 1980), showed that, the i.e.p values for low rank and oxidized coals were moved towards more acidic pH ranges. A generalized zeta potential versus pH values diagram for various ranks of coal and oxidized coal is shown in Figure 4.1.3. The i.e.p values were also found to change with rank, as described by Laskowski (Laskowski, 1968; Laskowski and Parfitt, 1989) and shown in Figure 4.1.4.

A good correlation was found between maximum flotation rate and isoelectric point for coals of different ranks (Laskowski and Lupa, 1966; Fuerstenau et al., 1983). This maximum floatability and hydrophobicity usually coincides with the neutral pH range for the unoxidized coals.

4.1.4 Petrographic composition

Unfortunately, very little is known about the hydrophobicity of pure macerals, mainly because of the difficulty in obtaining pure maceral concentrates. The only study of surface properties of pure macerals was recently reported by Chol-yoo (1988). The macerals were obtained by the density gradient separation technique, as introduced by Dyrkacz (Dyrkacz and Bloomquist, 1981). In this study on adsorption of surfactants on coal macerals, it was found that the change in the surface

properties of inertinite with rank is significantly less dramatic than for vitrinite and liptinite.

A comprehensive study of the structure of macerals (Crelling, 1979; Winans and Crelling, 1984; Winans et al., 1984) showed that the inertinite have the most aromatic structure (lowest H/C ratio), with vitrinite being next but with much higher contents of polar groups (oxygen functional groups). Liptinite contains much higher amounts of aliphatic hydrocarbons (paraffinic) in its structure. Based on this information one may expect that liptinite will be the most hydrophobic maceral, since aliphatic hydrocarbons are more hydrophobic than aromatic hydrocarbons, vitrinite less so, and inertinite least so. In most of the humic coals, especially at the rank where they display highest hydrophobicity (hvb-mvb), liptinite content is usually very small, and the vitrinite maceral is the most abundant. Therefore, the surface properties of liptinite are not so distinct.

Most of the studies assessing hydrophobicity of petrographic components were usually limited to lithotype samples, representing natural concentrates of macerals. The very first contact angle measurements were performed on lithotypes (Horsley and Smith, 1951), followed by many other researchers (Sun, 1954; Klassen, 1966). Horsley and Smith (1951) showed that the natural contact angles of different lithotypes differed by nearly 50 degrees, with vitrain being the most hydrophobic, followed by clarain, durain and fusain. Sun (1954) suggested that the order of hydrophobicity, based on the calculation of surface properties from

the elemental analyses (floatability index), decreases as follows:

clarain > vitrain > fusain > durain

Frequent discrepancies in the assessment of hydrophobicity of coal lithotypes are attributed to fundamental differences between coals, as well as variations in maceral and mineral matter composition of lithotypes from one coal to another.

Arnold and Aplan (1989) determined hydrophobicity of macerals from various ranks of coal by measuring the contact angle on microscopically identified macerals. They concluded that the liptinite is characterized by the highest hydrophobicity among all macerals, with contact angles as high as 114-132^{o} for resinite from hvb coal, and approximately 90^{o} for sporinite (hvA). Vitrinite is somewhat less hydrophobic than liptinite and appears to be significantly more hydrophobic than fusinite. The contact angle of [1]pseudovitrinite is generally slightly higher than for the corresponding vitrinite, implying higher hydrophobicity of this maceral.

4.1.5 Mineral matter

The minerals that are associated with coal are, as discussed in section 3.1.3, naturally hydrophilic. Consequently, any inclusions of mineral matter on the coal surface will have an

---

[1] Pseudovitrinite is a type of vitrinite which usually has higher reflectance than corresponding vitrinites. It appears as very smooth with characteristics slits in the structure, and occurs with fewer associations with other macerals. The term pseudovitrinite was introduced by Benedict (1968); this maceral was found to be less reactive in the coking process.

influence on its hydrophobicity.

Depending on the type of mineral matter and its form of association within a particular coal, its texture and liberation characteristics differ. Syngenetic minerals are usually part of the coal particles, whereas epigenetic minerals are the easiest to separate from macerals. In terms of hydrophobicity, the syngenetic mineral matter will influence the surface properties of coal particles the most. Epigenetic minerals, which are typically concentrated along cleats, are usually liberated during breakage, and are not part of the coal particle surface.

Caution has to be used when correlating the contact angle results with the floatability of coal particles, since the surface examined might not necessarily be the one which would be responsible for particle behavior in the flotation process. Apart from fracture planes and pores, mineral matter inclusions will greatly influence the final value of the contact angle. It was observed by Gaudin (1957) that an increase in the ash content of coal resulted in reduction of contact angle, and hence, in the hydrophobicity. Dramatic change in the surface properties of graphite was noted with an increase in ash content (Parekh and Aplan 1978).

In the work of Bustamante and Warren (1983) some conclusions were reached as to the direct influence of mineral matter content and flotation recovery of coal grains. In their study, relatively small amounts of mineral matter in the coal grains depressed the flotation of low rank coal, but when the coal

was of higher rank relatively large proportions of mineral matter had little effect on floatability. The low-rank coal in their study was hvb, and was regarded as being less hydrophobic, whereas the high rank coal was mvb, and was considered to be highly hydrophobic.

The very fact that large amounts of mineral matter are usually associated with fusinite has often been used to explain very low hydrophobicity of this maceral (Brown, 1962; Klassen, 1966; Bujnowska, 1985a).

4.2 Floatability of coal

4.2.1. Floatability of coal as a function of rank

An inherent hydrophobicity of coal is the prerequisite condition for natural floatability of coal. For this reason the contact angle is very frequently used to assess floatability of coals (Brown, 1962; Sun, 1954; Horsley and Smith, 1951; Aplan, 1983). High contact angles are always associated with high floatability.

It has long been known that coal floatability changes with rank. Many hypotheses have been put forward to explain this phenomenon. Taggart (1939 in Sun, 1954a) suggested that the difference between floatability of bituminous coal and anthracite was due to the variation in the hydrogen-carbon ratio. Wilkins (1947 in Sun, 1954a) implied that floatability increases with

carbon content, that is with the rank. The theory based on the change in chemical structure of coals with the rank, and taking into account the influence of oxygen functional groups on overall hydrophobicity of coal was proposed by Klassen (1953). In 1954 Sun developed the surface component theory, where he used an empirical formula to correlate floatability with ultimate analysis of coal. According to this theory, high carbon and hydrogen contents are responsible for high hydrophobicity, and therefore high floatability, whereas oxygen, nitrogen and water contribute to a hydrophilic character. Based on his calculations of floatability indices, medium or low-volatile bituminous coals contain more floatable components than anthracite. This was shown to be in a very good agreement with the minimum amount of fuel oil used as a collector for flotation of medium and low-volatile bituminous coals (Brown, 1962; Klassen, 1966, Aplan, 1989). The strongly hydrophobic coals may even be floated with a frother alone. In practice, up to 0.5 kg/tone of fuel oil is added to the coal flotation. The quantity of collector increases for lower rank coals. Subbituminous coals require not only more collector for flotation but also right combination of an oily collector and a frother (Klassen, 1966).

4.2.2. Floatability of lithotypes

The flotation response of coal lithotypes was usually observed as variations in composition of concentrates from different points of the flotation circuit. The first results on

lithotype flotation on commercial scale were obtained in 1954 and reported by Klassen (1966). He showed explicitly that vitrain had higher flotation rates. Almost all vitrain was recovered in the very first flotation cells, while only half of the fusain was recovered in the same cells. The bulk of the clarain and durain was recovered in the middle cells.

A number of studies into the floatability of lithotypes on the laboratory scale were reported by Horsley and Smith (1951), and Sun (1954a). In one study (Horsley and Smith, 1951) an order of decreasing floatability was found as follows: vitrain > clarain > durain > fusain. According to Sun (1954a), the order of floatability was established in decreasing order as clarain > vitrain > fusain > durain. In both cases the order of floatability was in very good agreement with the contact angle values for lithotypes. The discrepancies between results may be due to the varying amount of mineral matter content in lithotypes or most probably origin of coals and therefore variation in macroscopic appearance of lithotypes.

The selective flotation of coal petrographic components may significantly improve the quality of coal for coking process. A number of flotation studies in selective flotation of lithotypes were summarized by Klassen (1966), and dated as early as 1922. It was observed that there is certain selectivity in flotation when different collectors are used. For example, light oils were more effective in fusain flotation, while cresol in flotation of vitrain and durain (Majer and Cukierman, 1934). Other studies (Barysz-

nikow, 1940) confirmed that phenol promotes flotation of bright (vitrain) components of coal, and then was concluded (Deminowa, 1957) that in flotation without collectors vitrain has the highest floatability, while fusain the lowest. The salt flotation (2% NaCl) was shown to boost flotation of vitrain and somehow depress flotation of fusain. On the other hand, pine oil in salt flotation induced floatability of fusain and durain. Chapman (1922) claimed to separate durain from vitrain and clarain with the use of phenol and kerosene as the collectors. In his study, contrary to other results obtained later on, phenol promoted flotation of durain and kerosene aided recovery of clarain and vitrain.

Very interesting results were obtained on the floatability of low rank lithotypes by Roznowa (1963). She showed that in flotation of low rank coals only fusain is characterized by natural floatability. The higher floatability of fusain as compared to vitrain was attributed to the higher degree of aromatization of the fusinite maceral (fusain being a natural concentrate of fusinite) at this rank. Vitrinite structure is characterized by very high content of hydrophilic oxygen functional groups, rendering vitrain (natural concentrate of vitrinite) less floatable.

The layout for selective flotation of lithotypes was proposed and tested on industrial scale (Roznowa, 1963). With the careful selection of flotation reagents and flotation conditions three different products were obtained: low-ash vitrain concentrate, low-ash and high-ash fusain concentrates.

A comprehensive study on selectivity of collectors in flotation of lithotypes was carried out by Kroger and Bade (1961). They showed that there is selectivity in adsorption of different collectors onto the different lithotypes as a result of their surface properties. Vitrain was characterized by the highest hydrophobicity in high to medium-volatile coals and the best interaction with collecting reagents.

4.2.3 Floatability of macerals

Brown (1962) in his review of froth flotation suggested that distinctions between the floatability of the major maceral groups can be made. Since that time, very limited research was done on floatability of different macerals. The only coals which received adequate attention were the medium and low volatile bituminous coals. As a result, vitrinite macerals were identified as the most floatable for all rank of coals (Brown, 1962; Klassen, 1966; Hower, 1984).

In the more recent study by Sarkar (1984), selectivity of coal macerals during flotation and oil agglomeration was examined. The flotation tests were carried out with the use of standard flotation reagents (diesel oil as collector and pine oil as a frother) in the commercial flotation cell.

From the microscopic analysis it was concluded that vitrinite has superior response to flotation over other macerals.

Vitrinite was found to be selectively concentrated in the clean coal flotation products. The clean coal concentrates, collected at different time intervals during flotation, revealed that free vitrinite grains responded in the initial stage, while other grains were collected at a later stage of flotation. Fusinite was shown to be significantly less amenable to flotation. This is in a very good agreement with the earlier studies on the medium-volatile bituminous coals.

A somewhat controversial results on floatability of coal macerals of different ranks were obtained by Bennett et al., (1983). According to this study, coal particles of varying microlithotype composition; vitrinite, clarite, vitrinertite or trimacerite, with no visible mineral matter had similar floatabilities when recovered by batch flotation in the presence of frother. Inertinite particles were found to be a slower floating than grains of other macerals group, regardless of rank of coal.

The most recent and probably the most comprehensive study on floatability of petrographic components of low rank coals was conducted by Bujnowska (1985b). In this study various reagents were used to promote floatability of different macerals, which are otherwise nonfloatable. The reagents were chosen in such a way that they promoted the flotation of one maceral at a time. The mechanisms of interaction between the reagents and the surface of coal was explained on the basis of different surface properties of macerals.

In subbituminous coal, inertinite (mainly fusinite) was

shown to be more hydrophobic than other macerals. The chemical structure of fusinite in this rank is considered to have small amounts of side groups (alicyclic and aliphatic structures, bridges, functional groups) as compared to the vitrinite of the same rank. Fusinite aromatic structure is a result of its high degree of aromatization and condensation in the early stages of coalification (van Krevelen, 1961; Stach et al., 1982).

The high content of oxygen functional groups in the structure of vitrinite of the lower rank coal has a decisive role in decreasing its floatability. Low floatability of liptinite (exinite) can be explained by its less aromatic and more disordered structure, with low content of functional groups. Relatively small content of oxygen groups in liptinite macerals may indicate a less hydrophilic surface. In the case of nonfloatable low rank coal, however, the floatability has to be induced by adsorption of chemical reagents (usually polar), and this means, in the case of liptinite, weaker interaction sites for the flotation reagents. As a result floatability of liptinite in lower rank coals was shown to be decreased (Bujnowska, 1985b). For vitrinite, the large content of functional groups was shown to facilitate adsorption of polar reagents, but not enough to increase hydrophobicity of vitrinite to exceed that of fusinite.

The floatability of macerals of subbituminous coal were found to be in the following order (Bujnowska, 1985b):

inertinite > vitrinite > liptinite

more precisely:

fusinite > micrinite > vitrinite > liptinite

The floatability of petrographic components was shown to change with the rank, and for medium and high rank coals the following decreasing order was observed by several researchers (Brown, 1962; Klassen, 1966; Hower, 1984; Sarkar, 1984; Bujnowska, 1985a):

vitrinite > inertinite > liptinite

The structure of vitrinite changes with the rank, the content of aromatic hydrocarbons increases drastically with the substantial decrease in number of hydrophilic groups, whereas the structure of fusinite changes insignificantly throughout the coalification range. For this reason, floatability of vitrinite in high rank coals exceeds that of fusinite.

CHAPTER 5

OBJECTIVES AND SCOPE

The objective of this study was to investigate wettability and floatability of coal particles of different petrographic composition. Film flotation was used to evaluate wettability and a Partridge-Smith cell flotation was used to determine floatability of macerals and lithotypes.

The film flotation technique, as proposed by Fuerstenau (1985), utilizes concept of critical surface tension of wettability to assess hydrophobicity of an assembly of coal particles. In this test coal particles are separated into fractions according to their critical surface tension as defined by Zisman (1964). The flotation tests are carried out by placing coal particles on the surface of the solution. Aqueous methanol solutions are used to create different surface tensions. The cumulative wettability distribution of particles versus their critical surface tension of wetting is obtained.

In small-scale flotation tests, the concept of critical surface tension has been extended to the dynamic flotation tests (Hornsby and Leja, 1980; Hornsby, 1981; Hornsby and Leja, 1983). Since wettability and floatability are not necessarily synonymous, the term critical surface tension of floatability was proposed

(Hornsby, 1981). In flotation, the selective separation of two hydrophobic solids may occur even though they may have the same critical surface tension, γ_c, but different γ_{cf}, the critical surface tension of floatability. Cumulative floatability distribution of particles according to their critical surface tension of floatability was obtained from the small-scale flotation tests in methanol solutions.

Maceral concentrates obtained from density fractionation of medium-volatile coal, as well as hand-picked lithotypes of the same coal, were used for the film flotation and the small-scale flotation tests. Cumulative distributions of wettability and floatability for maceral concentrates and lithotypes were compared. Furthermore, microscopic analyses of the flotation products were performed in order to determine flotation response of coal grains of various petrographic composition in solutions of changing surface tensions.

The coal sample properties were characterized by proximate and ultimate analyses, petrographic examination and Free Swelling Index. The narrow size fraction of coal was used to minimize the effects of particle size on floatability. The size ---210+149 μm, (65x100 mesh, Tyler) was chosen following Hornsby (1981).

CHAPTER 6

MATERIALS - METHODS OF PREPARATION

6.1 Glassware

All glassware used for experiments was washed in detergent solution of Extran MN-1 (1g per 1 liter of water), then cleaned with acetone and in chromic acid solutions ($K_2Cr_2O_7$ / H_2SO_4) when necessary, and thoroughly rinsed in single distilled water.

6.2 Solutions

A single distilled water used in experimentation, was obtained from a Barnstead still\ distillation unit. Fresh distilled water was stored in large Pyrex glass containers.

The methanol solutions were prepared from Fisher Certified ACS grade methanol, Cat. No. A-412-4 UN 1230. Solutions of different surface tensions were prepared by pipetting the required volume of methanol into volumetric flasks with distilled water at room temperature (20 -/+ 3^{o} C). The surface tension of methanol solutions was measured by the DuNouy ring method. The measurements were carried out at 20 +/-2^{o} C. The mean experimental

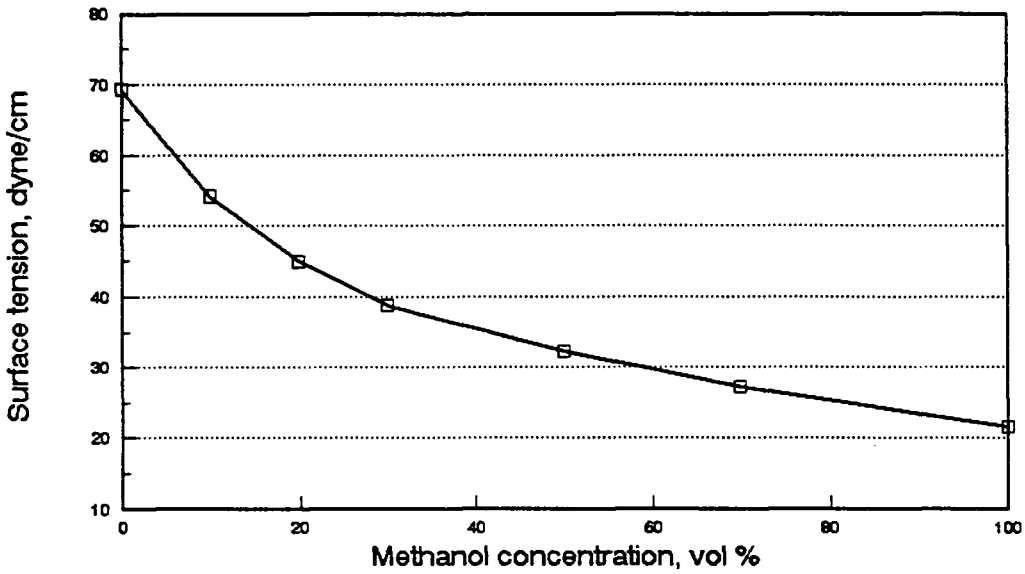

Figure 6.2.1 Surface tension of methanol solutions (temp. 20+/-2° C).

values of surface tensions are plotted in Figure 6.2.1 and Table B.1 The description of apparatus and procedure are given in Appendix B.

6.3 Coal Samples

6.3.1 Sample Description

The coal samples used in the study were from the mid Albian (Lower Cretaceous) Gates Formation from northeastern British Columbia. The main run-of-mine sample was obtained from Bullmoose Operating Corporation. According to the ASTM D 3888-66 (1972) this coal can be classified as medium volatile bituminous (Fixed Carbon, d.a.f. of the composite sample was 69.51%). Complete geological descriptions of Bullmoose seams are available from publications by Kalkreuth and Leckie (1989) and Drozd (1985). The reflectance (R_{omax}) of the seams varies from 1.14% in seam A, considered as the oldest, to 1.02% of Seam E, the youngest (Kalkreuth and Leckie, 1989).

Seam A lithotype samples were available thanks to Michelle Lamberson and Marc Bustin of Geological Sciences of the University of British Columbia. Lithotypes were collected as described by Lamberson (Lamberson et al., 1989) according to a modified Australian classification scheme as discussed in section 3.2.4. A minimum thickness of one centimeter was used to delineate a lithotype in the field. A representative sample of approximately

Table 6.3.1 The proximate and ultimate analyses of lithotypes. The results are presented on a dry and ash free basis.

Lithotype sample	B	BB	BD	BC	FIBROUS
Moisture, % . .	0.92	1.23	0.50	1.97	2.07
Ash, % . . .	4.20	5.23	6.12	8.00	3.46
Volatile Matter (d.a.f)	30.41	27.07	29.46	26.73	26.99
Fixed Carbon . . (d.a.f)	69.59	72.93	70.54	73.27	73.01
F.S.I . . .	8.5	6.5	4	1.5	0
Ultimate					
Total Sulphur . . (d.a.f)	.42	.55	.29	.37	.24
Carbon . . . (d.a.f)	87.37	88.56	87.57	86.3	87.06
Hydrogen . . . (d.a.f)	5.43	4.86	4.84	4.69	3.44
Nitrogen . . . (d.a.f)	1.04	1.20	1.18	1.12	.60
Oxygen . . . (diff)	5.74	4.84	6.12	7.52	8.66
Atomic Ratios					
H/C	.75	.66	.66	.65	.47
O/C	.004	.03	.05	.05	.06

B - bright; BB - banded bright; BD - banded dull; BC - banded coal
d.a.f - reported on dry ash free basis

50 grams (whenever available) was taken, sealed in plastic bags and stored in the refrigerator. The complete set of proximate and ultimate analyses of lithotypes is included in Table 6.3.1.

6.3.2 Sample preparation

6.3.2.1 Composite sample

A 100 kg barrel of run-of-mine Bullmoose seam A coal was spread out on the drying floor. The sample was dried for 48 hours to equilibrate with the laboratory atmosphere, and then reduced to 37.5 mm (1/2 inch) size. After crushing, the total sample was split according to the standard preparation procedure, ASTM D 2013-72 in order to obtain representative 12.5 kg sample. A further 1/8th of total sample was split by riffling into 6 lots of approximately 2 kg each. Then each sample was ground in a rod mill in water suspension at approximately 40 % solid concentration for 20 minutes. After grinding, samples were wet screened on vibrating screens. All size fractions were stored separately in sealed plastic bags. The -212+149 µm (65x100 mesh) size fraction was chosen for experimental work. This size fraction was found to be particularly high in ash content (28.34%). High density mineral particles were removed with the use of "gold-pan" washing technique. Both samples were used in experiments; high-ash composite sample was the initial -212+149 µm size fraction, whereas the "cleaned" sample was the low-ash composite. For ultimate and proximate as well as other bulk analyses 1/8th of the head sample was split again to obtain 125 grams of composite representative sample.

6.3.2.2 Density fractions

To obtain maceral concentrates from the composite sample, a float-and-sink technique was used. Macerals are known to have different densities. The density fractionation was carried out in aqueous $ZnCl_2$ solutions ($ZnCl_2$, Fisher Certified ACS, Cat. Z33-500). In each run 50 grams of -212+149 μm size fraction of composite sample was introduced into 1 liter separatory funnel with density solution. The lowest density solution was 1.3 g/cm^3 and it was subsequently increased by .5 g/cm^3 up to 1.5 g/cm^3. After the sink and float were completed, samples were washed with 20% methanol solution and with warm distilled water to remove traces of $ZnCl_2$. The fractions were dried and stored under N_2 in sealed glass containers.

6.3.2.3 Lithotypes

Lithotypes were received as fresh samples in sealed plastic bags. To obtain a -212+149 μm size fraction, each sample was reduced in pestle and mortar under nitrogen atmosphere, to 100% passing .50 mm (28 mesh) size and required size fraction was isolated. The lithotype samples were sealed under vacuum in tight plastic bags and stored in the refrigerator.

6.3.3 Proximate and Ultimate Analyses

The proximate analyses of the composite Bullmoose seam A, lithotype samples and density fractions were obtained in the analytical laboratory of the Department of Mining and Mineral Process Engineering in accordance with the ASTM procedures. The results are presented in Tables 6.3.1 and 6.3.2 on a dry and ash free basis. Total sulphur and FSI were also obtained in the same laboratory and reported with proximate analysis. The ultimate analyses of coal samples used in the experimental work were obtained from the Canadian Microanalytical Service Ltd., Delta,B.C. and Analytical Laboratory of the Alberta Research Council, Edmonton. The ultimate analysis data are the mean of the set of analyses performed in duplicate by Alberta Research Council and one set of analysis by Canadian Microanalytical Services, Delta.

Table 6.3.1 presents ultimate and proximate analyses of lithotypes. The proximate and ultimate analyses of the composite Bullmoose A, -212+149 μm size fraction (isolated from the composite) and the corresponding density fractions of the -212+149 μm size fraction are given in Table 6.3.2. The ultimate analyses are reported on dry, ash-free basis; the Oxygen is calculated by difference. A comparison of the analytical data of the composite sample with the analytical data for density fractions has not revealed any significant differences in elemental composition except for the heaviest density fraction, where carbon content is decreased. The elemental composition of lithotypes exhibits expected variation of C,H,N and O.

Density frac.	<1.30	1.30 -1.35	1.35 -1.40	1.40 -1.45	>1.50	Compo -site	Hi-ash	Lo-ash
Moisture, % . . .	0.65	0.48	0.48	0.72	0.51	0.75	0.61	0.55
Ash, %	3.01	7.87	14.89	20.89	62.74	35.25	28.34	16.03
Volatile Matter (d.a.f)	24.94	24.21	23.02	22.56	32.76	30.49	27.60	26.16
Fixed Carbon . (d.a.f)	75.06	75.79	76.98	77.44	67.39	69.51	72.40	73.84
F.S.I	9.0	4.0	3.0	1.5	1.0	4.5	6.0	8.0
Ultimate								
Total Sulphur . . (d.a.f)	0.45	0.55	0.50	0.51	1.07	0.70	0.78	0.56
Carbon . . . . (d.a.f)	87.51	86.94	88.00	88.96	85.74	83.89	82.54	89.29
Hydrogen . . . . (d.a.f)	5.05	4.76	4.71	4.86	5.58	4.80	5.12	5.11
Nitrogen . . . . (d.a.f)	1.25	1.10	1.06	1.05	1.28	1.14	1.04	1.22
Oxygen . . . . . (diff)	5.74	6.65	5.73	4.62	6.33	9.47	9.56	3.83
Atomic Ratios								
H/C	0.69	0.68	0.66	0.68	0.78	0.69	0.74	0.71
O/C	0.043	0.042	0.045	0.037	.042	0.043	0.080	0.090

d.a.f - reported on dry ash free basis

Table 6.3.2 The ultimate and proximate analyses results of the composite samples and the corresponding density fractions.

6.3.4 Petrographic Analyses

Petrographic analyses included three type of examinations: maceral analysis, R_o (random) reflectance measurement and grain type analyses. Additionally, microscopic examination of the mineral matter has been performed on the composite seam A sample.

Maceral analyses were performed on the representative composite sample of Bullmoose A seam, the -212+149 μm size fraction from the composite sample, density fractions obtained from gravity separations of the -212+149 μm composite sample, and the hand-picked lithotypes from the same seam.

Reflectance (R_o) was obtained on the vitrinite maceral of the Bullmoose A composite sample and hand-picked lithotypes. Reflectance data are included with the petrographic analyses of composite and lithotypes samples.

The examination of flotation products required a more efficient method to determine floatability of coal particles. Therefore grain type analyses were used instead of traditional maceral counting. Every counted particle has been described on the basis of its maceral composition, association with the mineral matter and observed oxidation. Detailed description of the grain analysis is given in section 7.3.2.

The maceral analyses of the Bullmoose seam A and -212+149 μm size fraction obtained from the same seam are reasonably similar in their petrographic composition, with the exception of the semifusinite content. The -212+149 μm size fraction has almost half

Table 6.3.3 Maceral analysis of the composite and the -212+149 μm size fraction from the composite sample.

Maceral	Composite Run 1	Composite Run 2	Composite Average	Composite (149-212μm)
Vitrinite	81	78	80	85
Liptinite	0	0	0	0
Semifusinite	9	11	10	6
Fusinite	4	4	4	3
Inertodetr	6	7	6	6
Total Inerts	19	22	20	21
R_o,mean	1.10			

of the semifusinite of the composite sample. Table 6.3.3 presents petrographic analyses of the total composite sample and size fraction (-212+149 μm) from the composite.

Petrographic examination of the density fractions showed significant distribution of macerals into different density ranges. It was found that vitrinite (volume percent on mineral-matter-free basis) was concentrated in the < 1.3 specific gravity fraction and that its volume reached a minimum in the range of 1.40-1.50 specific gravity, and progressively increased again in the fraction with density higher than 1.50. Similar changes in relative abundance of macerals from sink-and-float analysis were reported by Bustin (1982). Distribution of macerals in density fractions, as obtained from maceral point counting, is shown in Figure 6.3.1. All of the samples contained very small amounts of the recognizable

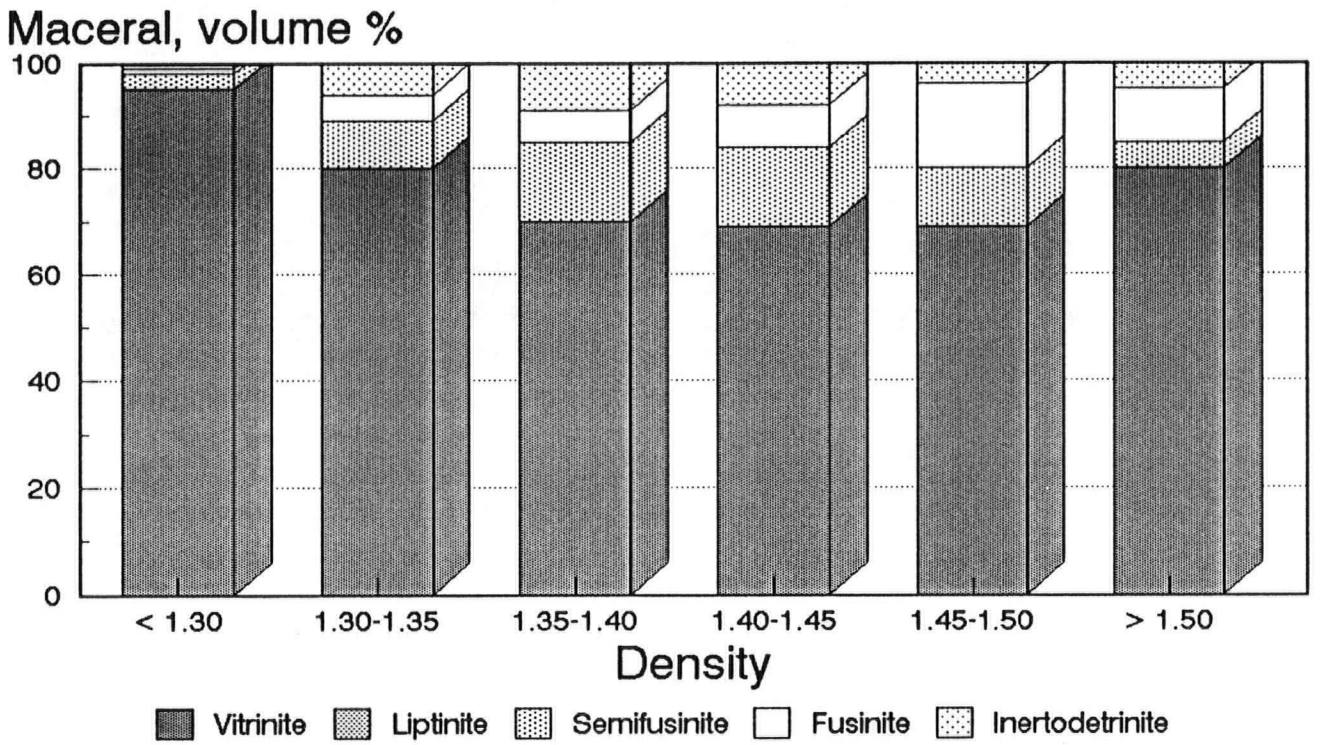

Figure 6.3.1 Distribution of macerals in the density fractions of +149-212 µm composite sample, (mineral matter-free-basis, obtained from point counting technique).

liptinite. The reasons for the low level of liptinite may be the difficulty in its recognition at higher rank, or a combination of original vegetation and peat chemistry (Lamberson, 1990).

From grain type analysis it is evident that mainly homogeneous clean vitrinite and pseudovitrinite particles occur in the lightest density fractions. A total of 63% of the free vitrinite particles and 24% of the pseudovitrinite are present in the 1.3 specific gravity fraction. Pseudovitrinites mostly occur as separate particles. Further, only 4% of the total accountable vitrinites are associated with the mineral matter. The number of free vitrinite particles decreases as the density increases. The minimum occurs at 1.45 specific gravity, where free vitrinite accounts for only 36% of the total volume of vitrinite. However, at the same time 100% of those vitrinite particles are in association with mineral matter. With the increase in density, the number of vitrinite particles in association with inertinites rapidly increases.

At 1.3 specific gravity, vitrinite in association with the inertinite accounts for only 13% by volume. In the next density fraction, 1.30-1.35, the number increases dramatically to 35% and then increases steadily until it reaches 63% in the 1.45-1.50 density range. In the heaviest, 1.50 specific gravity, the amount of vitrinite in association with inertinite sharply declines to 39%, and at the same time the amount of free vitrinite with mineral matter increases to 61 % of total vitrinite. It is noteworthy that the 1.30 specific gravity fraction is enriched in pseudovitrinite,

which may be of practical use when metallurgical coals are considered. The presence of pseudovitrinite leads to the deterioration of coke quality (Benedict et al., 1968). Distribution of grains in density fractions and their description in terms of association with mineral matter as well as the visible oxidation is presented in Figures 6.3.2 a and b, and is summarized in Table A.4 (Appendix A).

Lithotypes of Bullmoose seam A were described using the Australian classification scheme (Diessel, 1965; Marchioni, 1980). The examples of coal lithotypes found in Bullmoose coal seams are shown in Figure 6.3.3. Seam A, as described by Lamberson (1989) is primarily composed of banded coal and banded dull layers. Maceral analyses of the lithotypes (Lamberson, unpublished data) shows that there is a significant decrease in vitrinite, along with an increase in inertinite, from bright to duller lithotypes. There is also an increased abundance of pseudovitrinites in the bright lithotype. Among the inertinite maceral group, semifusinite is the most abundant. The maceral analyses of lithotypes of the Bullmoose seam A on the mineral-matter-free basis are given in Table A.1 (Appendix A) and illustrated in Figure 6.3.4.

The reflectance data for Bullmoose seam A lithotypes, as well as the composite sample, were again made available by Michelle Lamberson and Maria Mastalerz of the Department of Geological Sciences, University of British Columbia. The random reflectance ($R_{o)}$ of the vitrinite particles was determined by measuring reflectance of at least 50 relief-free vitrinite particles using

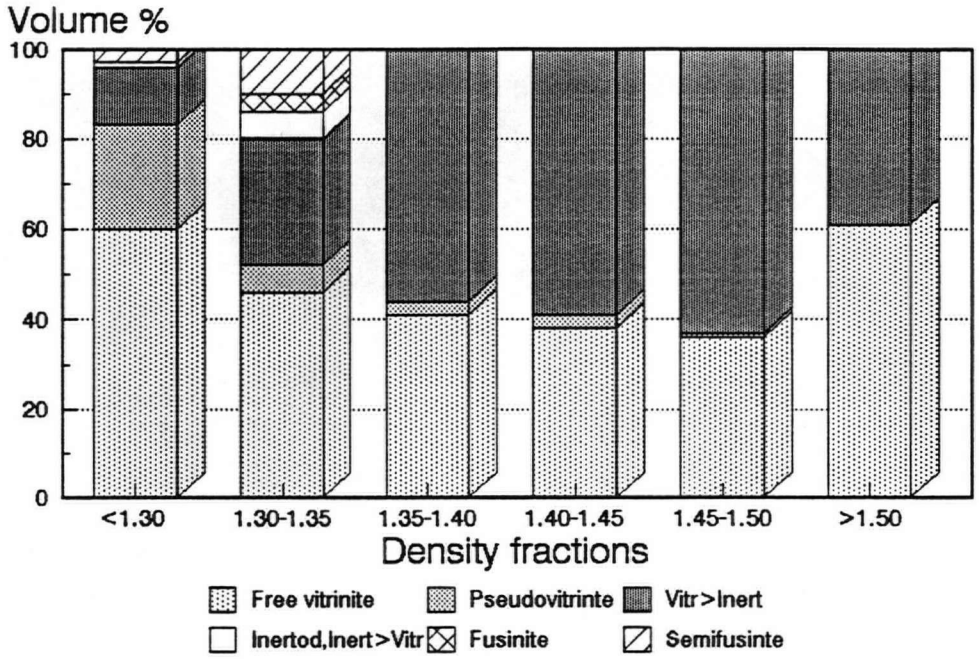

a

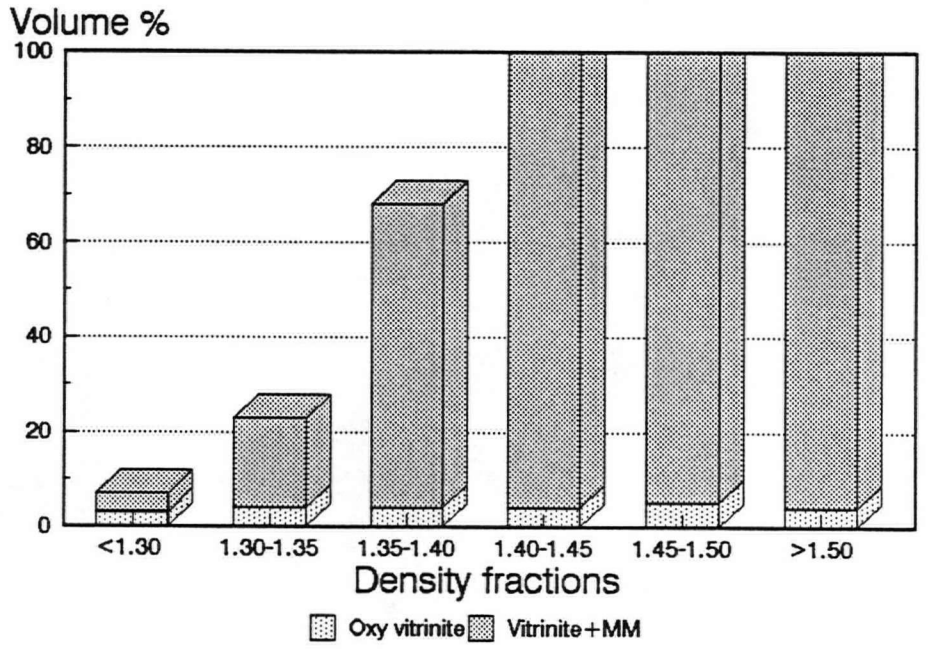

b

Figure 6.3.2 Distribution of coal grains in density fractions (a); distribution of grains associated with mineral matter and those with oxidized surface (b).

established techniques (ICCP, 1971). A Leitz Orthoplan reflecting light microscope equipped with a MPV2 photomultiplier was used for reflectance measurements. The mean random reflectance R_o, of lithotypes varied from 0.88 % for banded dull to 1.06% for bright, with the values of 1.0% and 1.04% for banded bright and banded coal, respectively. The composite sample was found to have the mean random reflectance R_o = 1.10%. The reflectance values for lithotypes are included in Table A.1 (Appendix A).

Figure 6.3.3 Examples of coal lithotypes found in Bullmoose coal seams, (Lamberson, 1989). A - dull coal; B - banded dull; C - banded coal; D - banded bright; E - bright; F - fibrous; G,H - sheared.

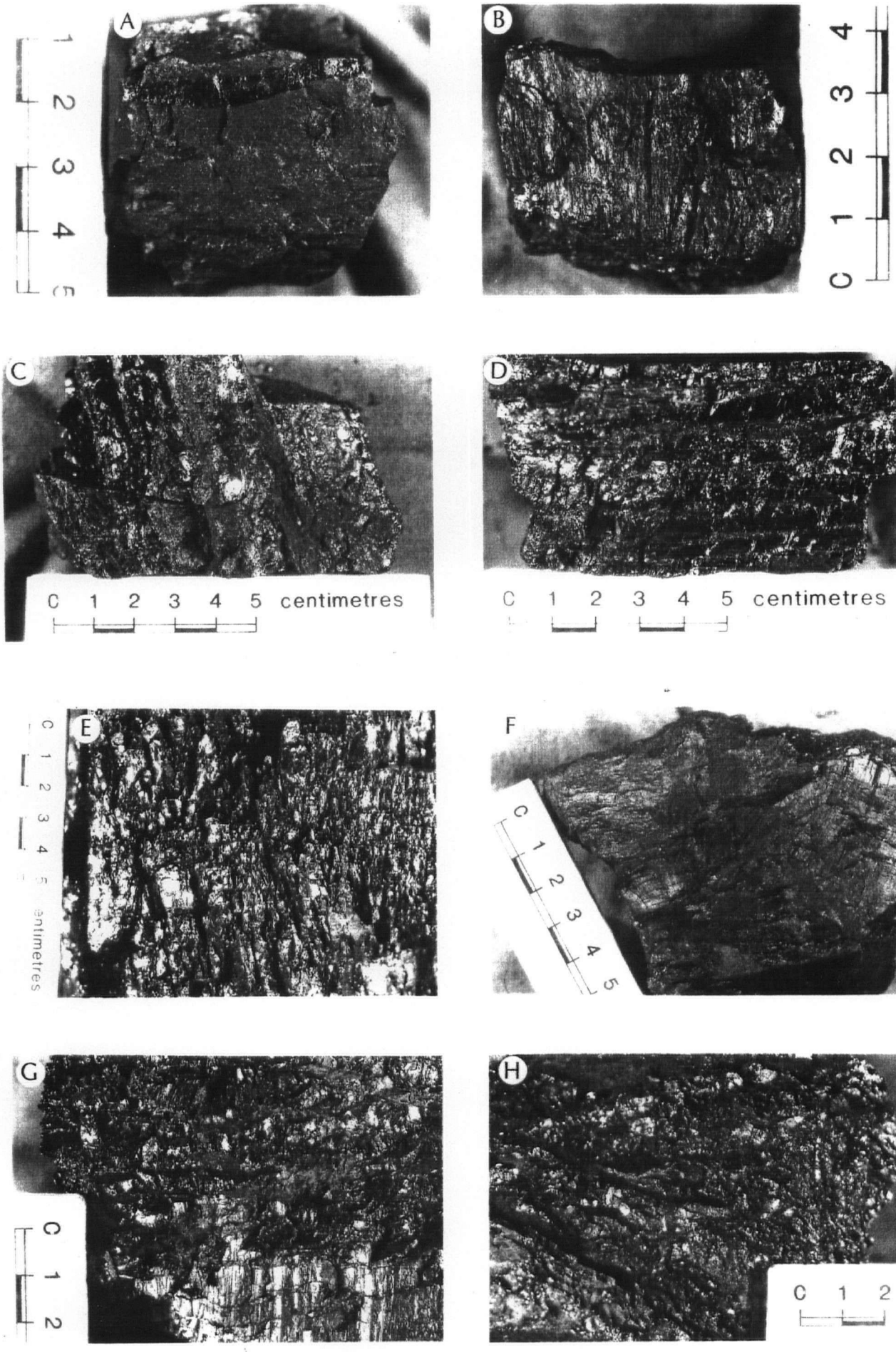
A
B
C
D
E
F
G
H
C 1 2 3 4 5 centimetres

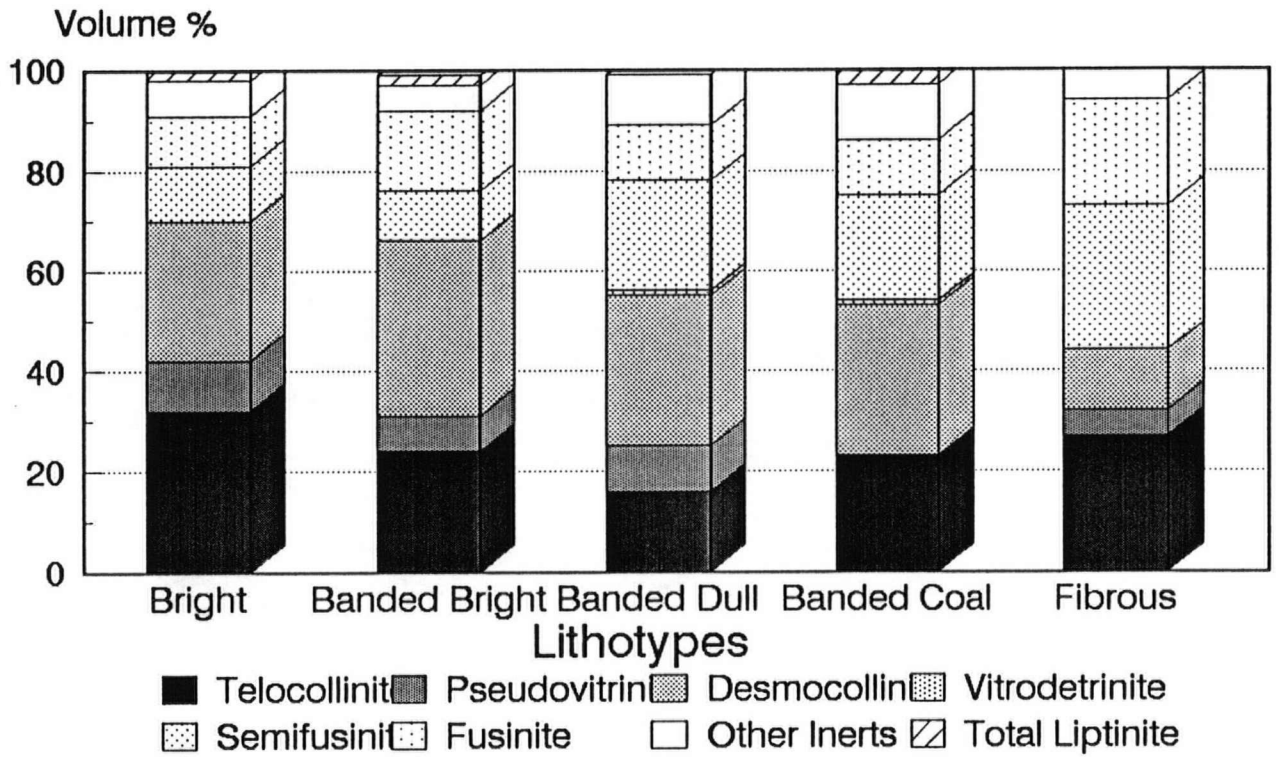

Figure 6.3.4 Maceral analyses of lithotypes of Bullmoose seam A. (mineral-free-basis, obtained from point counting technique)

Figure 6.3.5 Mineral matter present in composite sample (a) massive clay on the vitrinite particle; (b) small quartz grains in vitrinite; (c) clay filling the cracks; (d) clays intergrown with the vitrinite.

(a)

(b)

(c)

(d)

Microscopic examination of the mineral matter in the composite sample of the Bullmoose seam A revealed an abundance of clay-type minerals and relatively small amounts of quartz. The clays were mainly in two forms: as finely dispersed inclusions in coal particles, or as clay bands. The fine inclusions were mostly confined to the vitrinite or in the cavities of fusinite. Photographs of the mineral matter in composite sample are included in Figure 6.3.5.

CHAPTER 7

METHODS - EXPERIMENTAL PROCEDURES

7.1 Film Flotation Tests

A sample of 0.2 to 0.3 gram of coal was placed on the surface of a liquid to form monolayer of particles. These tests were carried out in small 150 ml separatory funnels. The funnels were used instead of shallow evaporating dishes as recommended in original film flotation procedure (Fuerstenau et al.1985). Initial tests were carried out following the above procedure, but since it was difficult to collect floating material and to obtain reproducible results, separatory funnels were chosen to carry out the tests.

For each complete run, six different solutions of decreasing surface tension were prepared and transferred using burette, into the separatory funnels. The highest surface tension corresponded to the 2% by volume of methanol in distilled water, and the lowest to the 30% by volume. After a coal sample was placed onto the surface of the solution two minutes was allowed for the immersion. There was no significant change in amount of floating material after prolonged immersion time. Two minutes time was the shortest immersion time for the amount of coal used. The coal which sank was removed from the funnel by opening the three way stopcock, and collected in the evaporating dish with a minimum of flotation

Figure 7.1.1 Film flotation set-up. (a) seaparatory funnels used for the flotation procedure; (b) film flotation test with the methanol solutions, increasing methanol concentration from left to right.

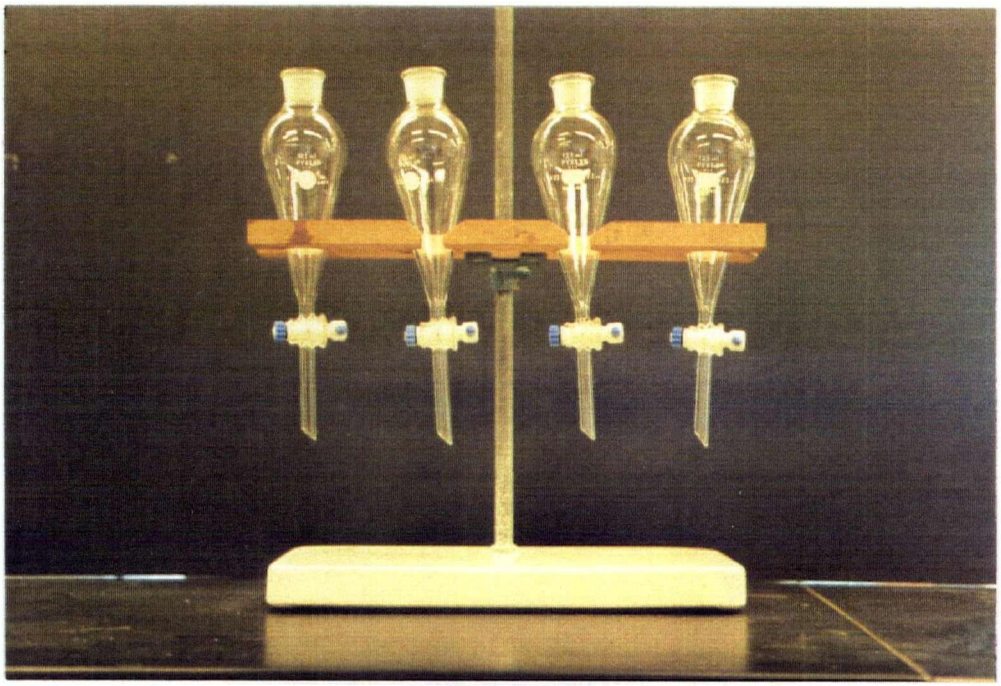

(a)

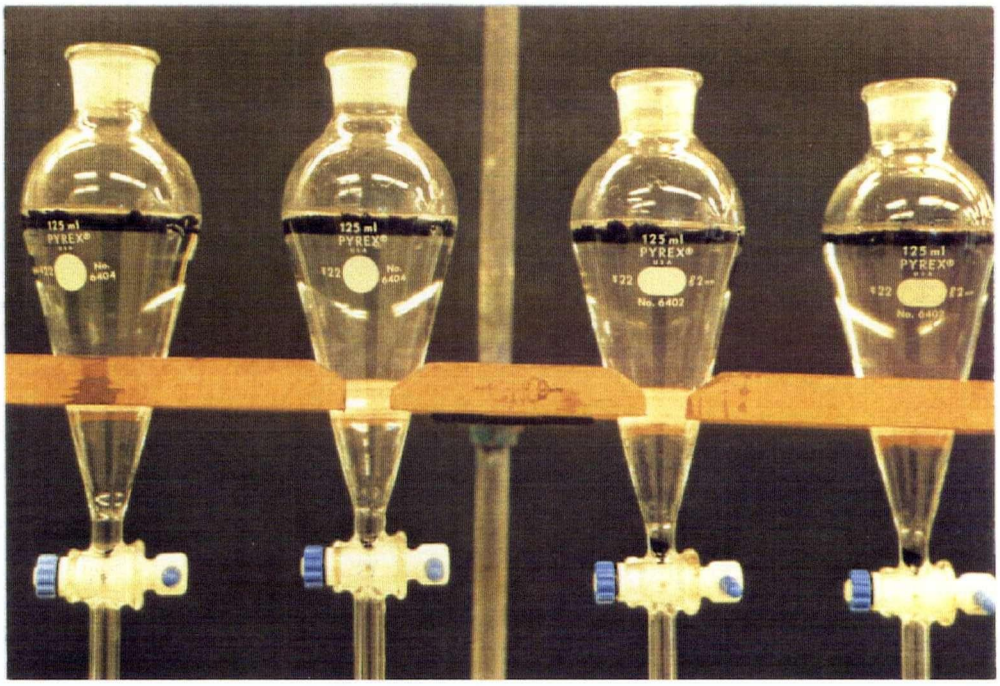

(b)

solution. The floating material was recovered by vacuum filtration in a Millipore filtration unit. The floats and rejects from film flotation tests were dried in the oven at about 105° C, cooled and equilibrated with laboratory atmosphere before they were weighed. Figure 7.1.1 shows the film flotation set-up.

7.2 Small-Scale Flotation Tests

7.2.1 Apparatus

The small-scale flotation experiments were carried out in a plexiglass Partridge and Smith flotation cell usually referred to as P/S cell (Partridge and Smith, 1971). The dimensions of the central flotation column were as follows: diameter, 30 mm; height 200 mm. The collection chamber was 60 mm in diameter, 125 mm in height and the central column projected about 42 mm into it. The total height of the flotation column was 335 mm, and the volume was about 950 ml. The plexiglass P/S flotation cell is sketched in Figure 7.2.1.

The design of the column was such that hydrophobic minerals (or in this case, hydrophobic coal particles), after being conditioned with the flotation solution and gas bubbles by the impeller, were brought to the top of the central column. When the particles reached the top of the column they were collected in the collection chamber. The central column was long enough to avoid mechanical carry over of fine particles. The only particles which

Figure 7.2.1 The plexiglass "frothless" Partridge-Smith flotation cell used for the floatability studies; (a) assembled; (b) basic operation, (Hornsby, 1981).

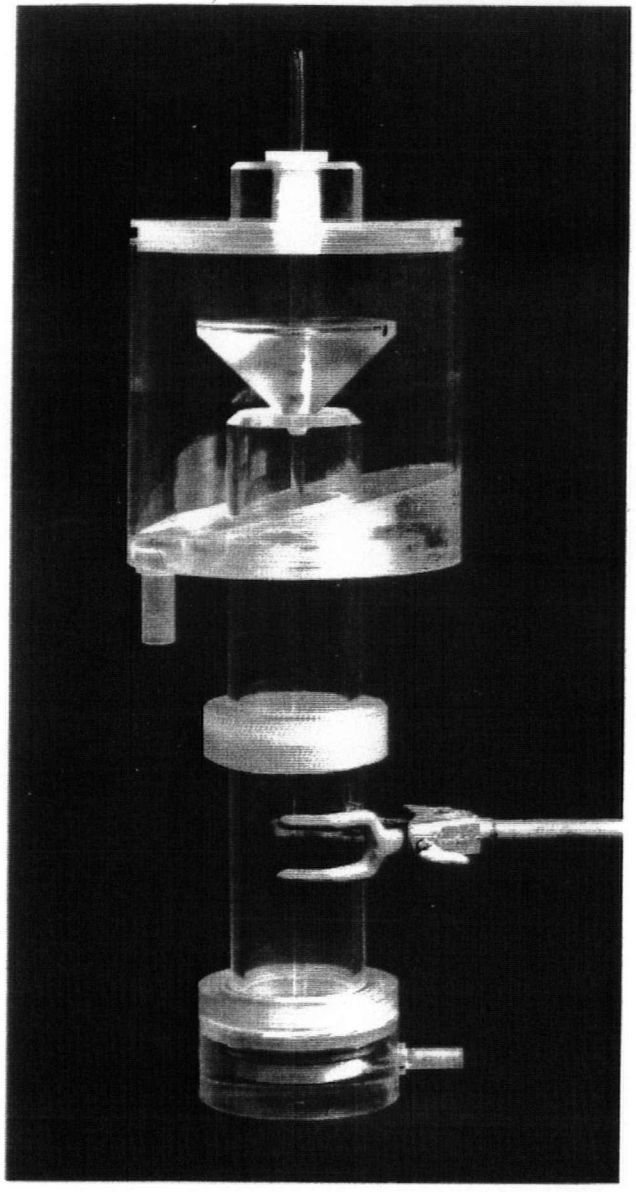

(a)

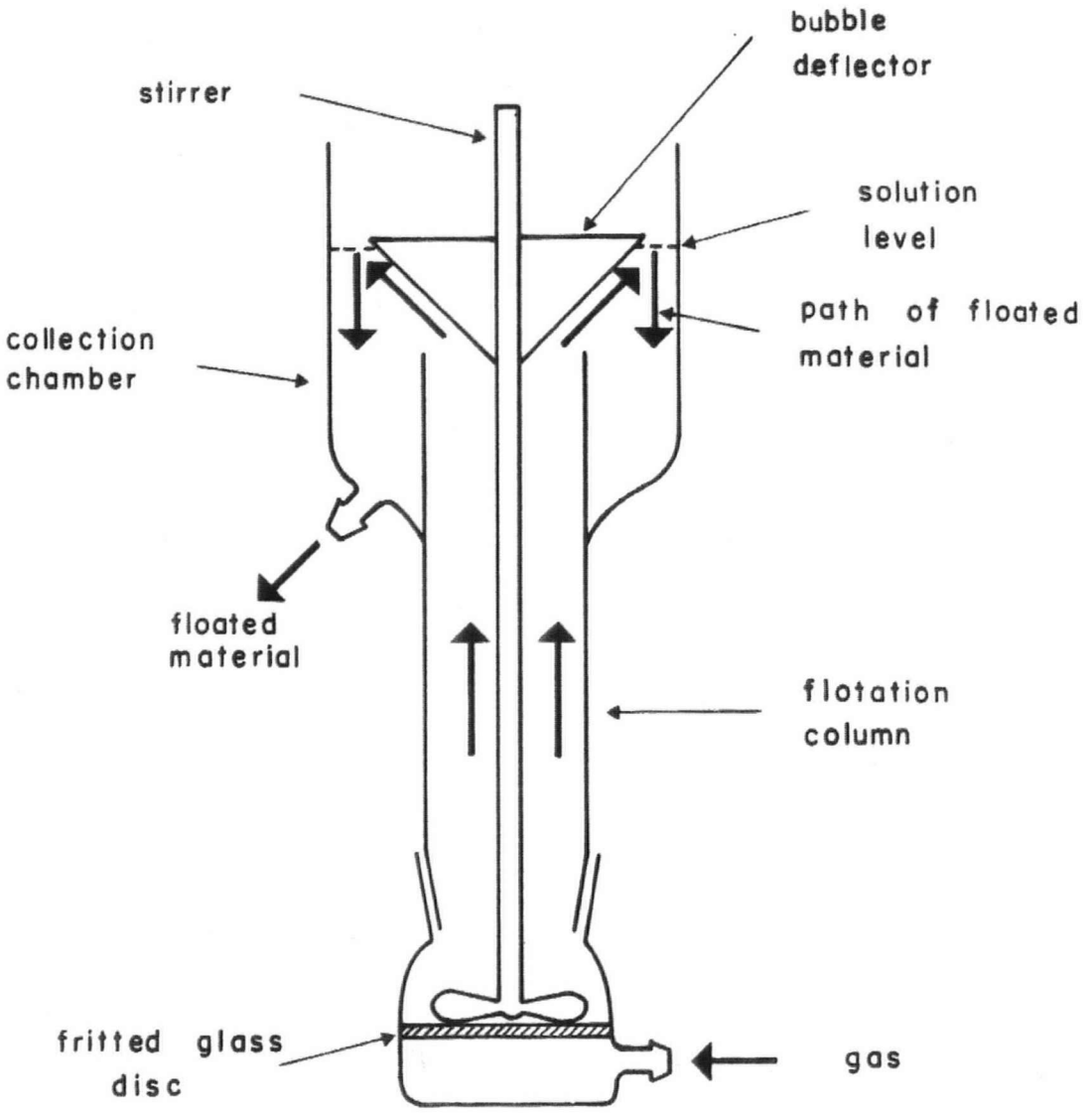
bubble
deflector
stirrer
solution
level
path of floated
material
collection
chamber
floated
material
flotation
column
fritted glass
disc
gas

(b)

reached the top of the column, under the given test conditions, were the most hydrophobic ones.

In its original design, the Partridge-Smith flotation cell was equipped with a bubble deflector, as shown in Figure 7.2.1, to deflect flow of bubbles at the end of the flotation column. However, as indicated by Hornsby (1980), better ash rejection and higher flotation rates were achieved without a bubble deflector. Therefore a bubble deflector was not used in the flotation tests.

The coal samples and flotation solutions were transferred through the glass funnel into the flotation cell. The flotation gas was grade K nitrogen supplied by Linde. The nitrogen was delivered at a pressure of 10 p.s.i.g. by Tygon tubing. The gas flow was regulated by a Dwyer rotameter, which has a capacity of 20-250cm^3/min. From the rotameter nitrogen was directed to the flotation cell.

7.2.2 Procedure

The procedure for flotation tests in P/S cell was based on that described by Hornsby (1981) with a few modifications.
For each flotation test, 2 grams of coal was placed in a small weighing boat and allowed to equilibrate with the laboratory atmosphere. Before each test, the flotation cell was taken apart and all the parts were washed with distilled water and then with the appropriate methanol solution used in the test. Prior to the

flotation test, nitrogen under pressure was passed through the fritted disc to make sure that pores in the disc were free of solid particles.

The following flotation procedure was used for all the flotation tests, unless specified otherwise.

1. Clean parts of the P/S cell were assembled and checked for appropriate functioning. Special attention had to be paid to the stirrer alignment and its clearance (1 to 2 mm) from the fritted disc.

2. Each coal sample was preconditioned in 100 ml of distilled water for 10 minutes by mechanical mixing. The speed of the stirrer was set at 1100 rpm. This speed was necessary to break down coal particle aggregates. The total volume of solution used for flotation was 750 ml, therefore the remaining 650 ml was used to prepare an adequate concentration of the methanol.

3. After conditioning, the coal sample was carefully transferred into the column using a glass funnel, and rinsed using as little of the flotation solution as possible. The coal suspension was allowed to settle for 5 to 10 minutes.

4. After coal particles settled in the column, the cell was filled very slowly, to prevent any carry-over of particles into the collection chamber, with the remaining methanol solution

5. The flotation cell was carefully fitted onto the rotor stirrer, as the fritted disc at the bottom of the cell was very fragile, and the stirrer should not touch it.

6. The nitrogen supply tube was connected to the bottom

section of the cell and controlled by the three way stopcock.

7. The coal slurry was conditioned for additional 5 minutes, without nitrogen flow, at 1100 r.p.m.

8. Shortly before conditioning was completed the stirrer speed was reduced to the setting required for flotation (300 r.p.m) and the N_2 was introduced at the rate of 30 ml/min. This flow rate generated a sufficient number of bubbles but did not cause significant turbulence to carry over non-floating particles.

9. Time of flotation was counted from the moment the first bubbles reached the top of the flotation cell.

10. After the flotation time expired, the stirrer was stopped and the gas supply disconnected.

11. Floating coal particles were removed from the collection chamber by releasing the clamp on the teflon hose from the chamber outlet, and letting it drain into the clean beaker. Similarly, the non-floating "rejects" were collected into another beaker. Any remaining material in the central column or at the bottom of the cell was rinsed into the "rejects" beaker, and remaining material from the collection chamber was washed into the "floats".

12. The floats and rejects were filtered using the micropore vacuum filtration unit and then dried in an oven at about 105^{o} C. Flotation products which had cooled and equilibrated with the laboratory atmosphere were weighed and submitted for ash analysis.

7.3 Microscopic Examination

For all microscopic examinations representative samples were used to prepare standard 2.54 cm (1 inch) coal pellets. In most cases coal samples were crushed to -850 microns (ASTM D 2797-75), split and mixed with polyester resin to make a pellet. In instances where the -212+149 μm size fraction was used, no crushing was necessary prior to pellet preparation. Coal pellets were prepared using a hydraulic press with elevated temperature (110^{o} C) to melt polyester resin into transoptic powder, and coal particles were mounted in it. Following that, pellets were placed in a holder for grinding and polishing with an automated grinder/polisher. Detailed procedures are in ASTM D 2797-75. A Zeiss-2 reflecting light microscope, with total 640 X magnification, one eyepiece cross-hair, and a Swift mechanical stage and registering counter, was used to carry out maceral counting. The mechanical stage was capable of advancing the specimen laterally by equal steps. The point counts were recorded on the counter in six different categories. The microscopic equipment used was in accordance with the ASTM D 2799-72 (reproved 1976) standard procedure as well as with the ICCP standards (ICCP, Handbook, 1963).

7.3.1 Maceral Analysis

Macerals are microscopically recognizable organic consistuents of coal and can be categorized into three groups:

vitrinite, liptinite (exinite) and inertinite. It is possible to distinguish one maceral from another based on their appearance under the microscope. The macerals can be identified mainly by their differences in reflectance, color, morphology and other optical properties, which are particularly striking in low rank coals.

The proportions of these petrographic components in all coal samples used in the study were determined by point counting a statistically adequate number of points, and summing those representative of each component. Three hundred points were counted (mineral matter free, i.e. mineral matter particles were not counted) using the established maceral counting procedure for bituminous coals (Bustin et al., 1983). A maceral was counted when it appeared directly under the cross hairs. The specimen was advanced by mechanical stage in steps of 0.1mm. The point-to-point distance was chosen according to the ASTM D 2799-72 procedure, which recommends that stepping distance be half of the diameter of the largest grain.

The maximum size of the particle in most cases was 0.20 mm, as in all the experimental work the particle size range was -212+149 μm, except where otherwise specified. The number of points counted for each individual maceral or maceral group were calculated as a percentage of the total of all points recorded. The values were expressed as volume percent, and results were recorded as an integer, because maceral analyses may be in error of at least +/- 1 percent (Hevia-Rodriguez and Prado, 1961). The accuracy of the

analyses are usually given by the reproducibility of the results. For this type of analysis it is required that accuracy of two analyses made by one operator on the same polished surface should be +/- 1.5 %. The results must not differ by more than 3% by volume for any maceral or maceral group if they are to meet ICCP standards.

7.3.2 Grain Type Analysis

Flotation products of the studied coal, the concentrates and the tailings were analyzed for maceral and grain type composition simultaneously. The efficiency of the flotation process depends primarily on the surface properties of the separate grains. The surface property and therefore behavior of a coal grain in flotation can be greatly influenced by the presence of mineral matter, and, to a lesser extent, by its maceral make-up. It was important to know how the mineral matter was distributed among coal grains and in what proportions, and also how the macerals were associated with each other, and whether these particular association and the presence of mineral matter would have an effect on flotation. However, this type of information could not be supplied by simple maceral analysis. An analysis describing each grain separately in terms of its association with other macerals as well as with mineral matter was required. The grain-type analysis was performed following the modified maceral analysis procedure (Cudmore et al., 1986). Definitions of the examined grain types are

Figure 7.3.1 Grains found in the examined samples; (a),(b) free vitrinite; (c) pseudovitrinite; (d),(e) vitr+inert, V>I; inert-+vitr, I>V; (f),(g) fusinite, free; (h) vitr+mineral matter.

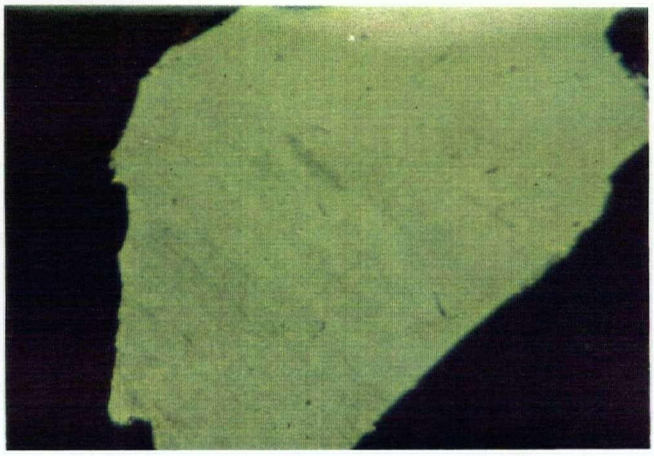

(a)

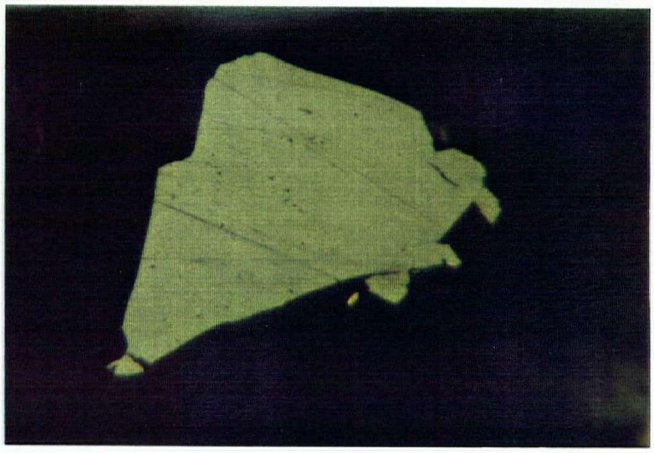

(b)

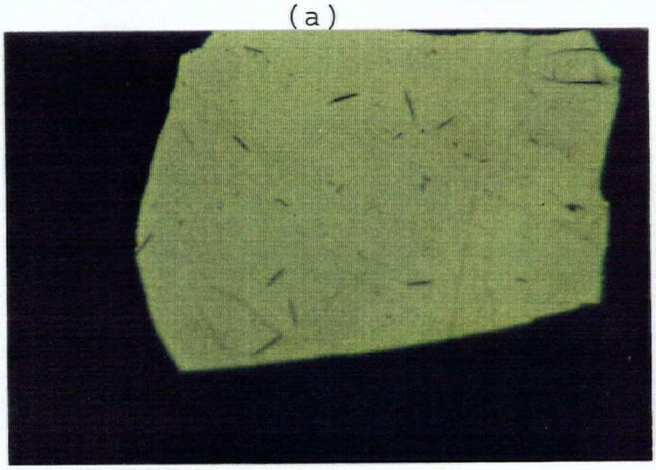

(c)

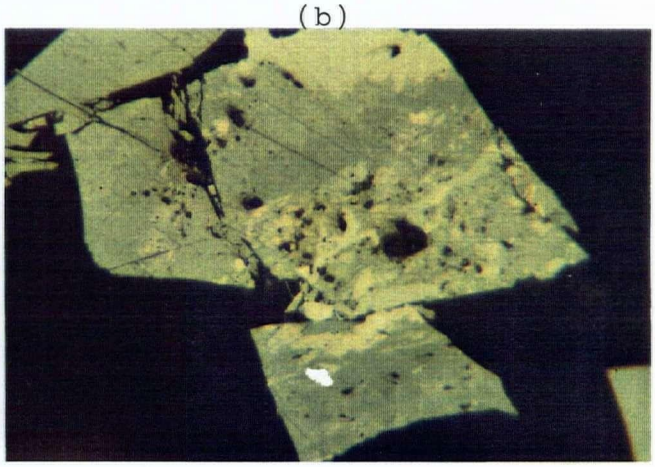

(d)

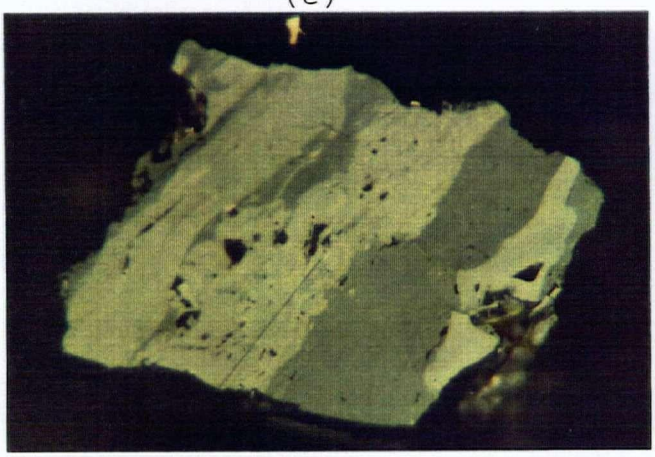

(e)

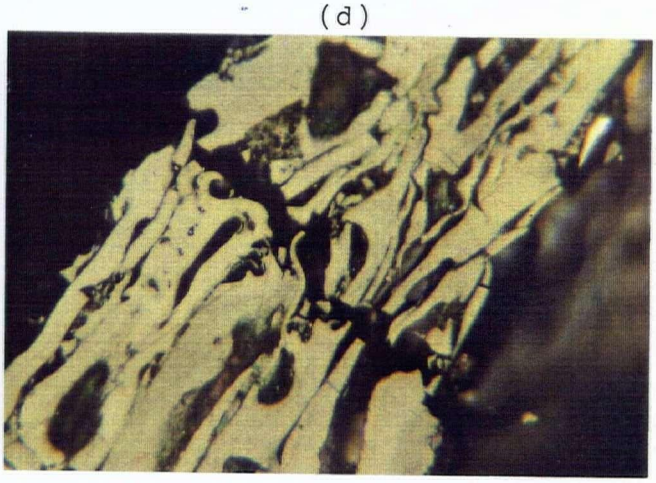

(f)

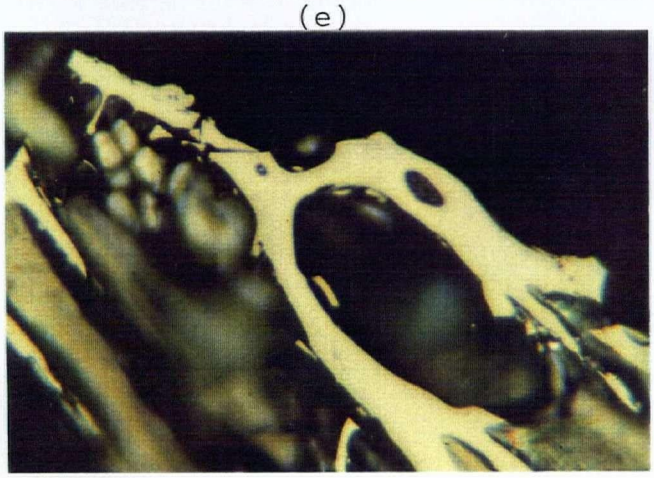

(g)

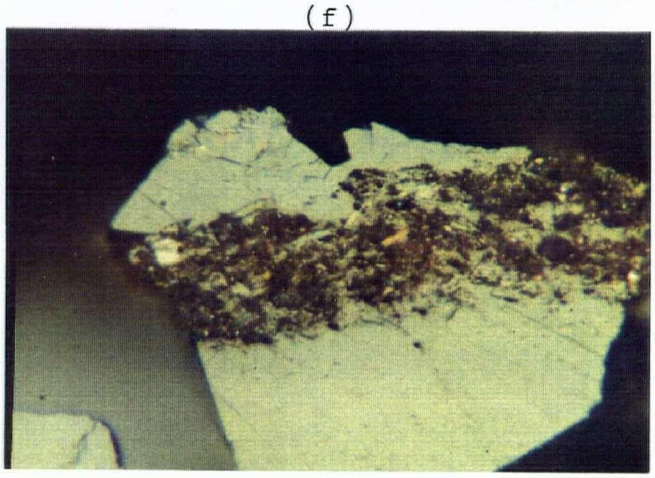

(h)

Figure 7.3.2 Different degrees of oxidation. A,B - extensive oxidation of vitrinite; C,D oxidation on the edges of grains; E,F physical changes appearing in grains; cracks and fissuring.

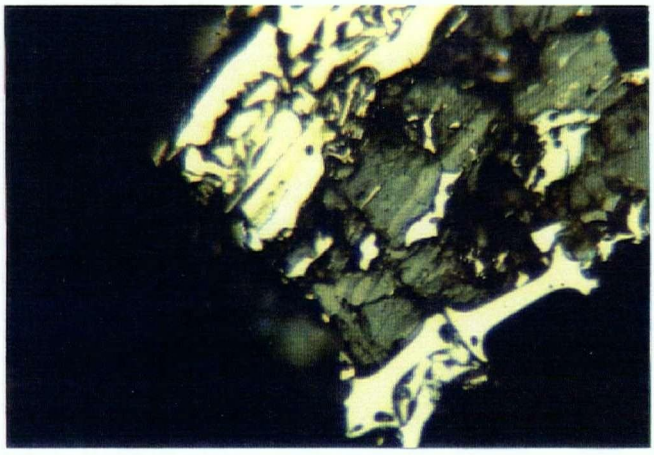

A

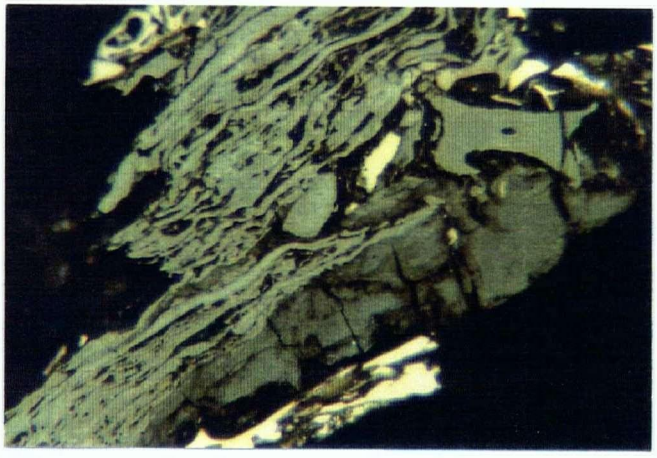

B

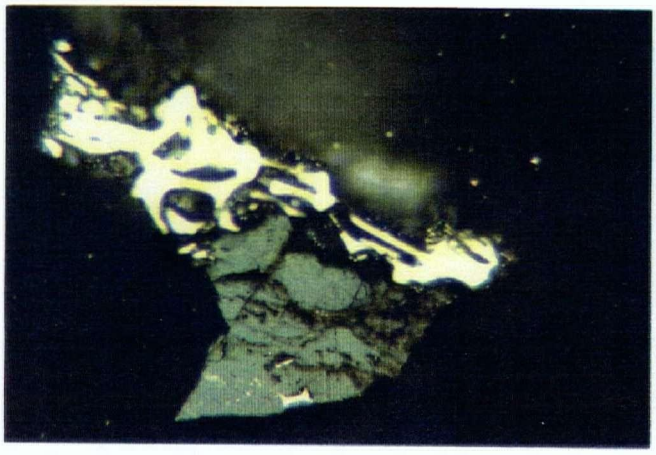

C

D

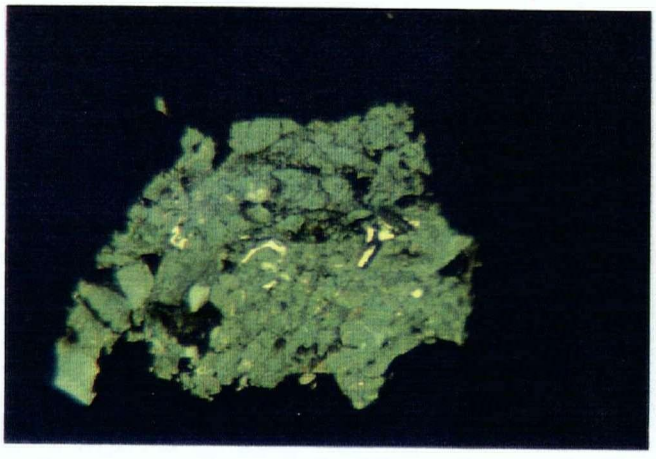

E

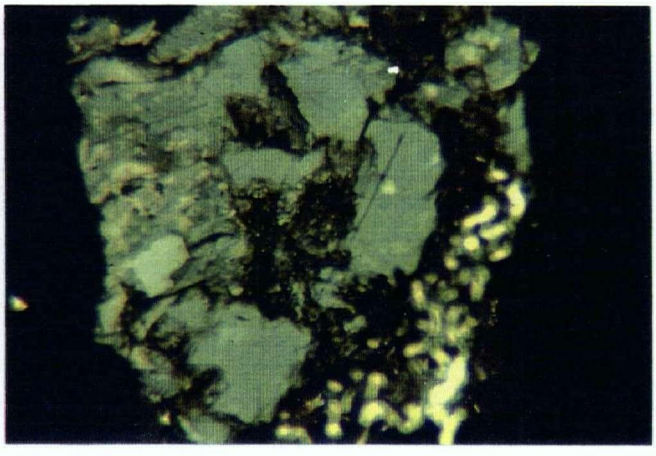

F

Table 7.3.1 Summary of grain-type analysis.

Grain type	Proportion of maceral groups
Free vitrinite	100 % vitrinite
Pseudovitrinite	100 % pseudovitrinite
Vitrinite + Inertinite V>I	V > 50 %, I < 50 %
Inertodetrinite I, I>V	100 % I, other inerts, and V + I, where I > 50 %
Fusinite	free fusinite or F > 50 % if associated with other macerals
Semifusinite	free semifusinite or SF > 50 % if associated with other macerals
Oxidized vitrinite	observed as oxidized particles under the microscope, and reported on the total vitrinite basis
Vitrinite with Mineral Matter	V + MM, where MM > 30 %

in Table 7.3.1. and illustrated in Figure 7.3.1. In general, the grain type was determined on the same particle, on which the maceral had been identified. For example, if the maceral under the cross-hair was identified as vitrinite, but the grain was also composed of lesser amounts of inertinite maceral, the grain would be recorded as vitrinite+inertinite (V+I) and at the same time was also identified in terms of mineral matter content. In terms of mineral matter content, only those grains which had an area more than 30% occupied by mineral matter were recorded. Under the

inertodetrinite category free inertodetrinite and grains of vitrinite with inertinite association, where I>V, were counted, while free semifusinite and fusinite were assigned to separate categories. A similar approach was used by Cudmore (Cudmore et al., 1986) when petrographically characterizing samples from froth flotation circuits. The oxidation is an important factor in rendering coal particles non-floatable. Therefore, the number of oxidized particles was also determined in the flotation feed and the product samples. To distinguish between oxidized and non-oxidized particles, coal pellets were soaked for 20 minutes in stain solution prepared from KOH + H_2O and safrinin "O" mixed in adequate proportions (Gray et al., 1976; Gray and Lowenhaupt, 1989). Stained particles were counted as oxidized and unstained were considered to represent fresh coal grains. The examples of oxidized grains as observed under the microscope (staining procedure) are in Figure 7.3.2.

CHAPTER 8

RESULTS AND DISCUSSION

8.1 Film Flotation Results

In the film flotation experiments as described in section 7.1, coal particles were separated according to their critical surface tension of wettability. At each surface tension of the solution, particles were partitioned into hydrophobic and hydrophilic fractions. The weight percent of the hydrophobic fraction was plotted as a function of solution surface tension and as a result the wetting tension distribution diagram was obtained. The plot represents cumulative distribution of particles in relation to their hydrophobicity. At the highest surface tension (2 % methanol concentration), the surface tension is insignificantly lower than that of water, and the partition is between hydrophobic and very hydrophilic particles; at the lowest surface tension only the most hydrophobic particles float. The wettability distribution is very sensitive to the surface properties of particles, therefore particles of different surface characteristics will have different wettability distribution curves.

The film flotation technique was used to obtain the wettability distribution of coal particles from a narrow size range (-212+149 μm) of Bullmoose seam A samples. In addition, wettability

distributions were obtained for lithotypes and different density fractions. To confirm that the technique is independent of particle size, different size fractions were also used.

8.1.1 Composite sample

The composite samples were represented by the -212+149 μm size fractions of low-ash and high-ash coal samples. The low-ash sample was the "cleaned" sample, while the high-ash was the initial composite sample received by sieving out the chosen size fraction from the total sample, as described in section 6.3.1. The wettability distribution was obtained for both composite samples by film flotation. The cumulative yield was plotted as a function of surface tension (methanol concentration, volume %) for the composite samples as shown in Figures 8.1.1. Three parameters can be determined from the wettability diagram: γ_{min}, minimum, the surface tension of the solution that wets all particles, γ_{max}, maximum, which represents the surface tension of the solution above which none of the particles are wetted; and the mean critical surface tension of wetting, γ_c. For the high-ash composite sample the minimum is at 39 dyne/cm, which corresponds to approximately 30 % by volume of methanol concentration, and the maximum yield of floating material, 73.58%, is observed at a surface tension of 68 dyne/cm (2 % by volume methanol concentration). The mean value of the critical surface tension is calculated as 54 dyne/cm for the high-ash sample, while similar value of 52 dyne/cm is found for the

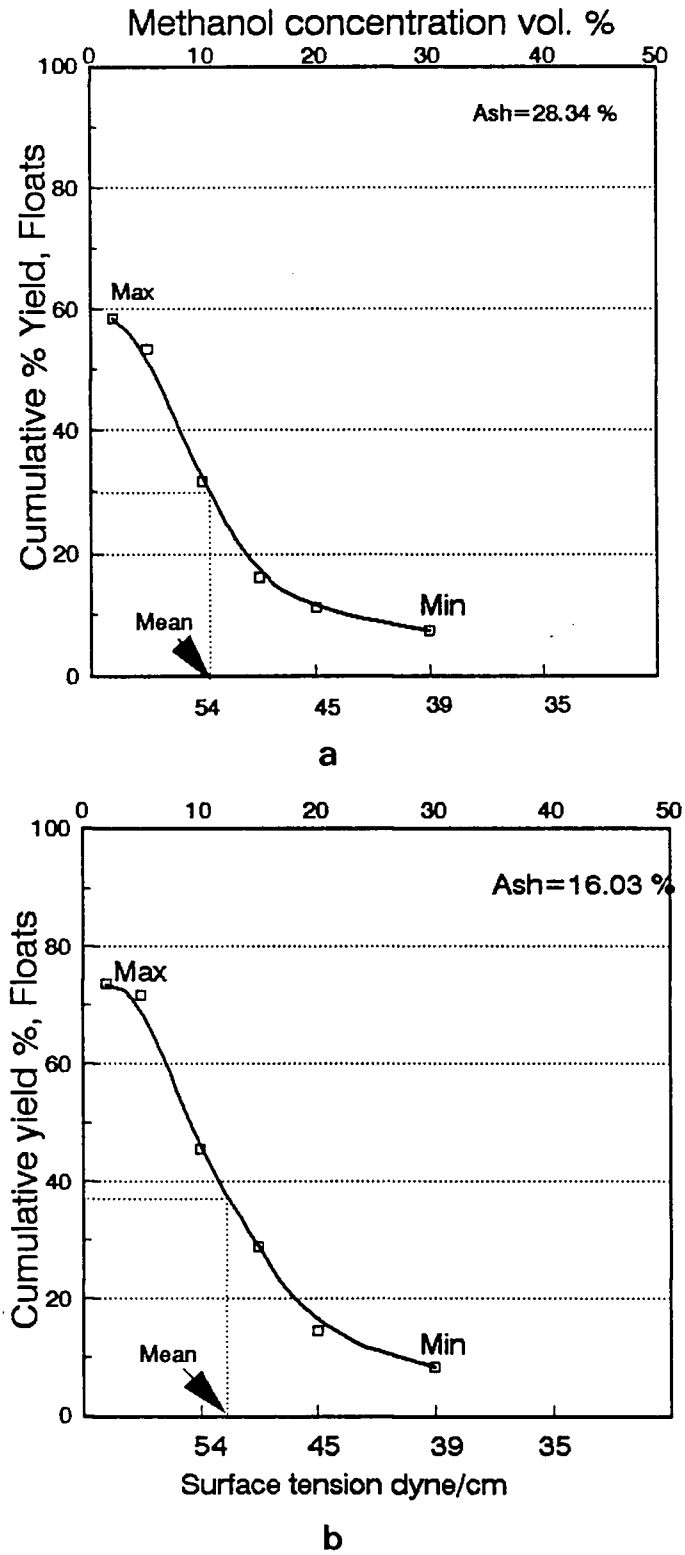

Figure 8.1.1 Film flotation. The cumulative yield plotted as a function of surface tension (methanol concentration, volume %) for the composite samples: (a) high-ash; (b) low-ash.

low-ash composite sample.

The amount of non-floatable material at the highest surface tension (2% methanol concentration by volume) for the low-ash composite sample was about 20 % wt. and for the high-ash sample almost 40 % wt. Microscopic analysis of the rejects indicates that most of the coal particles heavily contaminated with mineral matter, as well as oxidized particles are present in the non-floating fraction. Due to the small amounts of coal used for film flotation, and even smaller amounts reporting to floats and rejects,the point counting technique could not be applied to determine volume percent of different particles as the number of counted particles has to be at least 300 to be statistically valid. Therefore, only qualitative observations were made.

8.1.2 Density fractions

The film flotation experiments were conducted on the density fractions obtained from gravity fractionation of the narrow size fraction, -212+149 μm, (65x100 mesh Tyler) of the high-ash composite sample. A total of five density fractions were used for film flotation tests. The lightest density fraction was the <1.3 specific gravity, which has the least amount of ash, and as described in section 6.3.4, is the most enriched in vitrinite maceral. The abundance of vitrinite decreases with increasing density and for inertinite the opposite trend is observed (section 6.3.4).

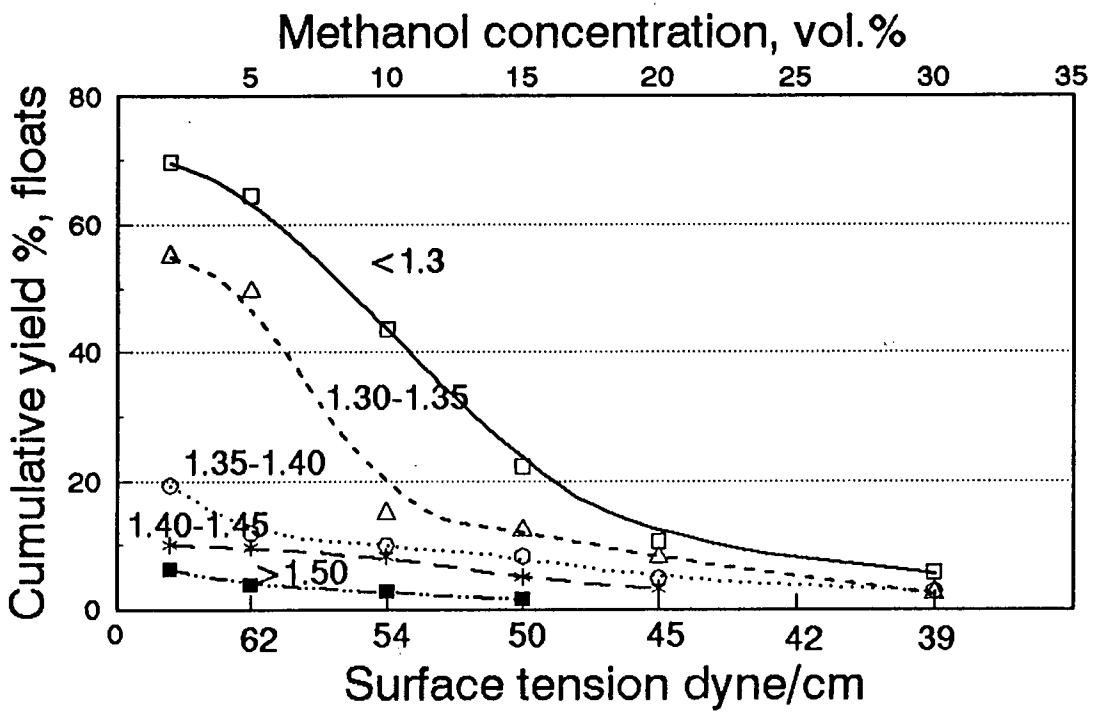

Figure 8.1.2 Film flotation. The wettability distributions of particles from various density fractions.

The cumulative distribution of particles according to their critical surface tension of wettability was obtained for all density fractions. These plots are shown in Figure 8.1.2. The wettability distribution of the lightest fraction indicates the best response to the film flotation. The highest recovery of coal particles in this fraction, 70 % by weight, is observed at 2 % by volume of methanol concentration, and the lowest is observed at approximately 30 % by volume of methanol concentration, corresponding to 39 dyne/cm.

About 30 % (by weight) of the material remained non-floating at 2 % methanol by volume, most of which, as in the composite, consisted of oxidized vitrinite particles, heavily contaminated with the mineral matter or relatively small amounts of fully liberated inorganic particles.

The 1.30-1.35 specific gravity fraction shows different wettability characteristics in terms of the cumulative distribution of particles versus their critical surface tension of wettability. The shape of the distribution curve is quite different as compared to the 1.30 specific gravity fraction.

The samples of higher density, such as 1.40-1.45 and > 1.50 g/cm^3 show no response to the film flotation, with the exception of the 1.35-1.40 fraction, which has low yield at 2 % methanol concentration. The primary reason for this behavior is that most of the particles, as examined under the microscope, are very heavily contaminated with mineral matter. Furthermore, all of the inorganic matter is associated with the coal particles

(unliberated). As a result of sink and float separation, the only fraction which contains liberated mineral matter is the heaviest, > 1.50 density fraction.

8.1.3 Lithotypes

Hand picked samples of five lithotypes from Bullmoose seam A, as described in section 6.3.2, were used in the film flotation tests using methanol solutions. The wettability distributions were obtained for all five samples. Figure 8.1.3 presents cumulative wettability distribution for different lithotypes, and ash content in floating fractions.

The wettability of "bright" and "banded bright" lithotypes (Australian classification) appears to be very similar. The maximum floatability of particles occurs for both samples at 2 % by volume of methanol (68 dyne/cm), with yields of 98.62 % by weight for bright, and 97.18 % for banded bright lithotype. The lowest yields of floating particles, 29.51 % for bright and 21.99 wt % for banded bright, are found at the level of 30 % by volume of methanol concentration (39 dyne/cm) for both lithotypes. The ash content (bright, 4.20 % ash; banded bright, 5.23 % ash) and maceral composition of these lithotypes are very similar (Table 6.3.1 and Figure 6.3.4).

Wettability distributions of "banded coal" and "banded dull" are very similar. Maceral analyses of both lithotypes are again very similar. The mineral matter content for both samples is

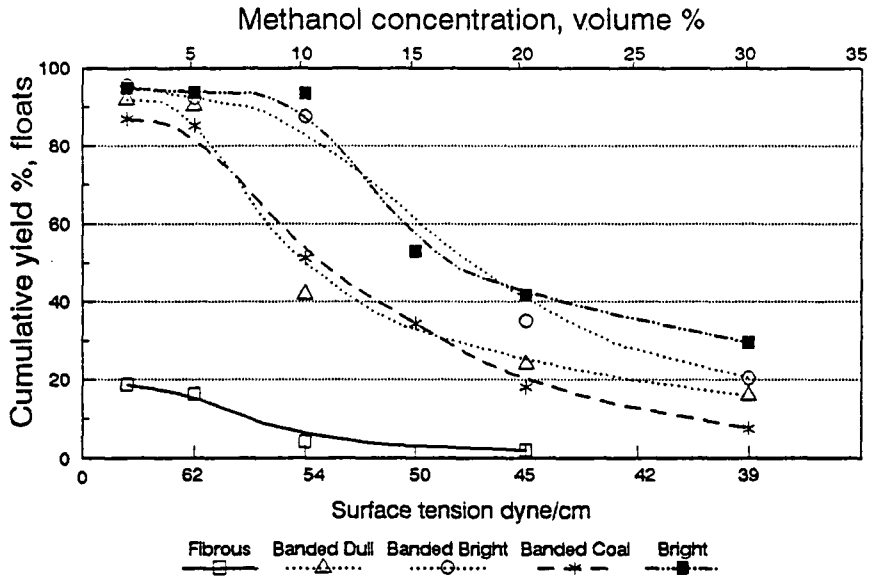

a

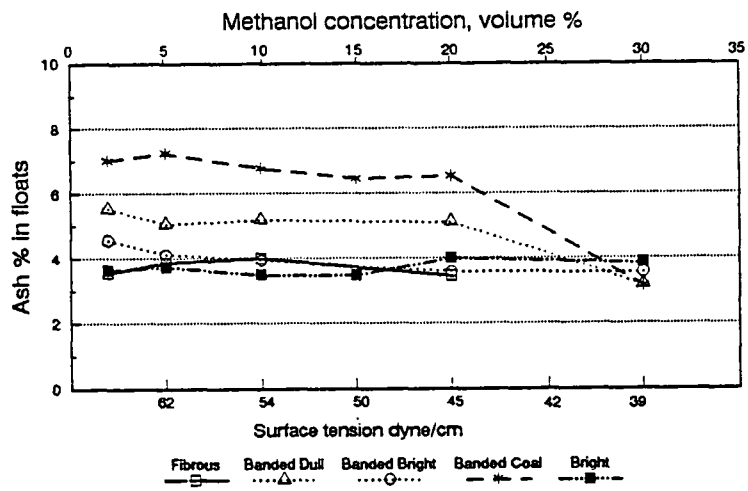

b

Figure 8.1.3 Film flotation. The cumulative wettability distribution for different lithotypes (a) wettability distribution; (b) ash content in the floating fractions.

very low. The maximum yield of floating particles is almost the same and occurred for banded coal and banded dull at 2 % by volume methanol concentration, and the lowest yield of floating particles is at 30 % by volume, methanol concentration.

Fusain (fibrous) shows the lowest response to the film flotation. The maximum yield of floating particles at 2% by volume of methanol concentration is 18 % by weight, and the minimum yield is observed at 10 % by volume of methanol concentration and corresponds to a surface tension of 54 dyne/cm.

It is evident from petrographic analysis, that fusain is enriched in inertinite macerals. The inertinite macerals at this coal rank (medium volatile bituminous) are known to have significantly lower hydrophobicity (Brown, 1962; Klassen, 1966; Hower, 1984; Sarkar, 1984; Bujnowska, 1985; Aplan, 1989) and therefore much lower flotation response, as compared with the vitrinite macerals.

An additional reason for high wettability of fusain, is that this particular lithotype contains exceptionally high amounts of elemental oxygen. From the H/C, O/C or O/H, atomic ratios it is noticeable, that fusain is the most aromatic (lowest H/C ratio) of all lithotypes and has the highest content of carbon, along with high content of oxygen. This might have also contributed, to its low floatability.

Low floatability of fusain, which is usually composed of fusinite, has been frequently linked to the fact that cavities in fusinite are usually filled with mineral matter. Mineral matter

represents strongly hydrophilic sites on coal particles, which consequently results in the lower flotation response. In the fusain studied here mineral matter content is very low and its effect on the floatability is probably negligible.

8.1.4 Different size fractions

Film flotation technique is predominantly controlled by interfacial forces. The effect of particles density, shape and size was studied by Fuerstenau et al., (1988a). They concluded that the technique is nearly independent of all factors other than the surface properties of the particles.

The hand-picked vitrain particles were separated into the four different size fractions (35x48, 48x65, 65x100,and 100x200 mesh) and used in film flotation experiments. Wettability distributions of different size fractions were obtained. The wettability distributions of all different size fractions are nearly identical. Figure 8.1.4 presents wettability of different size fractions of vitrain. The vitrain lithotype was chosen to maintain the same petrographic composition for all the size fractions. The segregation of macerals into different size fractions was reported previously in the sizing process (T. Laskowski, 1948; Hower et al., 1987; Falcon and Falcon, 1987).

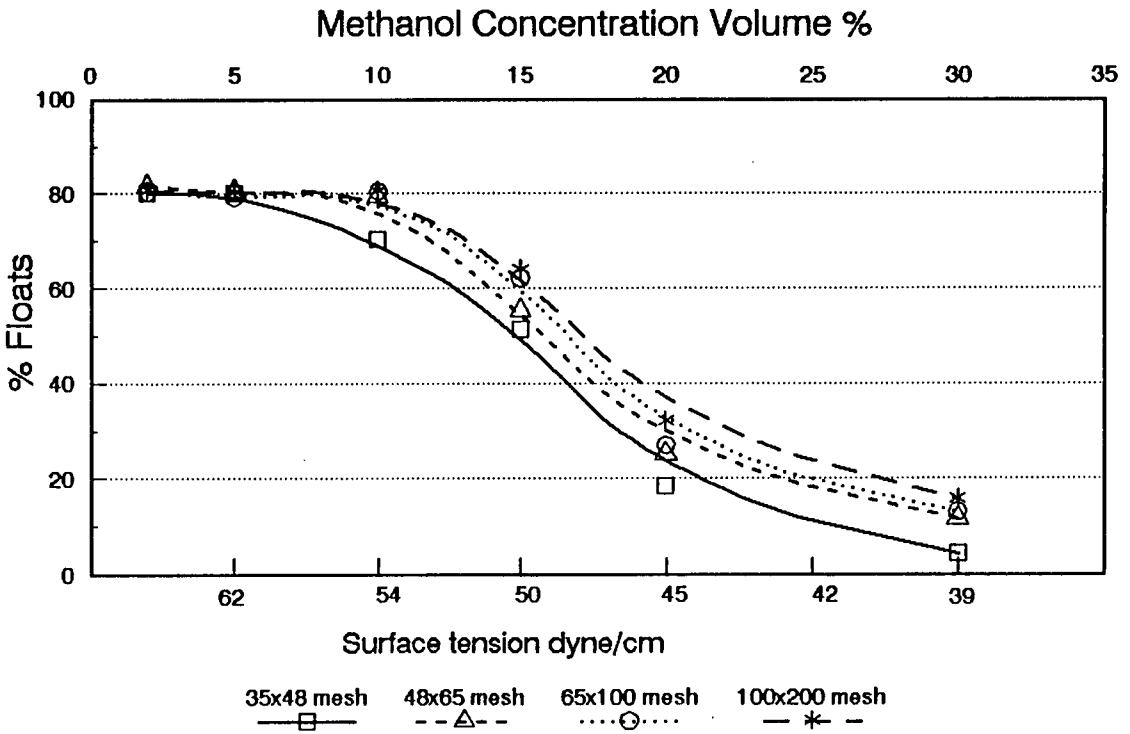

Figure 8.1.4 The effect of size on the wettability. Film flotation of different size fractions of vitrain (Bullmoose seam A).

8.2 Results of Small-Scale Flotation Tests

The small-Scale flotation as described in section 7.2 was used to evaluate floatability of coal samples of different petrographic composition. Flotation tests were carried out in a Partridge-Smith flotation cell without using reagents. Different methanol concentrations were used to vary surface tension.

The relative floatability of coal samples of different petrographic composition was analyzed in terms of the critical surface tension of floatability, γ_{cf}. The floatability distributions of coal particles according to their respective critical surface tension of floatability were obtained.

The cumulative yield % (weight percent of floated fractions) versus surface tension (methanol concentration) was plotted for each sample.

8.2.1 Conditions of flotation

The parameters such as flotation time and conditioning time were kept constant for all floatability tests. A preliminary series of tests was carried out to determine optimal flotation conditions.

8.2.1.1 Flotation time

The small-scale flotation tests were performed with the

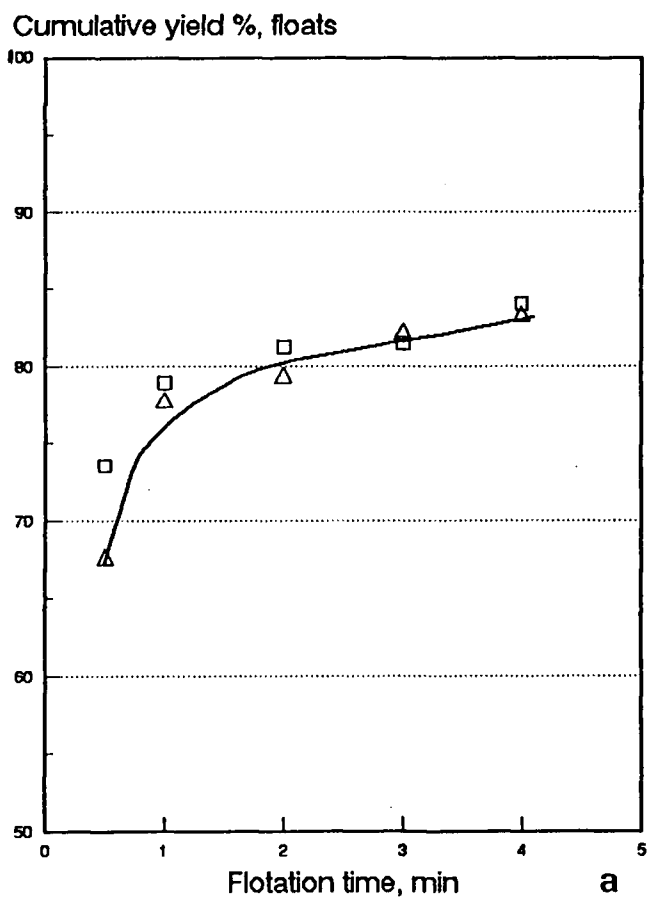

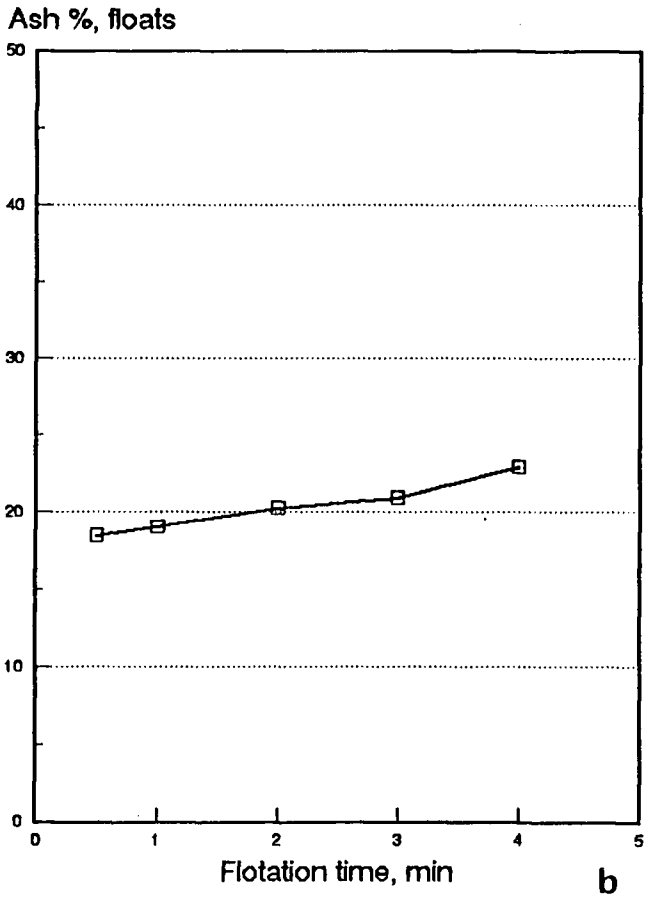

Figure 8.2.1 The effect of flotation time on yield and on ash of floats: (a) cumulative yield of floats versus flotation time; (b) cumulative ash % in floats versus flotation time.

-212+149 μm high-ash composite sample in order to establish the optimal flotation time. Flotation tests were carried out in 2 % methanol solution, keeping all the other flotation parameters unchanged except the flotation time, which varied over the range from .50, 1, 2, 3, to 4 minutes. Cumulative yield of floating coal particles becomes essentially constant after 3 minutes of flotation. An additional increase in flotation yield, beyond the 3 minutes flotation time, was found to increase ash content of the floating fraction (Figure 8.2.1). The flotation time of 3 minutes was therefore used for all experiments.

8.2.1.2 Conditioning time

Conditioning is needed to wet a coal sample with water. Conditioning is also applied to mix the flotation pulp after the reagent addition. The most common practice is to use 10 to 15 minutes conditioning to wet coal particles with water prior to the addition of reagents (Hornsby, 1981). Following the addition of methanol, only a short conditioning time (3 to 5 minutes) was used to mix coal with the reagents.

The effect of conditioning time in water on the yield and ash of floats is depicted in Figure 8.2.2. The conditioning times prior to the reagent addition were 0, 3, 5 and 10 minutes. The optimal conditioning time for all floatability experiments was set at 10 minutes.

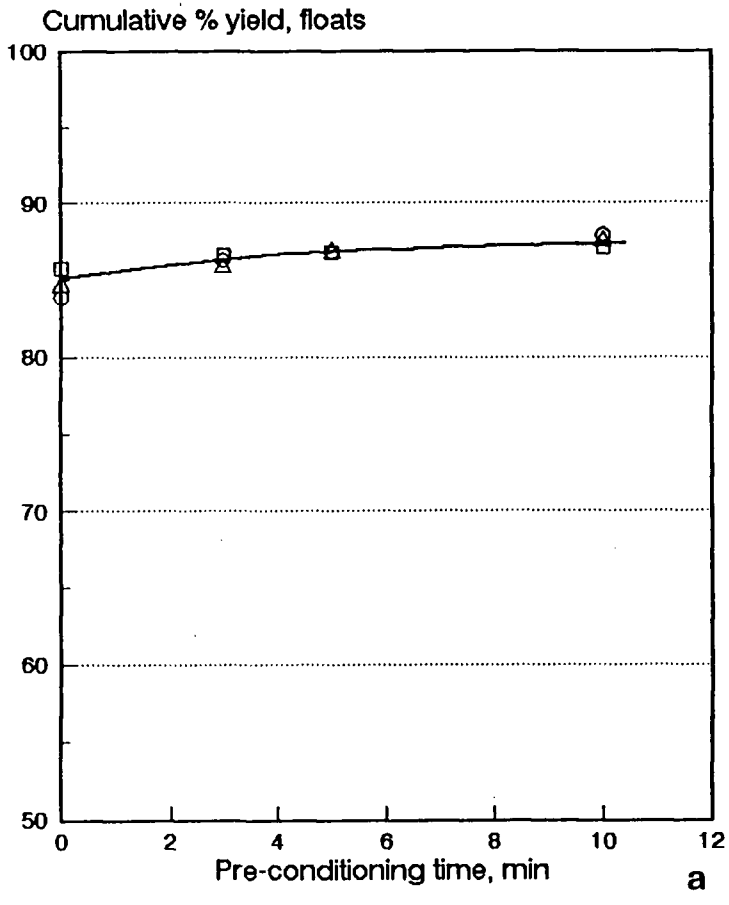

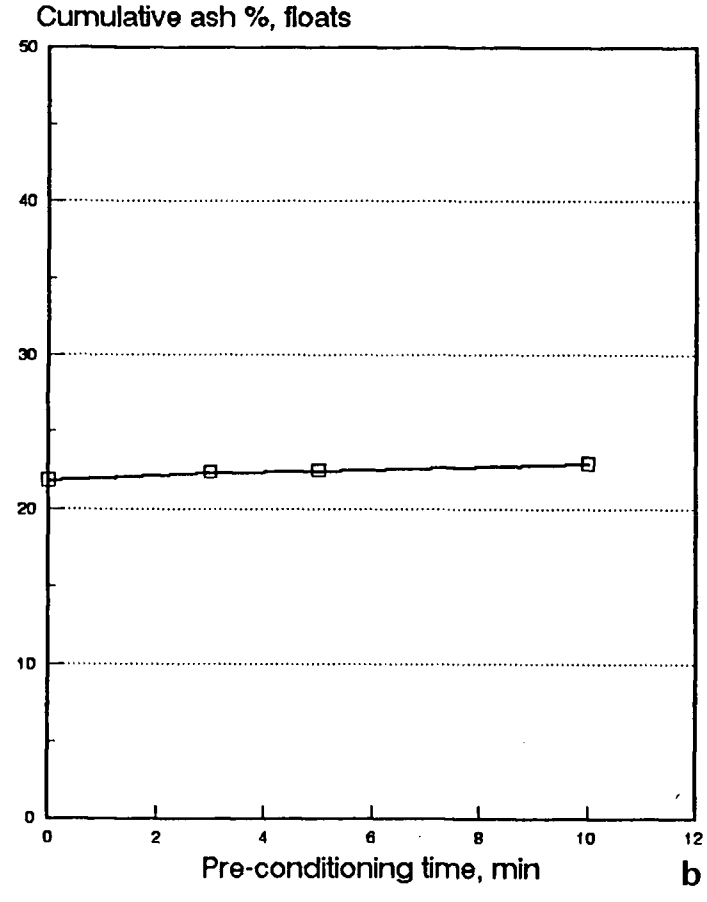

Figure 8.2.2 The effect of conditioning time on flotation. (a) Cumulative yield of floats versus preconditioning time; (b) Cumulative ash in floats versus preconditioning time.

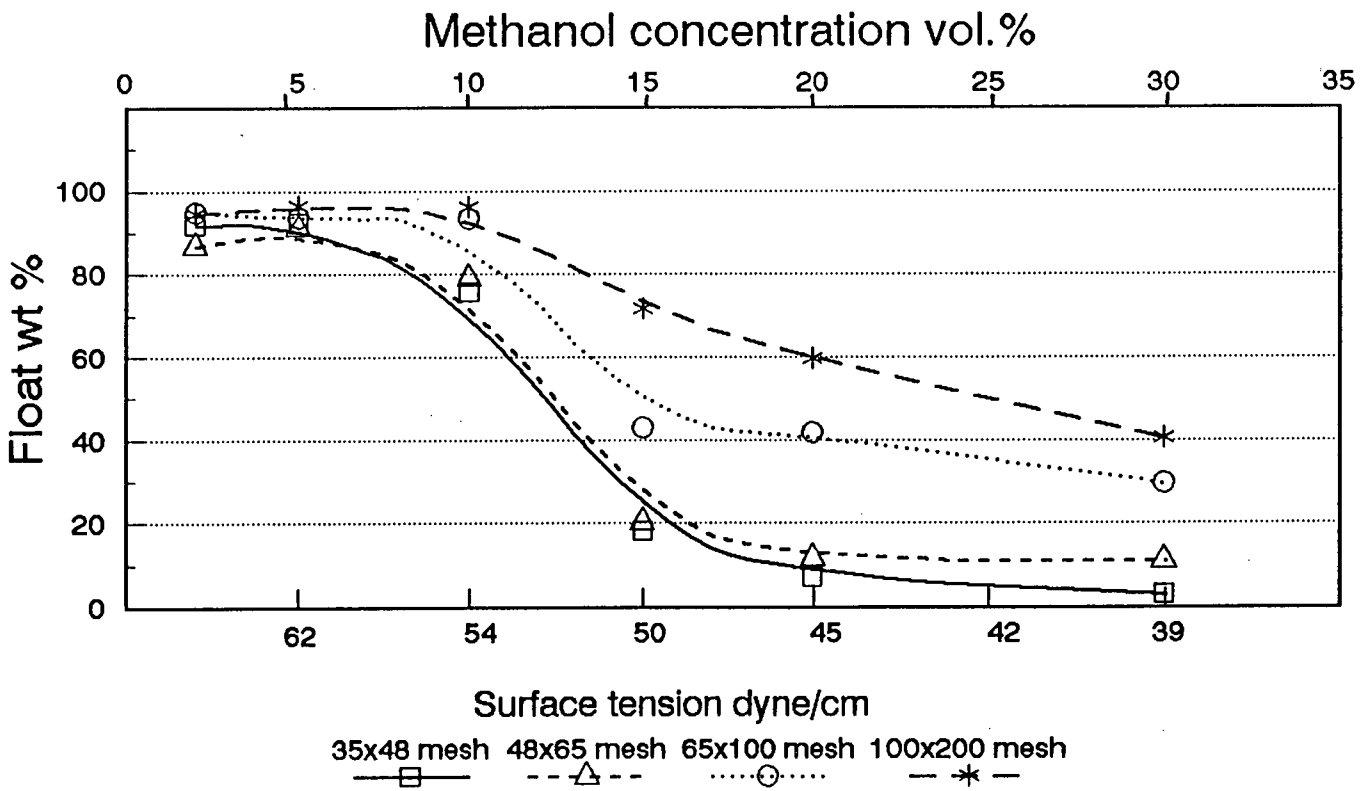

Figure 8.2.3 The effect of size on floatability of vitrain. Small-scale flotation tests in P/S flotation cell.

8.2.2 Floatability distribution of coal particles

The cumulative yield was plotted as a function of surface tension (methanol concentration) for a number of Bullmoose A-seam coal samples. The flotation tests were carried out under standard flotation conditions: 10 minutes conditioning in water time, 3 minutes flotation time, no bubble deflector. The curves have been fitted through the replicate data points whenever replicates were available. Density fractions of the composite sample (as described in section 6.3.1) were also used in the floatability tests. Since flotation is size dependant, different size fractions were used to examine the effect of size on floatability (Figure 8.2.3).

8.2.2.1 Composite sample

The cumulative yield versus surface tension (methanol concentration, volume %) plots were obtained for the two composite samples. Figure 8.2.4 presents floatability distributions for these samples. The initial composite sample has an ash content of 28.34%, and the low-ash composite sample referred to as "cleaned" has 16.03% ash; both were used in the flotation tests.

Both composite samples appear to be readily floatable. The cumulative yields for the cleaner sample are much higher at any given methanol concentration. The minimum yield of floating particles in both cases is at about 30 % methanol concentration. At methanol concentrations greater than 30 %, a constant amount of particles was reporting to the floating fraction.

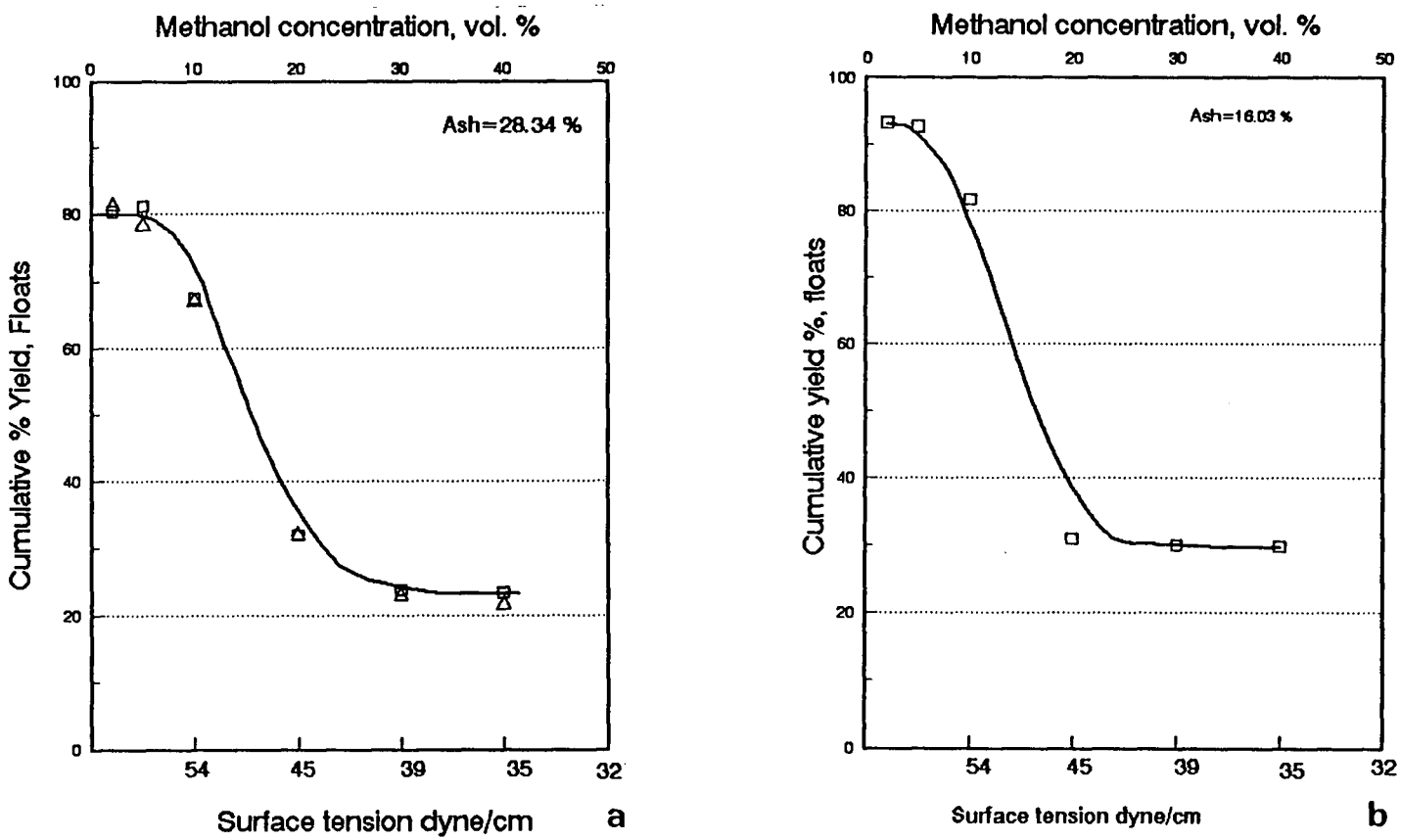

Figure 8.2.4 The cumulative yield versus surface tension for two composite samples: (a) high-ash composite sample; (b) low-ash composite sample.

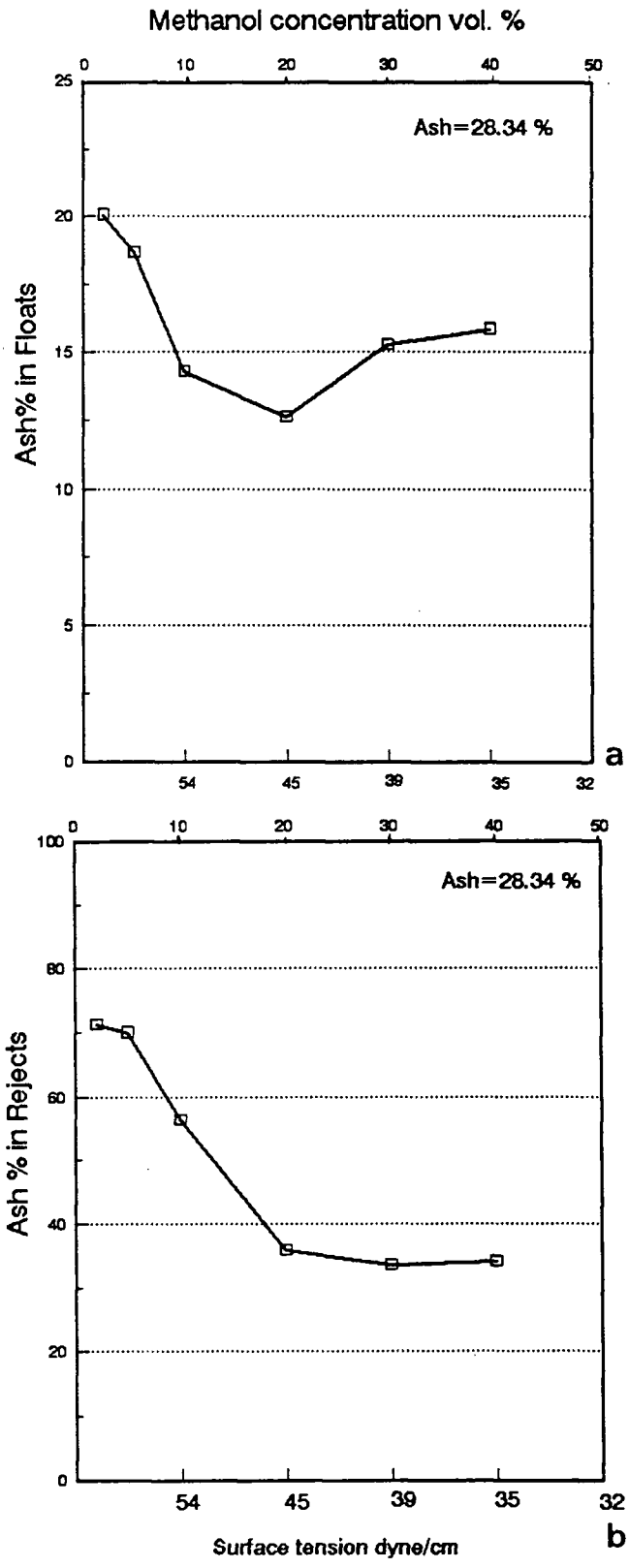

Figure 8.2.5 Ash content in floats and rejects for the high-ash composite sample: (a) floats; (b) rejects.

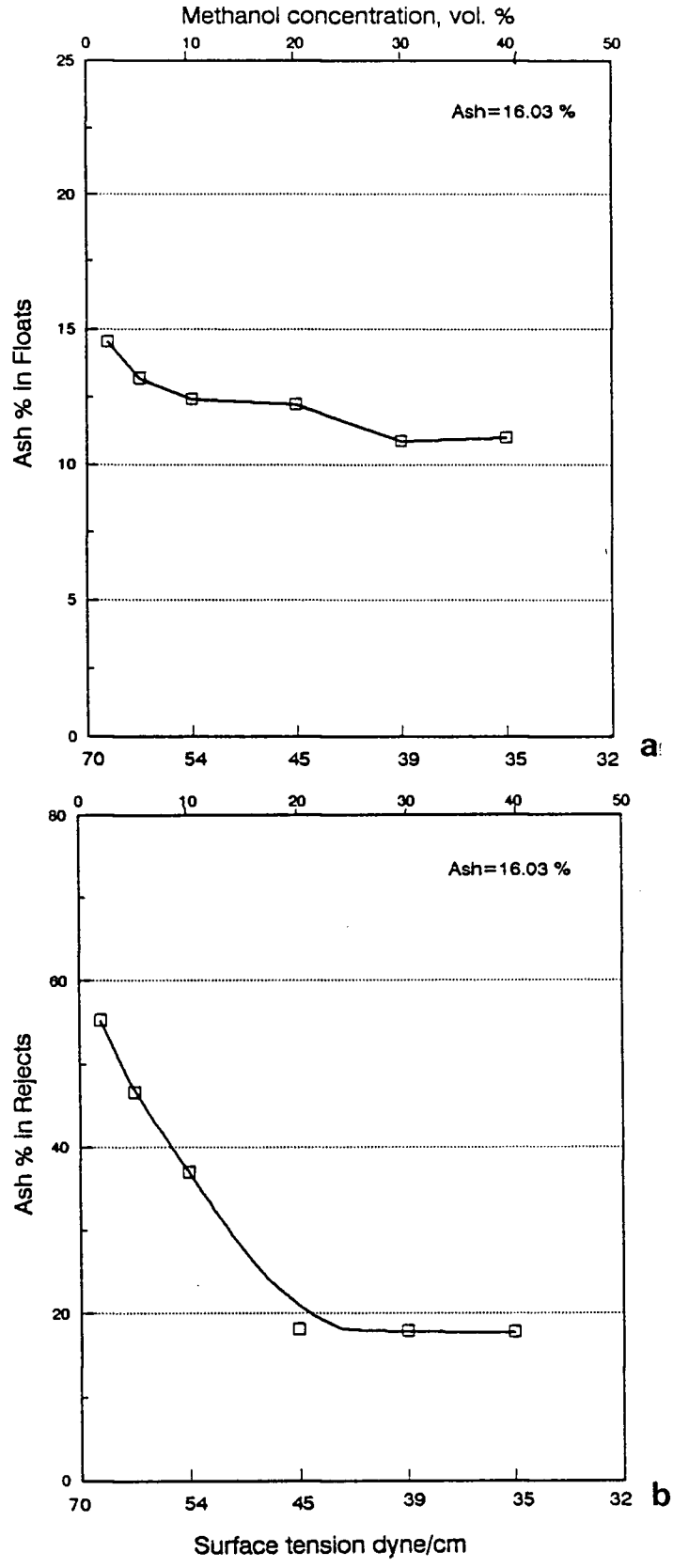

Figure 8.2.6 Ash content in floats and rejects for the low-ash composite sample: (a) floats; (b) rejects

The ash content of the floated fractions decreases with an increase in methanol concentration and reaches a minimum at 20 % methanol, and then tends to increase as the concentration of methanol is further increased. The higher ash content of floats at higher methanol concentration may indicate the presence of clays in the sample. This effect is especially visible in the high-ash composite sample. A reason for clay particles reporting to the floating fraction is the peptization of clays in high concentrations of methanol (Hornsby, 1981). Similar effects were observed in the floatability experiments by Hornsby (1981). Figure 8.2.5 and Figure 8.2.6 present ash content in floats and rejects for both composite samples.

8.2.2.2 Density fractions

Five density fractions were also used in the flotation tests. Floatability distributions were obtained for each of the density fractions (Figure 8.2.7). The three lightest density fractions show positive response to flotation in methanol solutions. The three heaviest have a constant amount of particles floating at each methanol concentration, with no evident floatability distributions.

The highest cumulative yields were obtained for the lightest fraction (<1.30 specific gravity), with the maximum yield at surface tension of 68 dyne/cm (2 % methanol concentration), and the lowest yield at about 39 dyne/cm of surface tension (30 %

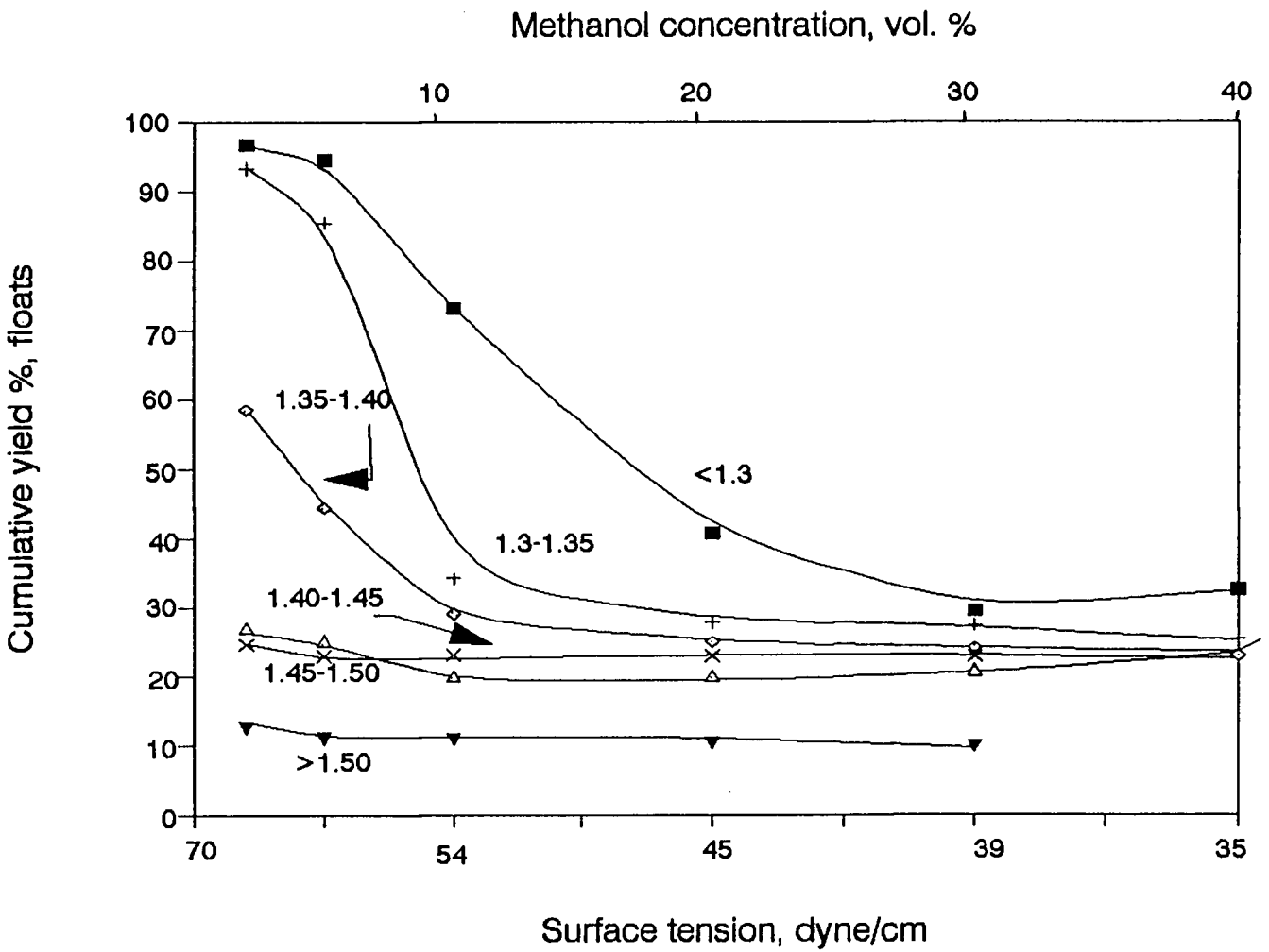

Figure 8.2.7 The cumulative yield vs surface tension curves for various density fractions as obtained from P/S small-scale flotation tests.

methanol concentration). The second lightest fraction (1.30-1.35 specific gravity) is characterized by a different floatability distribution, with much lower yields and a sharper change in shape of the distribution curve.

The third lightest fraction (1.35-1.40 specific gravity) shows considerably lower flotation response when compared to the two lighter fractions discussed above. The low yields at low methanol concentrations (high surface tensions) are mainly due to the fact that most of the coal particles within this fraction are heavily contaminated with mineral matter. The trends in ash content of floats and rejects for the three density fractions under discussion are depicted in Figures 8.2.8 and 8.2.9.

The ash content of floating coal particles for the two lightest fractions seem to be independent of methanol concentration (surface tension), while the ash content of rejects decreases as the methanol concentration increases; the minimum ash content occurs at about 10 % methanol concentration for both fractions. Further, the ash content of rejects becomes constant with decrease in surface tension. The high ash content of rejects at low methanol concentration (high surface tension) confirms that at that surface tension the separation is between all hydrophobic coal particles and only very hydrophilic mineral matter (or heavily contaminated coal particles).

The ash pattern for the floats of the third density fraction (1.35-1.40 specific gravity) is different from the pattern for the density fractions discussed above. The majority of the

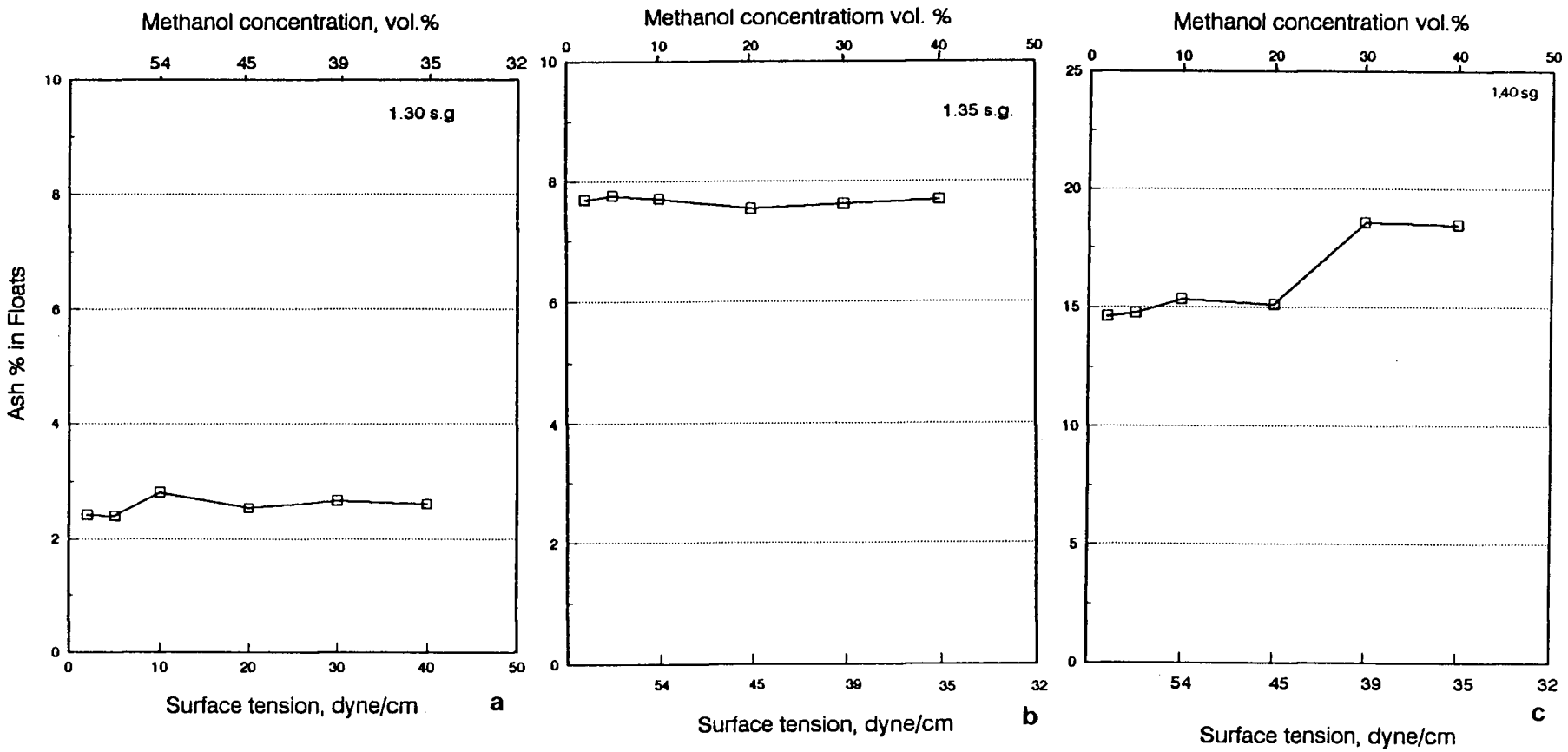

Figure 8.2.8 Ash content in the floats of the three density fractions: (a) < 1.30 specific gravity; (b) 1.30 - 1.35 specific gravity; (c) 1.35 - 1.40 specific gravity

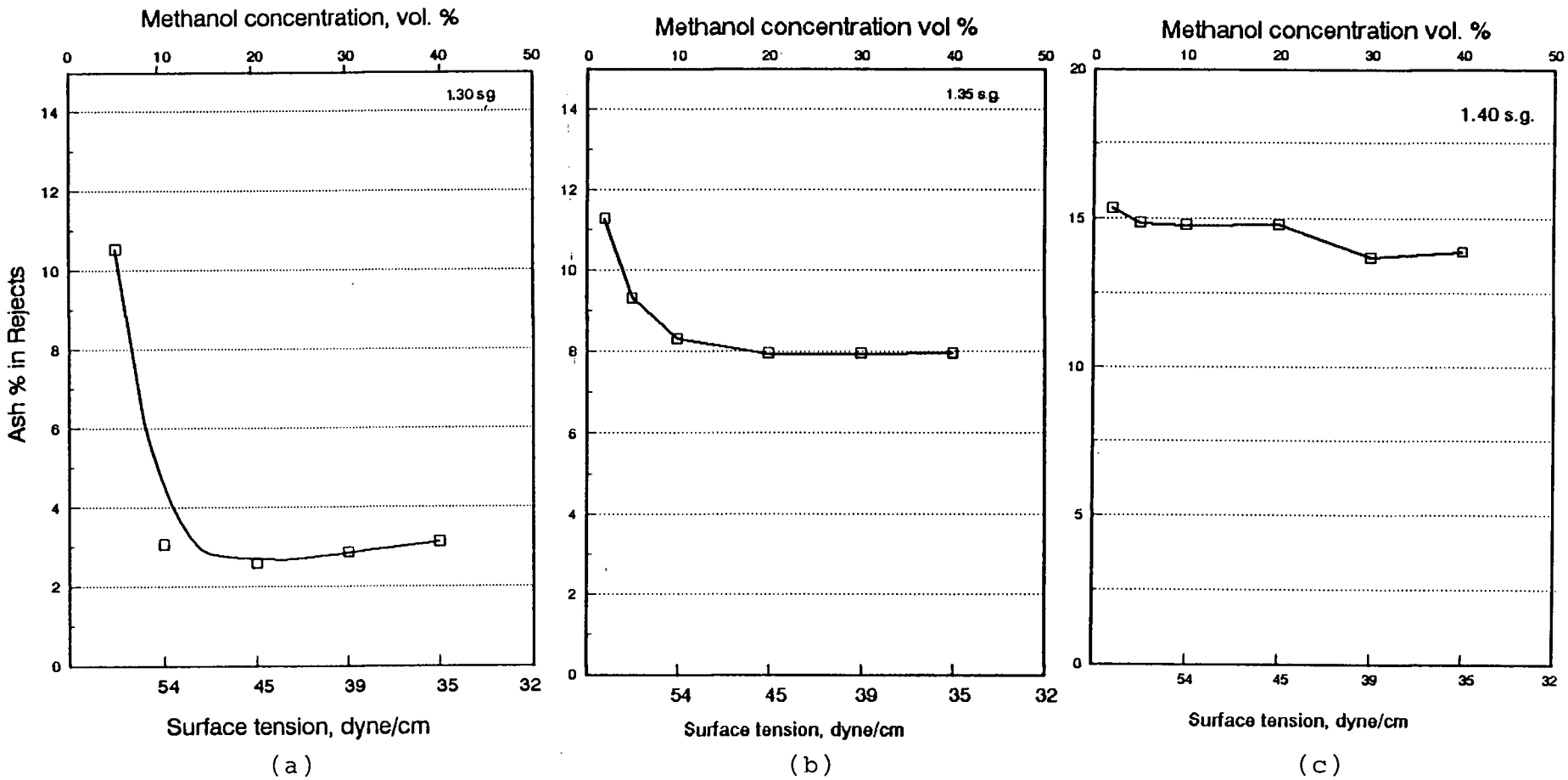

Figure 8.2.9 Ash content in the rejects of the three density fractions: (a) < 1.30 specific gravity; (b) 1.30 - 1.35 specific gravity; (c) 1.35 - 1.40 specific gravity

particles, however, within this density fraction are contaminated with mineral matter, and only a few particles float, and therefore the distribution obtained from floatability runs is only for those particles which are hydrophobic enough to be floated. The ash content of the rejects appears to be constant over the studied methanol concentration range. Since only a small amount of coal particles float at high methanol concentration, it is difficult to observe significant changes in the ash content of rejects.

8.2.3 Cumulative ash versus cumulative yield

The cumulative ash versus cumulative yield of the floats and rejects were plotted to characterize the floatability. The data in Figures 8.2.10 and Figure 8.2.11 represent two composite samples; results are plotted as cumulative ash versus cumulative yield of the floats and rejects.

For the high-ash composite sample, as the cumulative yield of floats decreases below 30 %, the ash content increases rapidly for the high-ash composite sample. The yield of 30 % of floats coincides with 20 % methanol concentration. This trend provides an additional evidence that clay slimes are released during prolonged conditioning in the more concentrated methanol solutions (over 20 % methanol concentration). According to Hornsby (1981), there is a strong peptizing effect of alcohol solutions on clay minerals associated with coal. The peptization effect is minimized at short conditioning times. The shape of the clean coal

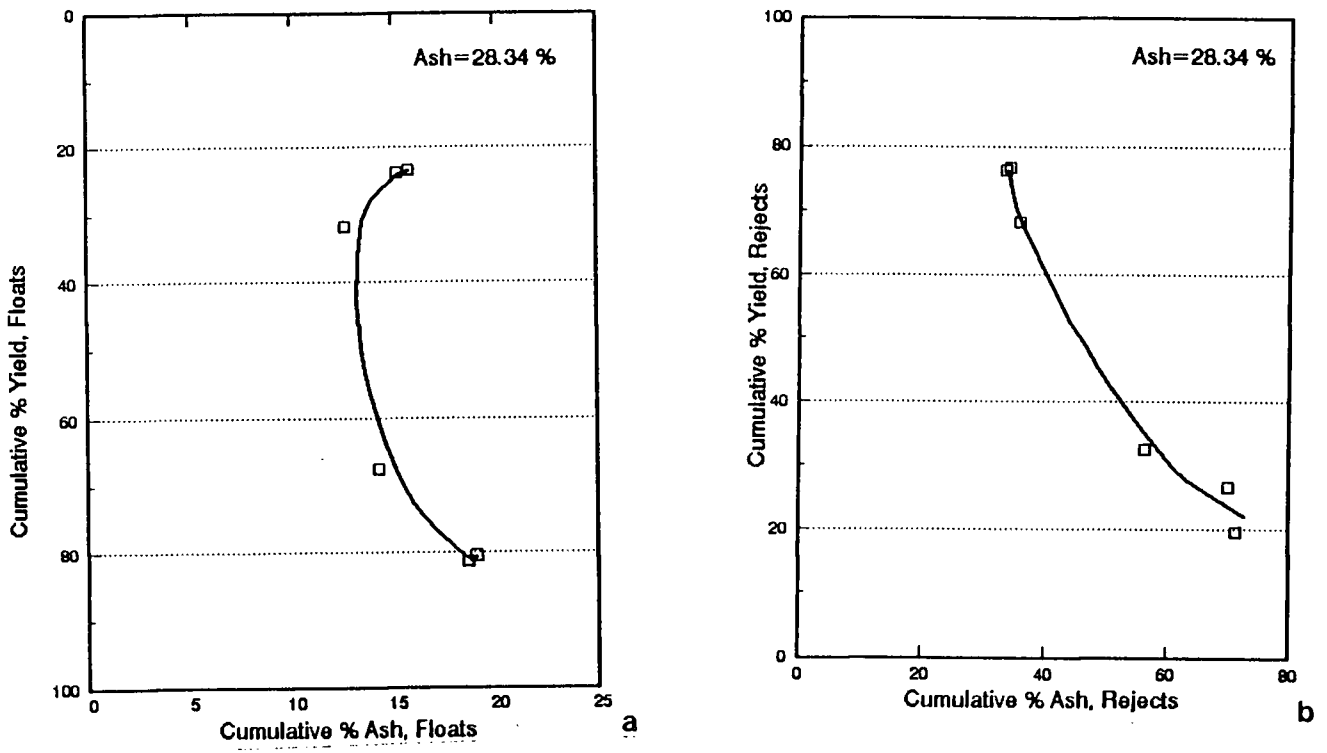

Figure 8.2.10 The cumulative yield versus cumulative ash for the floats and rejects for the high-ash composite sample. (a) floats; (b) rejects.

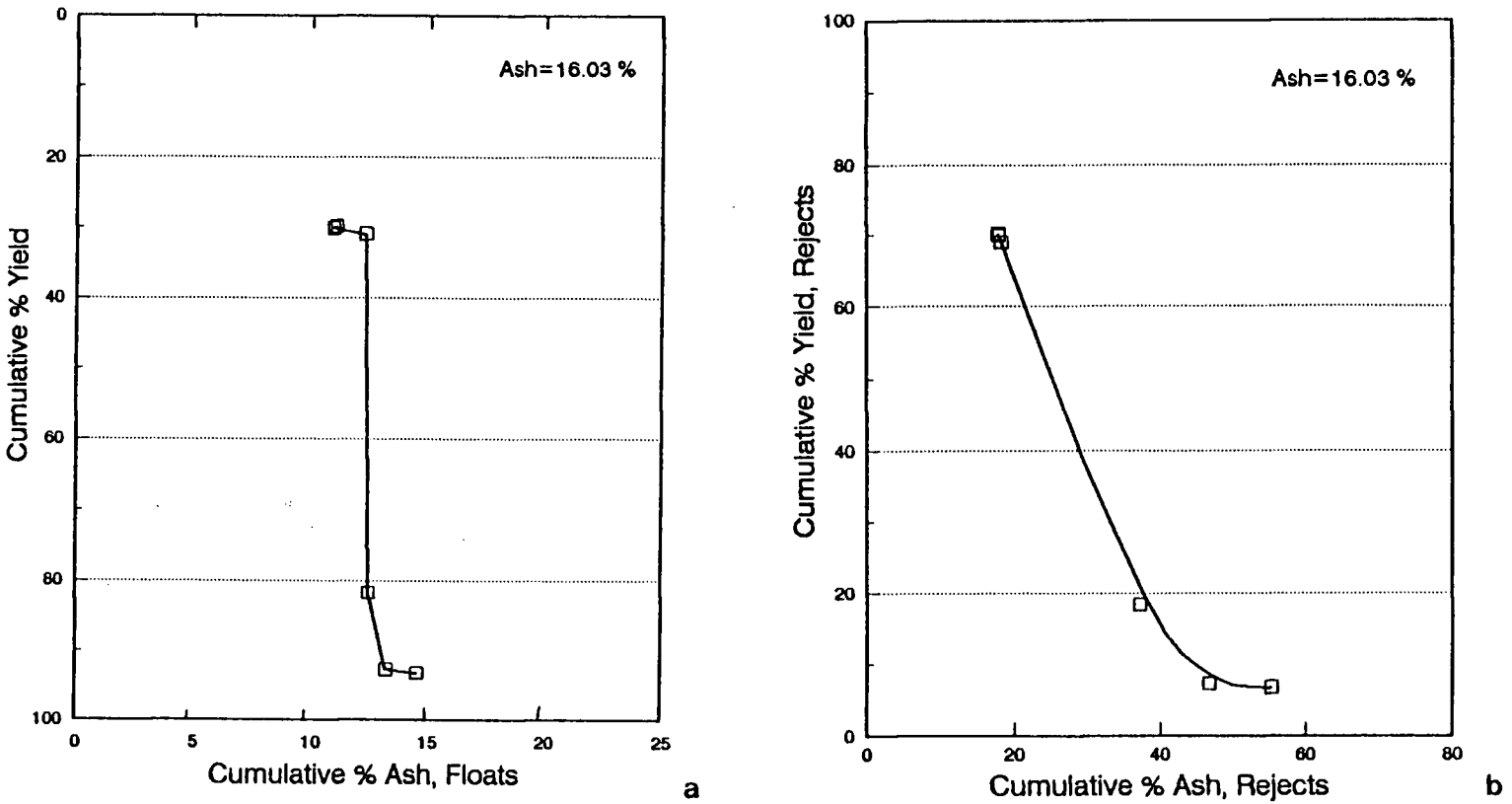

Figure 8.2.11 The cumulative yield versus cumulative ash curves for the floats and rejects for the low-ash composite sample. (a) floats; (b) rejects

curve for the low-ash composite sample indicates that, even though conditioning time for both samples was the same, the peptizing effect appears to be minimal when the ash content is lower.

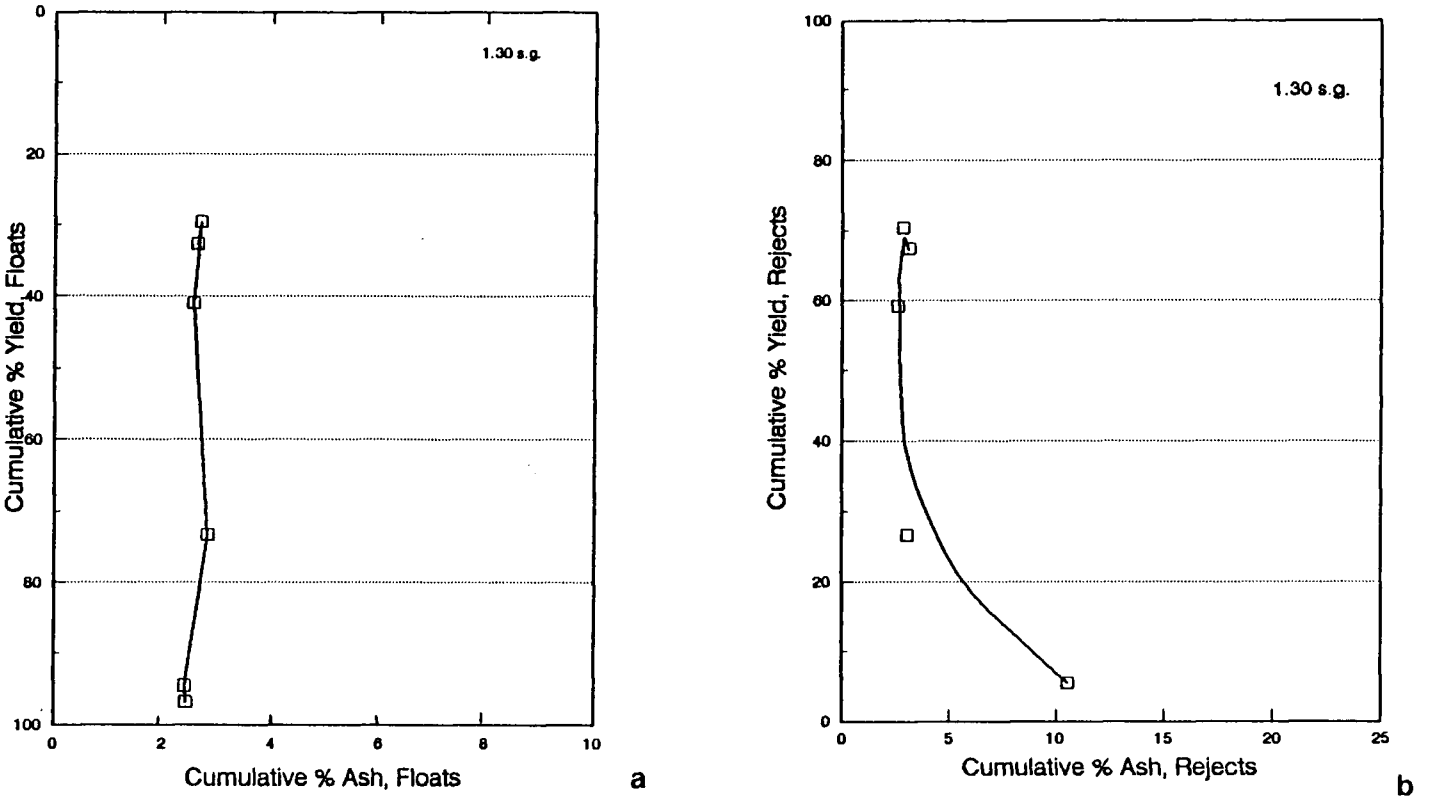

Figure 8.2.12 The cumulative yield versus cumulative ash for the floats and rejects for the < 1.30 specific gravity fraction: (a) floats; (b) rejects.

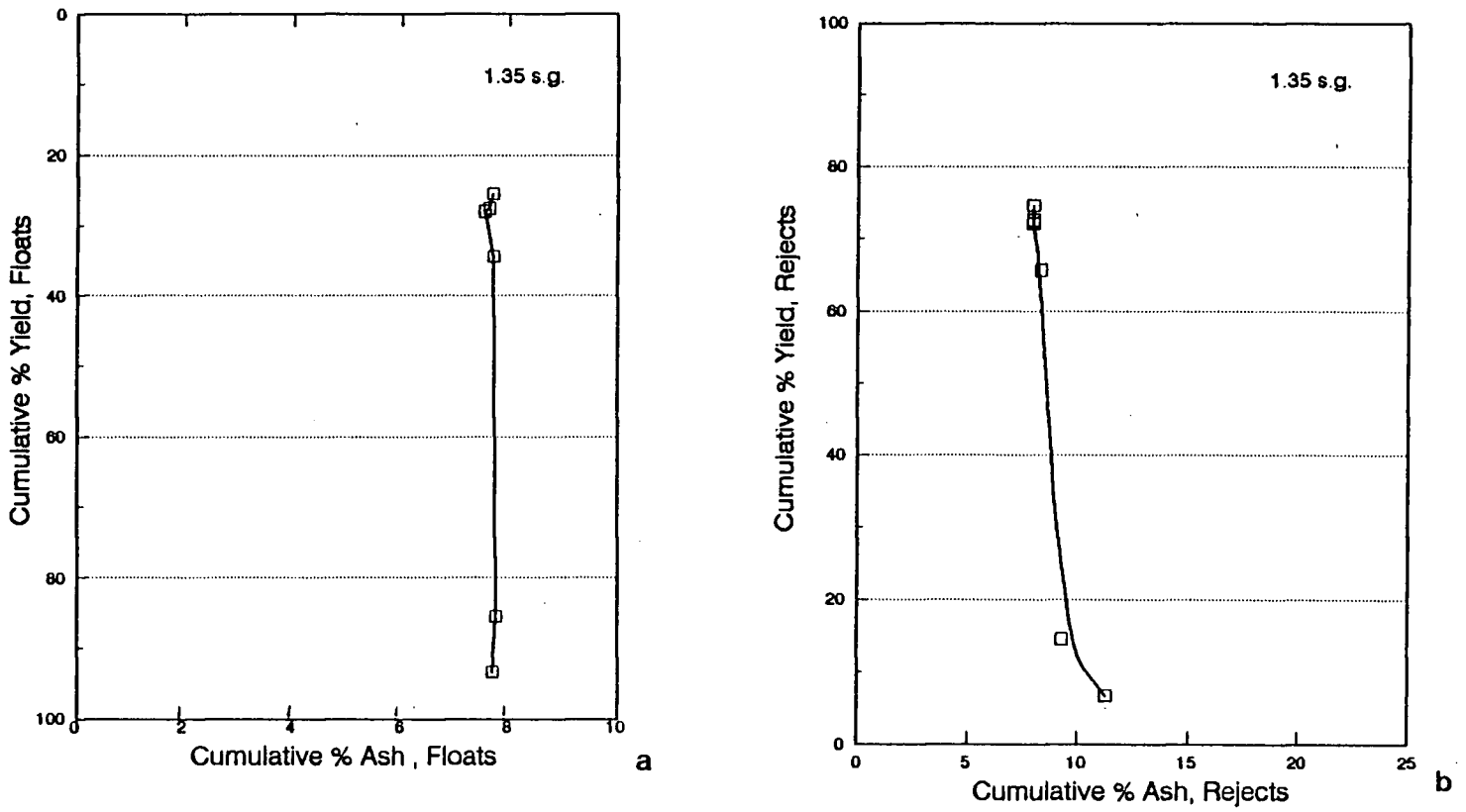

Figure 8.2.13 The cumulative yield versus cumulative ash curves for the floats and rejects for the 1.30 - 1.35 specific gravity fraction: (a) floats; (b) rejects.

The cumulative ash plotted versus cumulative yield of floats and rejects for density fractions are given in the Figures 8.2.12 - 8.2.14. For the two lowest density fractions, the plots indicate no change in ash content as the yield of floats is decreased. This clearly implies that for these samples the separation process does not depend on the ash content of particles. In other words, once the ash content becomes negligible, the other factors which contribute towards surface properties of a given particle become predominant. The third density fraction under consideration showed a different trend in the ash distribution. Apparently the effect of clay peptization becomes pronounced again, as the ash content in this fraction is much higher than in the other two density fractions.

The plots of cumulative ash versus yield of rejects reflect the change in the quality of the non-floating material. The calculated feed ash content obtained from float and reject fractions for all flotation tests has been statistically compared with the measured feed ash values for the corresponding samples and is presented in the Appendix D.

8.2.4 Floatability-washability characteristics

The cumulative ash-cumulative yield curves derived from the flotation in methanol solutions can be considered, by analogy to the washability curves, as floatability-washability curves (Hornsby, 1981; Laskowski, 1986b).

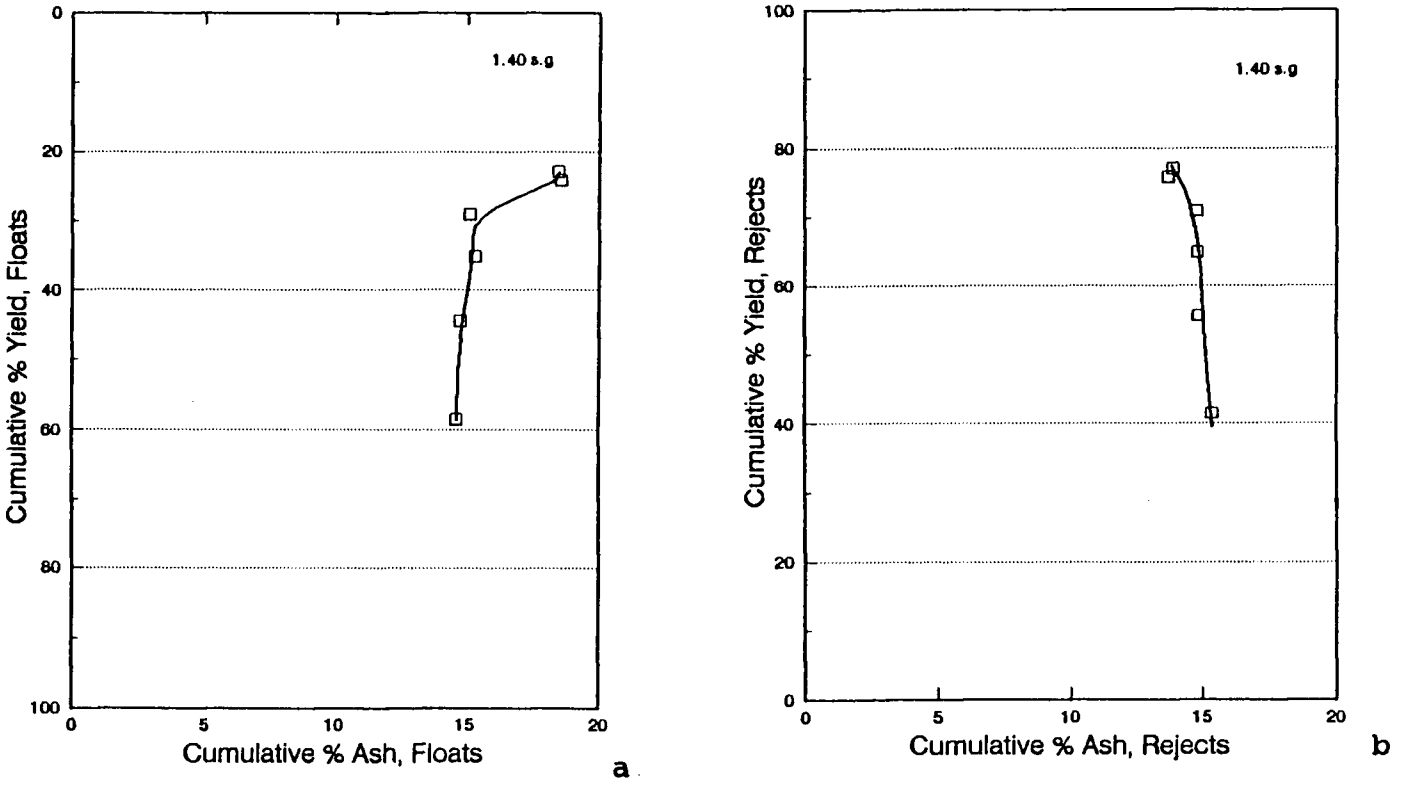

Figure 8.2.14 The cumulative yield versus cumulative ash curves for the floats and rejects for the 1.35 - 1.40 specific gravity fraction: (a) floats; (b) rejects.

In gravity washability tests, coal particles are separated according to their respective densities, and the relationship between the yield and ash is derived to predict the quality of the products from the gravity based processes.

In the flotation tests carried out at varying methanol concentrations, the aim is to separate particles according to their surface properties, namely their γ_{cf}, critical surface tension of floatability, to predict their flotation response.

In gravity separation the density of a single particle plays a decisive role. In general, density is directly proportional to the mineral matter content (density of minerals associated with coals range from 2.5 to 5 s.g.; density of macerals is within 1.1 to 1.45 s.g.). Therefore, the yield-ash relationship predominately depends on the mineral matter content and its association with coal particles.

In floatability tests, particles are separated according to their surface properties. Surface properties of each particle are believed to be an average value of factors such as: mineral matter content (strongly hydrophilic sites); oxidation degree (slightly to highly hydrophilic sites depending on the extent of oxidation) and finally petrographic composition (which represents sites of different degree of hydrophobicity). Mineral matter and the degree of oxidation have the greatest effect on the average surface properties because they present the highly hydrophilic sites on a given coal particle.

In some cases (e.g. medium volatile coal), flotation

response may be predictable from the gravity-washability characteristics because the only factor contributing to hydrophilicity is the presence of mineral matter. However, this does not necessarily mean that even in such a case the washability will be equal to floatability.

A comparison between the floatability-washability and the washability curves for the same composite sample can be made, Figures 8.2.10 and 8.2.15. The cumulative ash versus yield curve of high-ash composite sample obtained from the washability test shows more yield dependance on ash content than the same curve from the floatability-washability.

The cumulative floatability curves were recalculated into the incremental floatability distributions for the studied samples. The incremental ash content was calculated for composite and density samples. Figures 8.2.16 and 8.2.17 present the incremental data for two composite samples. Figures 8.2.18 to 8.2.20 show similar histograms and ash lines for the density fractions. The intervals corresponding to the methanol concentrations in flotation tests (2, 5, 10, 15, 20, 30 and 40 %) were used for incremental data calculation. The flotation fraction within each of the methanol concentrations can be defined by its mean critical surface tension of floatability, γ_{cf}.

The approach using the incremental yields and ash contents of each floatability fraction was introduced by Hornsby (1981). He used 2% intervals of methanol concentration to create incremental yields from the floatability distributions. The average

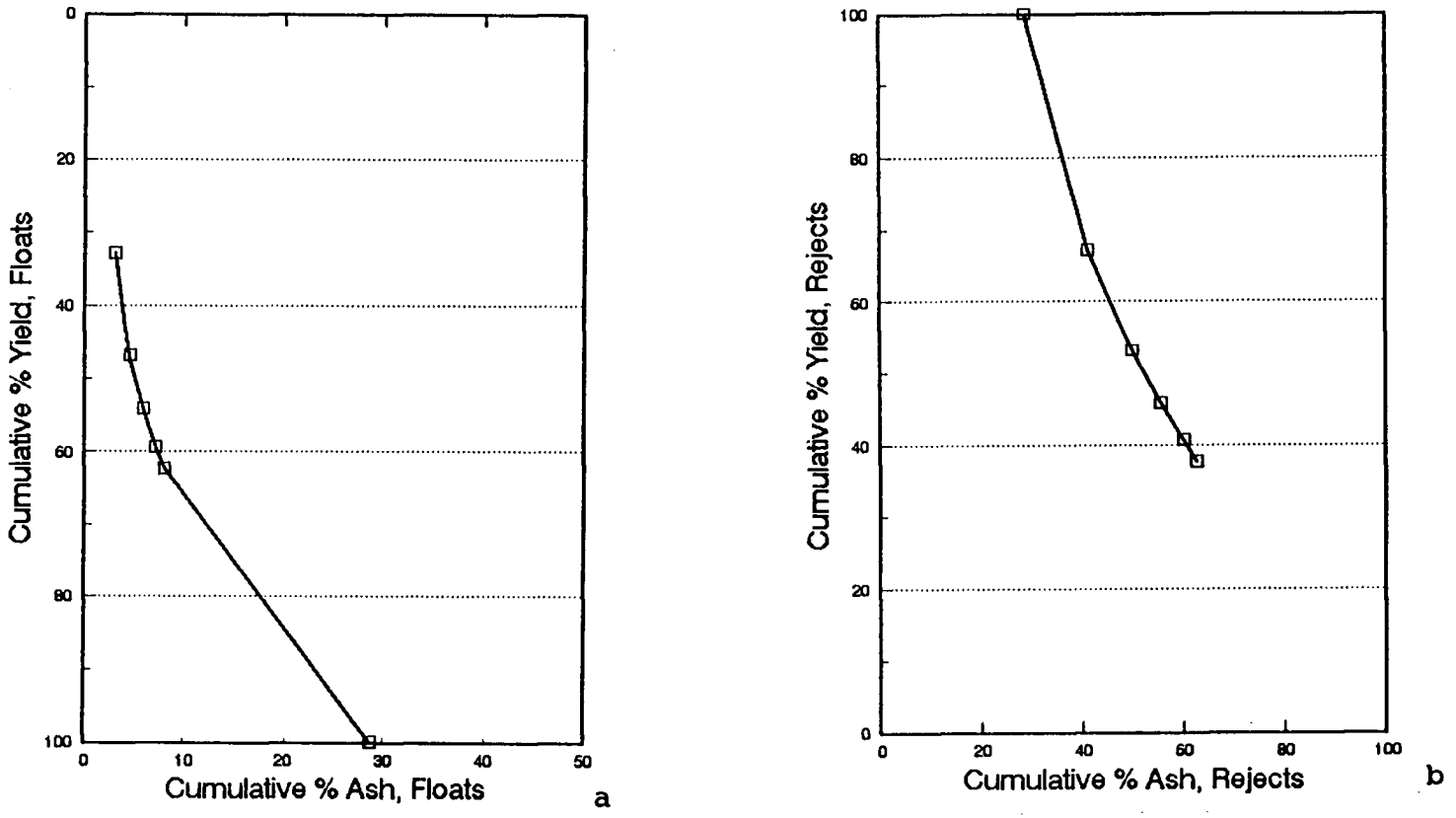

Figure 8.2.15 The cumulative yield versus cumulative ash curves for the high-ash composite sample (from washability): (a) floats; (b) rejects.

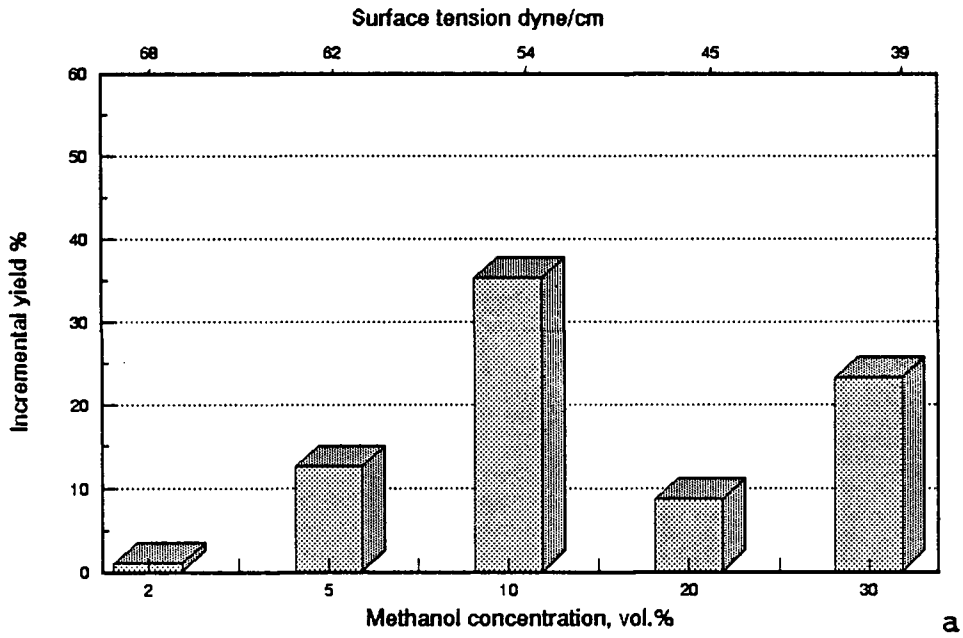

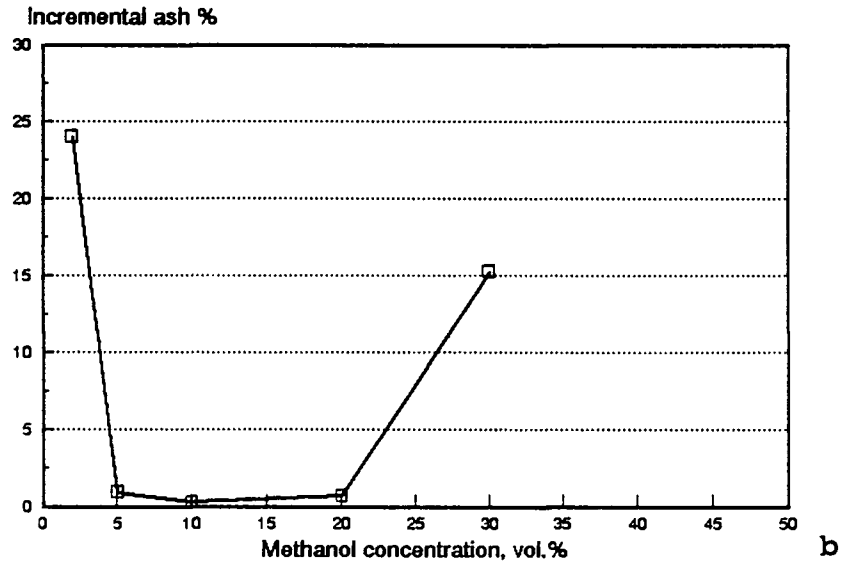

Figure 8.2.16 The incremental yield and ash for the high-ash composite sample: (a) incremental yield histogram; (b) incremental ash plot.

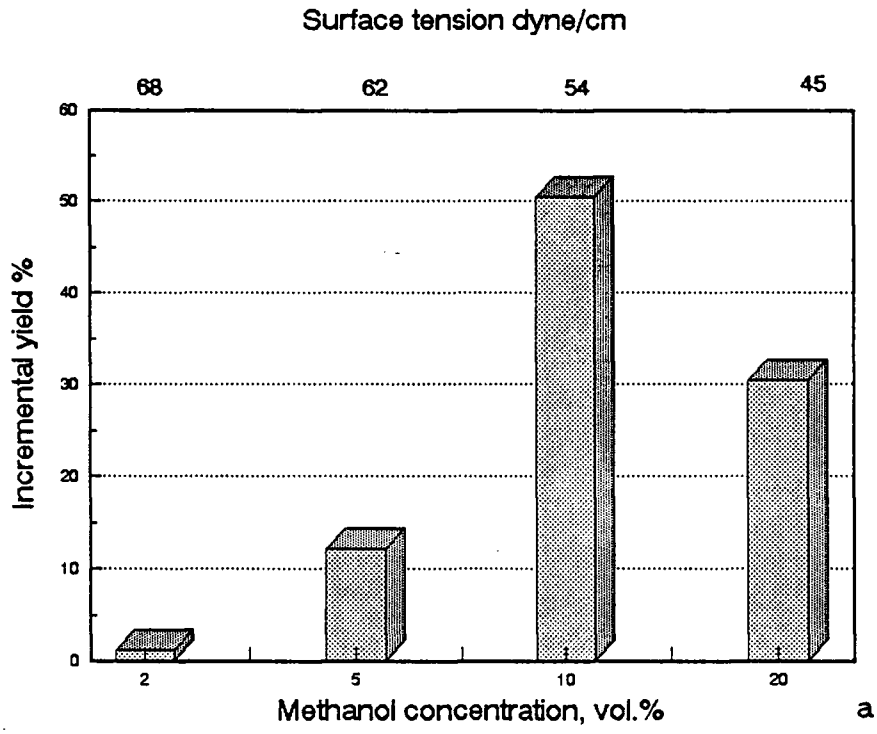

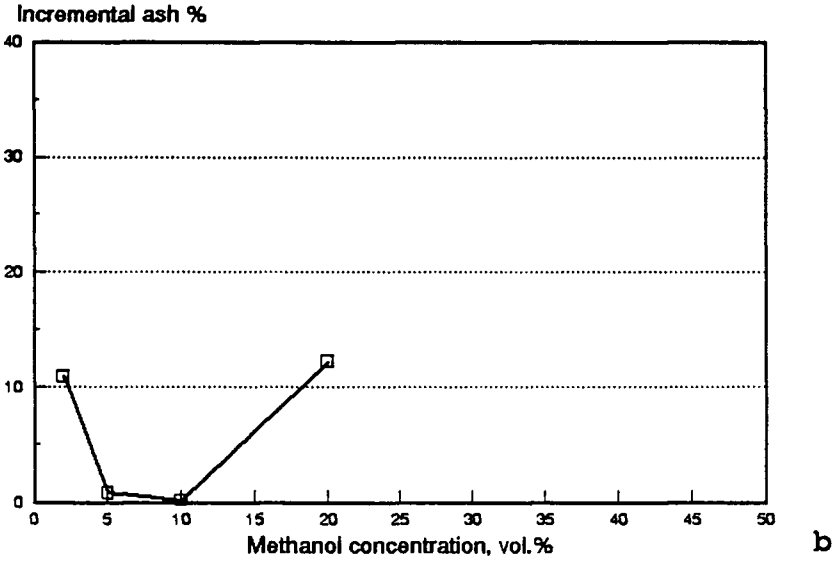

Figure 8.2.17 The incremental yield and ash data for the low-ash composite sample: (a) incremental yield histogram; (b) incremental ash plot.

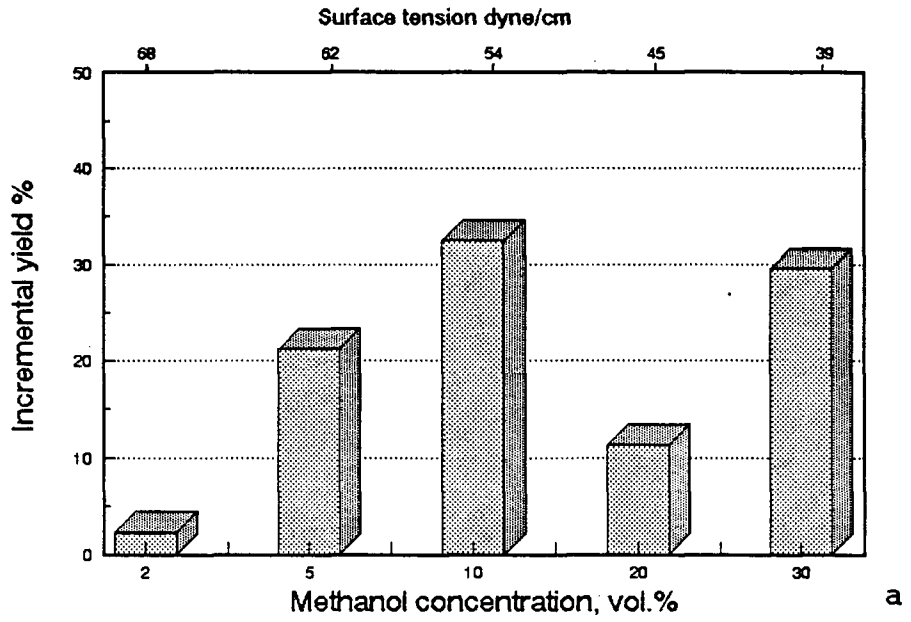

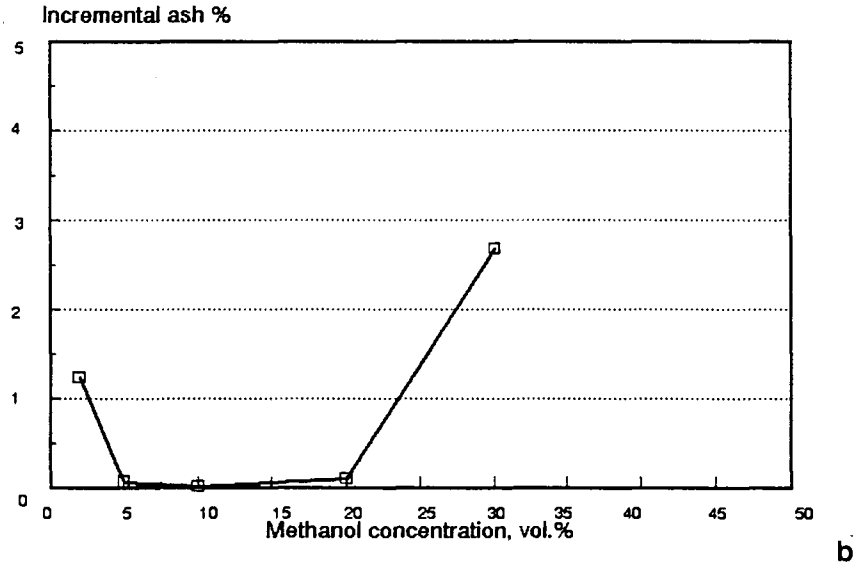

Figure 8.2.18 The incremental yield and ash for the < 1.30 specific gravity fraction: (a) incremental yield histogram; (b) incremental ash plot.

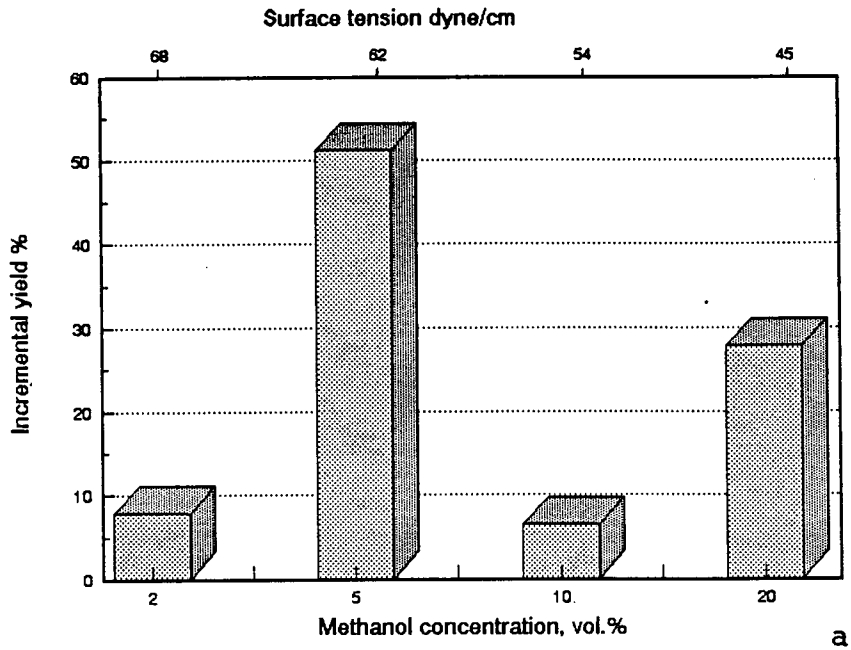

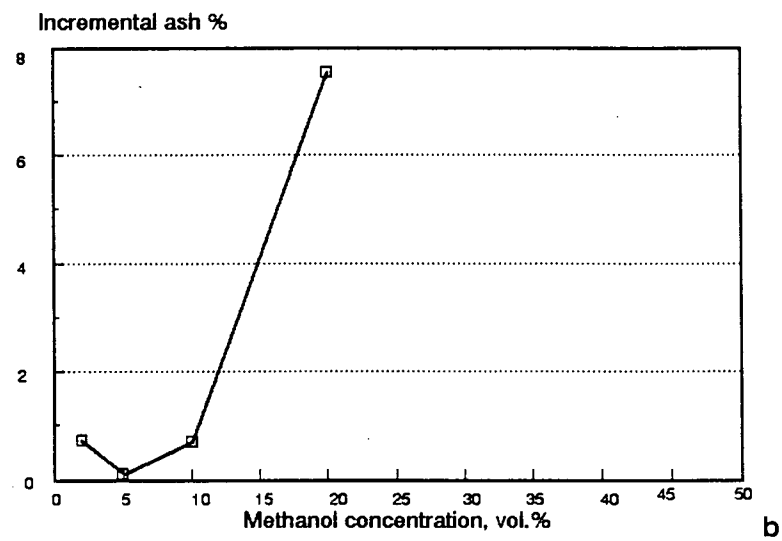

Figure 8.2.19 The incremental yield and ash for the 1.30 - 1.35 specific gravity fraction: (a) incremental yield histogram; (b) incremental ash plot.

floatability of each fraction was characterized by the "floatability number", FN, which is the arithmetic mean of the two boundaries defined by the methanol concentrations. Accordingly, the higher the floatability number of a fraction the more floatable material is in the fraction. Following the same reasoning, histogram distributions of each of the examined samples can be separated into low and high "floatability" regions.

The ash content and floatability are inversely interrelated for the low floatability regions of all samples. The incremental ash reaches minimum values at various methanol concentrations for different samples. For the two composite samples and the lowest density fraction, the minimum is reached at 10 % methanol concentration, the minimum ash content for the lowest density fraction (< 1.30) is at 20 % methanol concentration, for the next lightest (1.30 - 1.35 specific gravity) appears to be at 5 %, and for the 1.35 - 1.40 specific gravity fraction, the ash content is usually constant over the range of methanol concentrations up to 20 %. For all the samples, ash content increases drastically for the floatability fractions over 20 % methanol concentration with the exception of the 1.30 density fraction, where the ash content has the lowest value. This sudden increase in ash content in the high floatability region is attributed to the slimes carry-over into the floats, as discussed in section 8.2.3.

The incremental distributions of the yield versus methanol concentration are the distributions of hydrophobicity for a given sample. Depending on the surface characteristics of

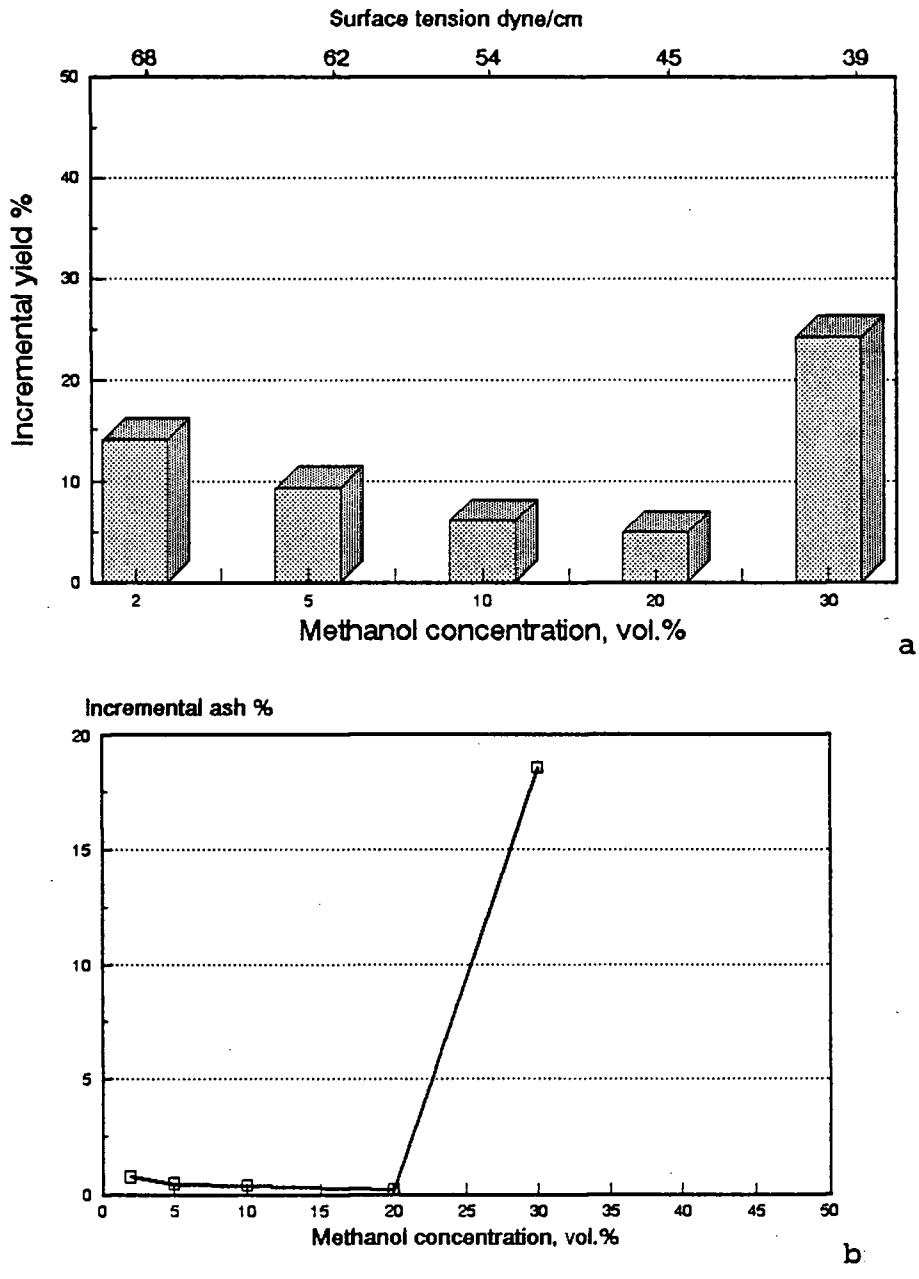

Figure 8.2.20 The incremental yield and ash for the 1.35 - 1.40 specific gravity fraction: (a) incremental yield histogram; (b) incremental ash plot.

particles within the sample, the distribution of floating particles may vary according to their individual average surface properties. For example, the distribution of hydrophobicity of one sample may be considerably different if the average surface properties of the particles are significantly different. In this approach, the average surface properties are characterized by the average critical surface tension of floatability, γ_{cf}.

The majority of the particles in the composite samples were found to be floating at 10 % methanol concentration, and the average γ_{cf}, corresponds to 54 dyne/cm. In the 1.30 specific gravity fraction, the maximum of floating particles appears to be at 10 % and an abundance of floating particles also occurs at 20 % methanol concentration (45 dyne/cm). Most of the particles within the 1.30-1.35 specific gravity fraction are found to be floating at 5 % methanol concentration, and their average γ_{cf}, was 62 dyne/cm, while for the 1.35-1.40 specific gravity fraction, the majority of particles float at 2 % methanol concentration, with average γ_{cf} = 68 dyne/cm.

8.2.5 Microscopic examination of flotation products

Microscopic analyses were carried out on flotation products obtained from the P/S small-scale flotation tests. Initially maceral counts were performed on the floats and rejects following the standard petrographic procedures (Bustin et al., 1983). From maceral analyses alone it was difficult to observe

significant changes in maceral composition in the floats and rejects at different levels of methanol concentration.

The maceral counting technique, as defined in International Handbook of Coal Petrology (1971) is frequently used to estimate quantitively the relative abundance of macerals. This type of analysis is usually satisfactory for petrographic predictions, where relative abundance of macerals provide adequate information. Petrographic analyses have been successfully used in predictions for carbonization processes.

The flotation process, however, relies on the surface properties of separate particles. Therefore, the nature of single particle is more important than the abundance of macerals. However, as each particle is composed of intimately intergrown macerals, grain-type analysis describing composition of each particle is more appropriate.

For the detailed microscopic analysis of flotation products, density fractions were chosen. The maceral counts were performed simultaneously, with full description of each encountered particle. The particles were recorded in the set-up grain-type categories. The important part of the analysis was to describe in the best possible way the association of macerals with each other as well as with the mineral matter. Grain-analyses of density fractions were discussed in section 6.3.4.

Tables A.5 and A.6 (Appendix A) present grain-type analysis of the floats and rejects for 1.30 s.g. and 1.30-1.35 s.g. at different methanol concentrations. The trends in recovery were

observed by comparing the volume percent of floating particles to their content in the feed sample. Figures 8.2.21 and 8.2.22 compare floatability of coal grains for two density fractions.

Detailed grain analysis of the flotation products as obtained from flotations in methanol solutions, shows the segregation of coal grains into fractions of different critical surface tensions. The flotation products of the two lightest density fractions were intentionally chosen for petrographic analysis, because both samples are low in ash content and represent specific maceral concentrates. The lightest (1.30 specific gravity) fraction is enriched in vitrinite and pseudovitrinite, whereas the 1.30-1.35 specific gravity fraction has greater abundance of vitrinite in association with inertinite. The number of vitrinite particles contaminated with mineral matter increases with the density. As the mineral matter level is reduced in low density fractions, the other factors such as petrographic composition become more important.

The grain-type analysis of the flotation products of the 1.30 specific gravity fraction (Figure 8.2.21), shows that there is significant recovery of free vitrinite particles in the floats, at 10 % methanol concentration. The volume percent of free vitrinite particles rose from 60 % by volume in the feed sample to 81 % by volume in the floats, at 10 % methanol concentration. The vitrinite particles in this fraction appear very little contaminated with mineral matter. The floatability trends for pseudovitrinite indicate that a minimum of floatability occurs at 10 % methanol concentration and a maximum at 20 % methanol concentration. In

general, pseudovitrinite levels are reported not to exceed the level in the feed sample.

The flotation of the 1.30-1.35 specific gravity fraction (Figure 8.2.22), shows less pronounced trends in floatability of petrographic grains, as the particles in this fraction have a more composite nature, more vitrinite associated with inertinite (V > I) and inertinite with vitrinite (I > V). Floatability of free vitrinite particles remains at the same level throughout methanol concentrations from 2% to 20 %. The maximum of floatability for free vitrinite is at 30 % of methanol concentration. Vitrinite particles with mineral matter were found to have their maximum floatability at 5 % and 30 % methanol concentrations, and their minimum at 10% methanol concentration (Table A.1.6). Free vitrinite grains included vitrinite particles which were free of association with other macerals, but not free of mineral matter. Therefore, free vitrinite particles floating at 10 % methanol concentration are the least contaminated with mineral matter. The higher floatability of vitrinite with mineral matter at higher methanol concentrations may be the effect of clay peptization at high methanol concentrations, as discussed earlier. The incremental ash for this fraction was found to be quite high, indicating excessive presence of mineral matter (8.2.19.b). Vitrinite with inertinite grains (V > I) were found to have their increased floatability at low methanol concentrations in the range from 2 to 10 % methanol concentrations, and show some drop in floatability at the 20 to 30 % methanol concentration range. Inertinite, inertinite with

vitrinite grains (I > V), and semifusinite were found to float better at 5 % methanol concentration.

8.3 Discussion of the wettability and floatability distributions results

8.3.1 Wettability distributions of different coal samples

Wettability distribution, as derived from film flotation in methanol solutions, is a very convenient way of describing the range of critical surface tensions of an assembly of particles. Three parameters derived from the wettability distribution, as discussed in section 2.1.2., γ_{cmin}, γ_{cmax} and $\overline{\gamma}_c$, characterize particles in relation to their hydrophobicity.

The value of γ_{cmin}, (the surface tension of the solution, that wets all particles), is found for both composite samples, two density fractions and lithotypes, at the same surface tension of 39 dyne/cm (Figures 8.1.1, 8.1.2 and 8.1.3). The γ_{cmax}, was found to be constant for these samples as well, and had a value of 68 dyne/cm. The γ_{cmin}, and γ_{cmax}, as discussed in section 2.1.2, reflects the range of surface properties of particles within an assembly. For particulate coal sample, a band on adhesion tension diagram,(see Figure 2.1.4) represents wettability instead of a discrete line (Hornsby, 1981), resulting in distinct γ_{max} and γ_{cmin}. The previously quoted work by Fuerstenau (1988) indicated

that, the γ_{cmin} for coal particles ranged from at least 30 to 40 dyne/cm. The difference between γ_{cmax} and γ_{cmin}, is a rough indicator of the surface heterogeneity of the sample. For homogeneous particles, γ_{cmax} is almost equal γ_{cmin}. These two values also describe boundaries for wettability of particles for a given assembly. For all examined samples, these limiting boundaries of wettability were the same.

The average critical surface tension of wetting, $\overline{\gamma}_c$, was the only parameter changing markedly for these different samples. For both composite samples was estimated at 54-56 dyne/cm, for lowest density fraction was found at 52 dyne/cm; and for the 1.30 - 1.35 specific gravity fraction at 56 dyne/cm. The values of average critical surface tension for lithotypes $\overline{\gamma}_c$, were as follows: bright and banded bright, $\overline{\gamma}_c$ = 48 dyne/cm; for banded dull and banded coal $\overline{\gamma}_c$ = 54 dyne/cm, and 58 dyne/cm for fibrous (fusain).

The mean value of $\overline{\gamma}_c$ is an important parameter describing each distribution. For the studied samples, even though the boundaries of wettability were the same, each of the sample had distinct wettability distribution. According to Fuerstenau (1988), the difference in $\overline{\gamma}_c$ for coal particles, can be a quantitive measure of variation in surface properties, and was found to be useful index in detecting oxidation. The $\overline{\gamma}_c$ values of fresh and oxidized coals were correlated with the decrease in hydrophobicity. Consequently, using the $\overline{\gamma}_c$, as a parameter, we can define the order of hydrophobicity as follows; among lithotypes the most hydrophobic

are bright and banded bright, then banded dull and banded coal and the least hydrophobic fibrous (fusain). The lowest density fraction (< 1.30 specific gravity) was found more hydrophobic than the next lightest gravity fraction (1.30 - 1.35 specific gravity). Three other fractions were found to be generally hydrophilic over the studied range of surface tensions.

The average critical surface tension of wettability of two composite samples, with significantly different ash contents (28.34% and 16.03%), is quite similar. Comparing wettability distributions of these two samples (Figure 8.2.4 a,b and Figure 8.1.1), one can notice the difference in the yields at any given methanol concentration. This is logical, since the yield of floating particles depends on the amount of mineral particles present in the feed sample. The higher the amount of mineral particles, or coal particles heavily contaminated with mineral matter, the lower the relative yield of the floating fractions. Evidently, the higher amount of mineral matter in the high-ash composite sample does not have a significant effect on the estimation of the average critical surface tension of wettability for these particles. The reason for this is a good liberation of mineral matter in the high-ash sample, as observed under the microscope.

All lithotype samples as described in section 6.3.1, are characterized by rather low ash content (Table 6.3.1), the only compositional difference are in their petrographic make-up. The lithotypes with increased vitrinite contents, bright and banded

bright, displayed the highest hydrophobicity as compared to those enriched in inertinite macerals (Table 6.3.4, Figure 6.3.4).

Similar trends are observed for the two density fractions. The lowest density fraction being a concentrate of free vitrinite macerals, is found to be more hydrophobic than the one which is composed of particles more composite in nature. The second density fraction (1.30 -1.35), is mainly composed of vitrinite with inertinite. In the remaining density fractions, as depicted in Figure 6.3.2 b, particles are heavily contaminated with mineral matter.

8.3.2 Floatability distributions of different coal samples

For an assembly of coal particles with a given range of wettability and other physical characteristics (size, shape, and density), a range of γ_{cf} values exist, as described in section 2.1.3. From the small-scale flotations, in solutions of varying surface tension, the distribution of particles according to their critical surface tension of floatability can be obtained. By analogy to the wettability (see section 8.3.1), the distribution of the critical surface tensions of floatability of a range of particles characterizes each sample. The mean value of critical surface tension of floatability, γ_{cf}, calculated from the floatability frequency distribution, is the actual measure of the average flotation response of a given assembly of particles. An

adjustment of the surface tension of aqueous flotation solutions, provides conditions for the separation of particles into fractions of different floatability.

The average critical surface tension of floatability, γ_{cf}, for both composite samples (Figure 8.2.4) is found at 48 dyne/cm, while for the < 1.30 and 1.30 - 1.35 density fractions (Figure 8.2.7), at 50 and 54 dyne/cm, respectively. Microscopic and ash analyses of the floating fraction at 30 % methanol concentration, of 1.30 specific gravity fraction, reveals that the particles floating at this surface tension should be considered as carried-over slimes, as discussed earlier. As a result, the minimum critical surface tension of floatability is considered to be at 45 dyne/cm (20 % methanol concentration) and an average critical surface tension of floatability for the 1.30 specific gravity fraction is reestablished at 45 dyne/cm. Accordingly, the floatability of the two composite samples appears to be the same, while the floatability of the lowest density fraction has superior floatability to that of other samples.

As quoted in the literature (Hornsby and Leja, 1983; Yarar and Kaoma, 1984; Kelebek and Smith, 1985), the actual shape of the floatability distribution curve indicates the nature of the particles. Highly homogeneous particles can produce almost a straight line, whereas heterogeneous particles will have much broader distributions, with the distinct values of γ_{cfmax} and γ_{cfmin}. Difference between γ_{cfmax} and γ_{cfmin} can also be indicative of relative heterogeneity of particles within the

sample. For the studied composite samples and density fractions, the widest spread between minimum and maximum of critical surface tension of floatability, is found for the lowest density fraction, and the least for the 1.30 - 1.35 specific gravity fraction.

Yarar and Kaoma (1984) related the critical surface tension of floatability of hydrophobic solids, derived from tests in a small-scale flotation cell, to the critical surface tension obtained from contact angle measurements. They found very good agreement between the critical surface tension values obtained by extrapolation of the linear part of the recovery curve to the zero recovery, and the γ_c from the contact angle measurements. The same extrapolation technique as described above is used to estimate the values of γ_c for composite samples and density fractions. These are as follows: 43 dyne/cm for composite samples; 39 dyne/cm for the < 1.30 specific gravity; and 50 dyne/cm for the 1.30 - 1.35 specific gravity fraction.

The evaluation of floatability using the average value of critical surface tension of floatability and critical surface tension reveals that the floatability of particles decreases with increase in density. However, the floatability of the 1.30 - 1.35 specific gravity fraction is by far inferior to that of the < 1.30 density fraction, than one might expect from the increased ash content of this fraction. The ash content of the < 1.30 and 1.30 - 1.35 specific gravity was 3.01% and 7.87%, whereas for the composite sample 16.03 %. The lower floatability of the 1.30 - 1.35 fraction is rather attributed to the increased content of inerti-

nite maceral than to the increased mineral matter content.

The frequency distributions of floatability for various density fractions indicate variations in the surface properties of particles within these fractions. For the 1.30 s.g. fraction (Figure 8.2.18), most of the particles float at 10 % methanol concentration, fewer are floatable at 20 % and 5 % and the least at 2 % methanol concentration. Minimum ash content is found for particles floating in the range from 5 to 20 % methanol concentration. From a floatability-washability point of view, this density fraction is composed of particles whose surface properties are defined by the boundary of 5 to 20 % methanol concentration. The most hydrophobic particles are found at 20 % methanol concentration, (45 dyne/cm), whereas the least hydrophobic at 5 % methanol concentration (62 dyne/cm).

For the next lowest density fraction, (1.30 -1.35 specific gravity), the majority of particles are floatable within a 5 % methanol concentration range, corresponding to 62 dyne/cm, the lowest incremental ash content corresponds to the most abundant fraction (Figure 8.2.19 a,b).

The microscopic analysis of the flotation products (Figure 8.2.21 and 8.2.22), reveals that inertinite particles, or those which are in association with inertinite, appears to have maximum floatability at low methanol concentrations (high surface tensions) and to have the lowest floatability at high methanol concentrations. The sudden drop in flotation of inertinite or particles containing inertinite at high methanol concentration, for

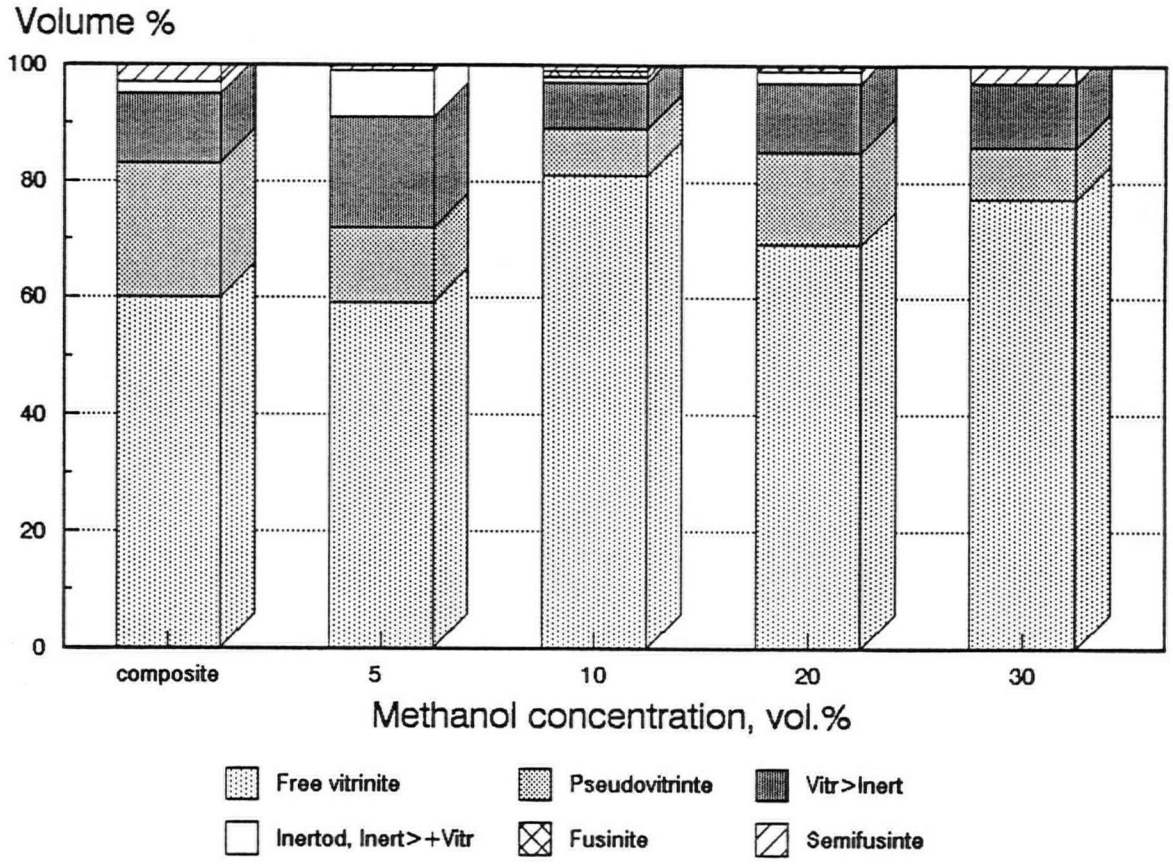

Figure 8.2.21 Floatability of the particles from the < 1.3 density fraction in methanol solutions. Petrographic composition of the floats.

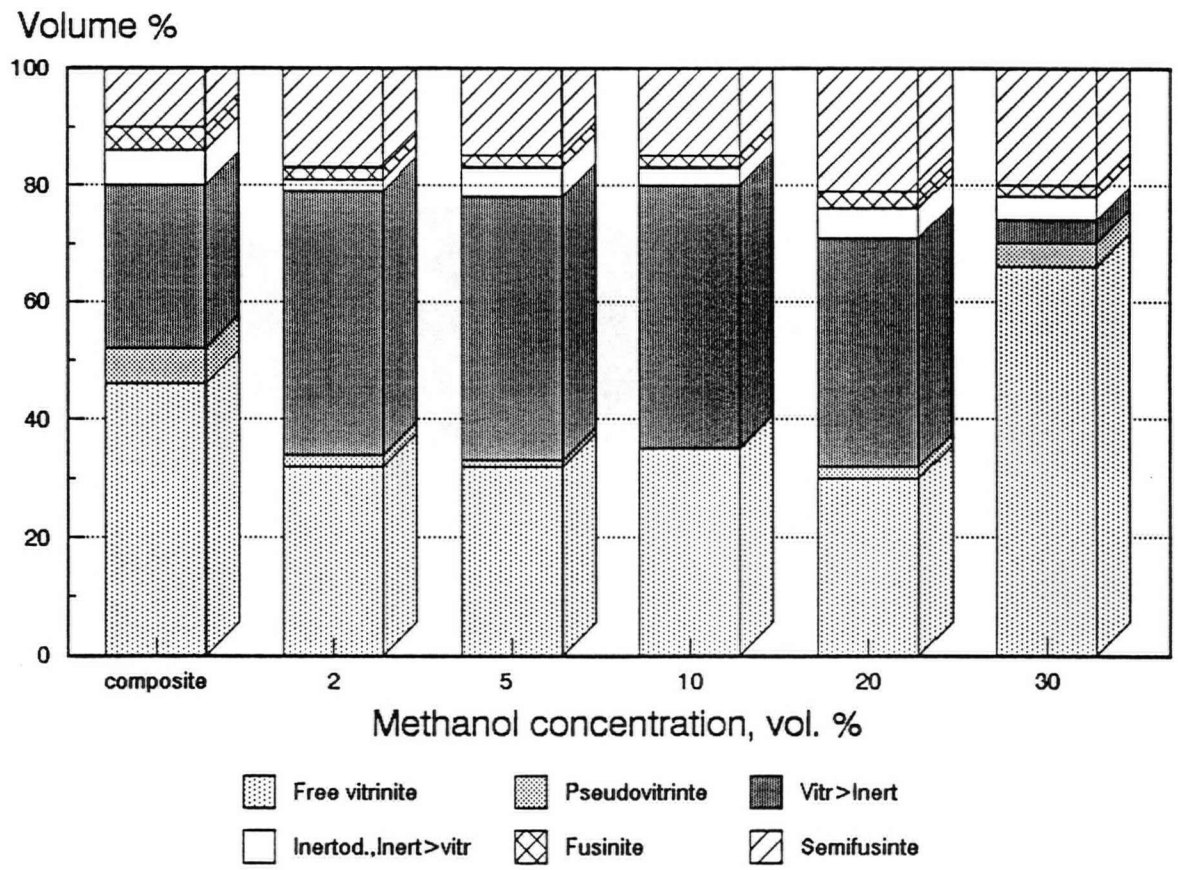

Figure 8.2.22 Floatability of particles from the 1.30 - 1.35 density fraction in methanol solutions. Petrographic composition of the floats.

examined density fractions, may be indicative of specific critical surface tension for these particles. The low floatability of inertinite particles, as compared to vitrinite in medium or low volatile bituminous coals was considered by many (Horsley, 1954; Klassen, 1966; Sarkar, 1984; Bujnowska, 1985) and was found to be related to the structure of this maceral.

8.3.3 Surface properties of coal particles

Surface properties of each coal particle are the result of the heterogeneous nature of coal. The first order of heterogeneity in terms of the surface properties is the presence of highly hydrophilic mineral matter. The second factor contributing to the hydrophilicity is the degree of oxidation of coal particle. Both are usually expressed as bulk parameters. The degree of oxidation is commonly determined by chemical titration, FSI index, transmittance measurements, elemental and IR analyses or other techniques. All of these methods describe bulk parameters for a given assembly of coal particles, and most of them are strongly dependent on and influenced by limiting factors such as ash content or petrographic composition (e.g. FSI, transmittance, etc). Frequently those bulk parameters are not sensitive enough to detect changes in the surface properties (e.g. FSI).

The mineral matter, commonly measured as the ash content, gives the same bulk dimension of this important parameter. The amount of ash in the sample does not necessarily influence the

actual surface properties of single particles, unless it is intergrown with the particle. According to some authors (e.g. Bustamante and Warren, 1983) only when the ash exceeds about half the weight of the grain does it have an effect on surface properties.

The next important component contributing to the surface property of coal is its rank. A change in rank brings about a change in the surface properties of all coal particles. For low-rank coals, relatively small amounts of hydrophilic mineral matter in the composite particle decrease its hydrophobicity, whereas for higher rank, relatively large proportions of mineral matter have little effect on its surface properties (Bustamante and Warren, 1983).

The degree of hydrophobicity may change if the coal particles are oxidized. Low temperature induced oxidation may actually enhance hydrophobicity of some coal particles as discussed by Fuerstenau (1988b) and Ramesh (Ramesh and Somasundaran, 1991). Figure 8.3.1 illustrates the effect of oxidation on a composite sample at various oxidation temperatures. Oxidation may be restricted to certain particles, or even be preferential for certain macerals (Mazeluaar, 1987; Miller and Ye, 1988), and in effect leading to the change in the hydrophobicity of only certain parts of the particle surface. Three different techniques were used to detect oxidation of particles in the examined coal samples. These were: stain test for detection of oxidized particles followed by microscopic observations, alkali-extraction test and a diffuse

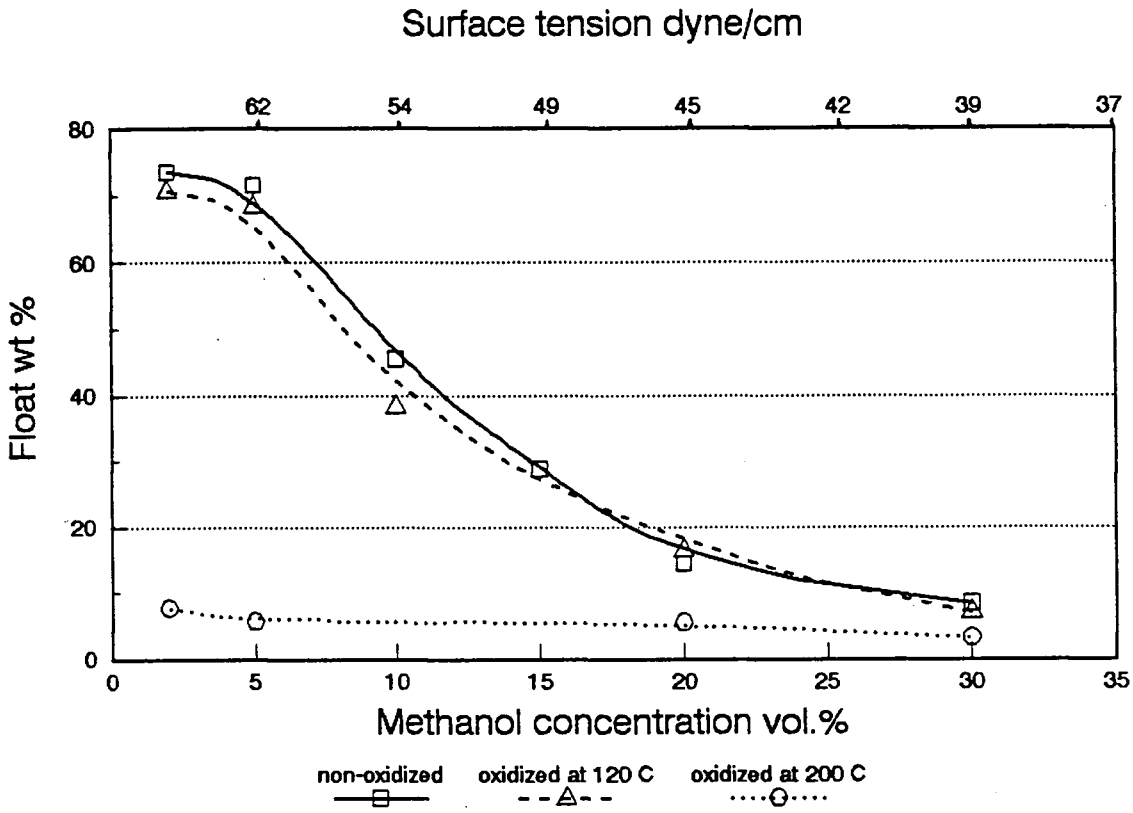

Figure 8.3.1 The effect of oxidation on the floatability of the composite sample at various oxidation temperatures. (a) non-oxidized; (b) oxidized at 120 C; (c) oxidized at 200 C

reflectance FTIR technique. According to these tests, coal particles in the studied samples appeared to have unoxidized surface with the exception of oxidized at 200^{o} C composite sample. A summary of detecting coal oxidation and discussion of the results are given in Appendix C.

A constant search for the explanation of surface heterogeneity in particulate coal population has led some researchers (Ramesh and Somasundaran, 1991) to the conclusion that the population of coal particles are mixtures of individual particles of heterogeneous surfaces. It has been established with the use of film flotation technique, that observed heterogeneity of an assembly of coal particles reflects the heterogeneity of each single particle. In other words, each coal particle possesses various surface sites which vary considerably in surface properties. These sites may represent different degrees of hydrophobicity for each particle.

According to Keller (1987) the surface of coal particle appears as a patchwork assembly of areas ranging from exceedingly hydrophobic identified as paraffinic, to areas exceedingly hydrophilic represented by mineral matter and pores filled with water. In this model, the organic matter is not, however, uniformly hydrophobic, but composed of very hydrophobic paraffinic areas, less hydrophobic aromatic areas and strongly hydrophilic spots with high content of oxygen functional groups. Assuming $\theta = 110^{o}$ for paraffins, $\theta = 88^{o}$ for aromatics, $\theta = 0$ for oxygen sites, $\theta = 0$ for mineral components and $\theta = 0$ for pores, Keller was able to

calculate reasonable wetting of coals of different ranks using Cassie-Baxter (1944).

Macerals as discussed in chapters 3 and 4, differ in chemical composition, and they may be identified as the elements building the patchwork assembly model of coal surface, as proposed by Keller (1987). The macerals are also known to have different surface properties (Klassen, 1966; Hower, 1986; Sarkar, 1984; Bujnowska, 1985; Arnold and Aplan, 1989) leading to their different response to flotation. When the samples are chosen carefully to represent coal particles with the minimum of oxidation and possibly with low mineral matter content, presumably, the only hydrophilic sites on the coal would be those which are the result of heterogeneous petrographic coal structure.

For the studied density samples, the heterogeneity of coal particles, as observed under the microscope, is evident as the variation in petrographic composition. The greatest petrographic variation among coal particles is observed in the two lowest density fractions (Figure 6.3.2). In these fractions coal particles are the least contaminated with the mineral matter, and their petrographic composition is significantly different. The < 1.30 specific gravity fraction, is mainly composed of liberated macerals, free vitrinite and pseudovitrinite, are the most abundant, while in the second lowest density fraction particles of composite nature (V+I; I+V) are increased in numbers. Distribution of particles from the lowest density fraction (Figure 8.2.21), according to their critical surface tension of floatability,

appears to be more pronounced with more apparent segregation of particles into fractions of surface tension. The distribution of particles from the 1.30 - 1.35 density, into fractions of different surface tensions, is less evident. The petrographic composition of the fractions floating at various surface tensions, up to 30 % methanol concentration, does not change drastically. This may indicate that particles composed mainly of two type of macerals, representing different surface properties, have less chance to be separated according to their respective surface tensions, as they are not liberated from each other.

8.3.4 Mineral matter characteristics

The amount of mineral matter becomes an important factor when parameters such as yield of clean coal and yield of rejects are considered. The more mineral matter present in the coal sample, the less the yield of clean coal. However, if the mineral matter is liberated, that is, not associated with the coal particles, it does not contribute to the difficulty of cleaning the coal. The quality of clean coal remains the same as long as the amount of mineral matter does not hinder the process of separation.

The comparison of the cumulative ash versus cumulative yield of floats curves for the two composite samples with considerably different ash contents (Figures 8.2.10 and 8.2.11), shows almost no differences in the quality of flotation products, at yields of clean coal from 30 to 80 % for the low-ash sample, and

from 30 to 70 % for the high-ash sample. The ash content of the clean coal obtained from the low-ash composite sample in this range is 12.5 %, and for the high-ash sample ranges from 12.5 to 13 %, even though the yield of clean coal increase for both samples. The quality of clean coal obtained by flotation of the low-ash sample improves as the yield of product decreases, whereas for the high-ash composite sample, the ash content of the clean coal fractions at low yields is much higher, which, as discussed before, indicates the effect of clay peptization at high methanol concentrations. In the low-ash composite sample at high yields of floats, ash tends to increase, even though the yield stays constant, which suggests that the more particles are floating, the greater the chance of mineral matter particles being trapped within the hydrophobic film.

The density distribution of the high-ash composite sample (Table G.1 in Appendix G) shows an abundance of the high density mineral matter fraction, which contributes to high ash in the sample. Most of which is in liberated form, since it was relatively easy to remove it in a simple gravity separation process without major change in hydrophobicity distribution, and reduce its ash from 28.34% to 16.03% in the composite sample. Microscopic examination of the composite sample confirms the presence of high amounts of clays as separate bands. In some cases, clays fill cleats and cavities in macerals, with fewer particles intimately intergrown with mineral matter.

The cumulative ash-yield relationships for the two density fractions (<1.30, and 1.30-1.35), shows that the quality of

products does not change when the yield increases. It can be concluded that for these samples floatability does not depend on the ash content (mineral matter). The ash content for these samples was 3.01% and 7.87% respectively. For the 1.35-1.40 fraction, the low-yield floatability is attributed to the higher ash content. As observed from petrographic analysis, this sample is very high in content of mineral matter confined to the coal particles. From grain analysis (Figure 6.3.2), over 60 % of vitrinite particles were contaminated with mineral matter; therefore, the yield of floating fractions in maximum floatability region was much lower than for the two lower density fractions. The low floatability of this and remaining density fractions may also be attributed to the fact that the mineral matter in these fractions was unliberated. It may also be concluded, that for this coal, the maximum acceptable mineral matter content at which the surface properties are still determined by coal organic matter (macerals) and not by mineral matter, is 14.89 % (ash content of 1.35 - 1.40 fraction). At higher ash contents, surface properties of this coal sample are predominantly determined by the mineral matter content.

8.3.5 Petrographic composition

Petrographic analysis of the density fractions (Figure 6.3.1) shows that the lightest fraction is overwhelmingly enriched in vitrinite, while the subsequent density fractions have shown to have greater abundance of inertinite macerals. Liptinite content in

examined coal is negligible, as discussed earlier. Grain-type analysis (Figure 6.3.2) reveals more details about the character of coal particles within each density fraction. On the basis of this examination, the two lightest density fractions, <1.30 and 1.30-1.35, represent the highest variation in the proportion of vitrinite and inertinite content. The 1.35-1.40 fraction, has more inertinite, however, most of it is in association with vitrinite, and almost 70 % of all vitrinite is contaminated with mineral matter. An increase in density above 1.35 specific gravity appears to be caused mainly by the increasing proportions of mineral matter in the composite grains, rather than variations in relative proportions of inertinite and vitrinite.

The wettability and floatability distributions of these two density fractions are different. As discussed in sections 8.1.2 and 8.2.2.2, the 1.30 specific gravity fraction has a much wider spectrum of surface tensions among coal particles. The 5 % methanol concentration region shows increased floatability of particles composed mainly of inertinite with vitrinite (I > V) and vitrinite with inertinite (V > I), (Figure 8.2.21). The particles floating at 10 % methanol concentration are the most abundant in this density fraction. This coincides with the maximum floatability for free vitrinite grains as found from microscopic analysis. Coal grains floating at 20 % methanol concentration are found to be enriched in free vitrinite and pseudovitrinite, which may indicate that this surface tension was the critical surface tension for those particles. This range is a high floatability region, and the most

hydrophobic particles would only be floatable at this surface tension. This implies that pseudovitrinite has higher hydrophobicity than other macerals, which is in agreement with the largest contact angle measured for this maceral (Arnold and Aplan, 1989).

The 1.30-1.35 fraction has the majority of particles floating at 5 % methanol concentration. From the microscopic analysis it was observed that, particles floating at this surface tension are vitrinite with inertinite (V > I and I > V) with fewer free vitrinite grains (Figure 8.2.22). There is some increased amount of free vitrinite floating at 10 % methanol concentration. For this density fraction it is more difficult to observe pronounced trends in maceral floatability, as the majority of particles are of a more complex nature. The critical surface tension for the majority of particles in this density lies at 5 % methanol concentration, corresponding to 62 dyne/cm.

For both density fractions, the yield of floating particles is independent of ash content, and therefore it is possible to assume that resulting floatability and wettability distributions are caused by variations in the petrographic composition of coal grains.

From wettability distributions of lithotypes one can notice that, lithotypes with increased inertinite content (banded dull and banded coal) have the region for the floatability (film flotation) of majority of particles shifted towards lower methanol concentration. The mineral matter content does not appear to have an influence on the floatability of the particles. The ash content

of floating fractions at different surface tensions is almost constant over the studied range (Figure 8.1.3 a,b). Banded bright and bright lithotypes have their majority of particles floating at 10 and 20 % methanol concentration, whereas banded dull and banded coal lithotype particles are floating at 5 and 10 % methanol concentrations.

In general, for the examined coals, vitrinite enriched samples have maximum particles floating at 10 % methanol concentration (55 dyne/cm). The maximum floatability region for pseudovitrinite is at 20 % methanol concentration (45 dyne/cm), and for composite vitrinite and inertinite particles it is at lower methanol concentration (2 to 5 methanol concentrations that is at 62-68 dyne/cm).

8.4 Comparison of the wettability and floatability distributions

Wettability distributions of coal particles for two composite samples, density and size fractions, were examined and compared to the floatability distributions. Since wettability and floatability are not necessarily synonymous, floatability established under dynamic conditions, does not have to be identical to the wettability, derived from the static test such as film flotation.

Film flotation, as implemented by Fuerstenau et al.,-(1985; 1987; 1987a; 1988a,b), provides the means to determine the

average value of critical surface tension of wettability for an assembly of hydrophobic particles. For heterogeneous particles the minimum and maximum surface tension are the values representing the range of the critical surface tensions for a given assembly of particles. A band of wettability lines on the adhesion tension diagram will be produced instead of one wettability line (Hornsby, 1981; Hornsby and Leja, 1983; see Figure 8.4.1 a,b). In some cases the band may be extended to $\theta = 0$. Only for very homogeneous solids, one wettability line characterizes the critical surface tension of wettability.

In film flotation, particles are placed on the surface of the solution and particles are imbibed at a given surface tension when their contact angle just reached zero. Due to gravitational effects, sinking usually occurs at contact angles slightly greater than zero (Fuerstenau, 1988b). The value of θ_{cw} is always higher than zero. The boundary of wettability for an assembly of particles can be found from the intercept of the adhesion tension line with θ_{cw}, the critical contact angle of wettability. The theoretical example illustrating the γ_{cmin} and γ_{cmax} of wettability, for the examined coal samples, is depicted in Figure 8.4.1, a,b. The values of γ_{cmin} and γ_{cmax} are taken from the estimated wettability ranges for the < 1.30 and 1.30-1.35 density fractions (see section 8.3.1).

In small-scale flotation under actual flotation conditions, a particle is floatable only if it successfully attaches to air bubble and is lifted with it out of the flotation slurry. For this to occur, not only does partial dewetting of the particle

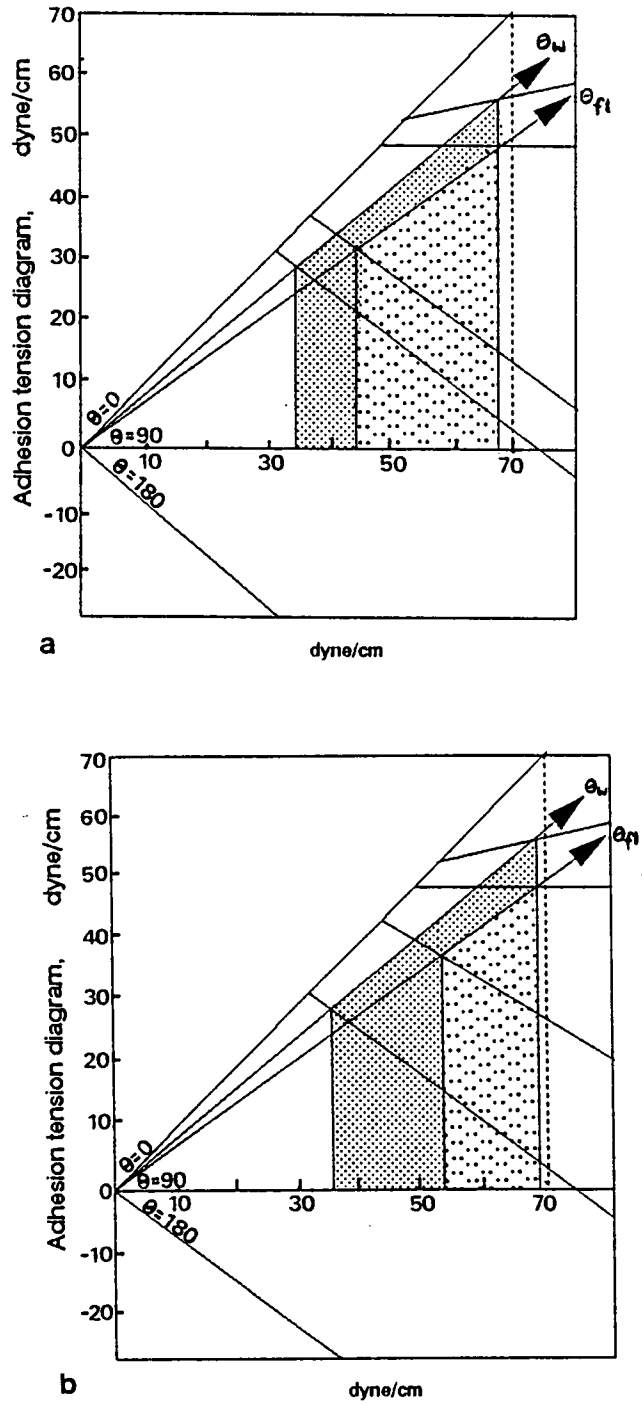

Figure 8.4.1 The theoretical adhesion tension diagram for the examined coal. Limits for wettability and floatability for: (a) the <1.30 density fraction; (b) the 1.30-1.35 density fraction.

surface have to be hydrodynamically possible, but several other criteria have to be satisfied (Laskowski, 1974; Trahar and Warren, 1976). The particle must collide with a bubble, the adhesion must occur within time of contact, and the particle-bubble aggregate must be stable enough to allow for the separation from the flotation slurry, as discussed in section 2.1.3. Under these conditions, size and density may become limiting parameters in floatability. Since, in both small-scale and film flotation tests, only narrow size and density fractions were used, such a comparison is more credible. The contact angle, θ_{cf}, corresponding to γ_{cfmin} and γ_{cfmax} (estimated from floatability distributions, section 8.3.1), for the examined samples is much greater than the one corresponding to γ_{cwmin} and γ_{cwmax} (critical surface tension of wettability). This would indicate that the minimum contact angle of floatability, θ_{cf}, is higher than minimum contact angle of wettability θ_{cw}, for the examined coal samples (Figure 8.4.1 a,b).

A comparison of the wettability and floatability distributions of the low-ash composite sample (Figure 8.1.1,b and 8.2.4,b) indicates very similar distributions of coal particles versus surface tensions. The yield of floating particles, at any given methanol concentration in the wettability distribution (film flotation), is much lower than for the same particles in the floatability distribution (small-scale flotation). The ash content of the flotation products from film flotation decreases as the methanol concentration increases (Table F.1.1). The same trend is noticed for the floats obtained from small-scale flotation (Table

E.1.1). The ash content of the floating products obtained from both types of flotation appears to be very similar. The small-scale flotation shows more selectivity; for the same ash content the yields of floating particles are higher in small-scale flotation than the yields of floating fractions in film flotation experiment. Lower selectivity of film flotation is believed to be due to the entrapment of small particles within the hydrophobic film.

The wettability and floatability distributions of density fractions can be compared (see Figures 8.1.2 and 8.2.7). Trends in the wettability and floatability distributions for the density fractions are very similar. Film flotation is again less selective than small-scale flotation, over the studied range of methanol concentrations. For the dynamic flotation conditions (small-scale flotation) in high methanol concentrations the small-light hydrophobic particles are more selectively separated than in the film flotation.

To delineate the dependance of both methods on the size of floating particles, the small-scale and film flotations were carried out with four different size fractions as described in sections 8.1 and 8.2. Different size fractions were obtained from the vitrain lithotype (natural concentrate of vitrinite) to avoid the influence of petrographic composition on wettability and floatability distributions (Figure 8.1.4 and 8.2.3). It is evident that small-scale flotation is more dependant on the size of the floating particles than film flotation.

CHAPTER 9

CONCLUSIONS

The aim of the study was to show an influence of petrographic composition on the surface properties of coal particles. Concepts of critical surface tension of wettability and critical surface tension of floatability have been used to investigate the floatability and wettability of coal samples with varying petrographic composition.

9.1 General

The heterogeneity of a coal particle surface was examined microscopically. It was shown that surface heterogeneity of coal is strongly influenced by the amount of unliberated mineral matter, degree of oxidation and petrographic composition.

The petrographic contribution to the surface heterogeneity, as determined from wettability and floatability tests, becomes dominant only when the effect of other factors such as mineral matter content, degree of oxidation and size of coal particles are negligible. The petrographic components represent only different degrees of the hydrophobicity, whereas parameters such as mineral matter and oxidation represent strongly hydrophilic sites on the surface of coal particle.

Under certain conditions, wettability and floatability

distributions of particles according to their critical surface tension are shown to be sensitive to variation in petrographic composition of coal grains. Once petrographic composition becomes a significant factor in hydrophobicity, the yield-ash relationship is independent of the mineral matter content.

Petrographic heterogeneity of coal might not necessarily match its surface heterogeneity, it certainly contributes towards its complexity.

9.2 Wettability distribution of various coal particles

Wettability distributions were obtained from film flotation for a number of coal samples varying in petrographic composition. The lithotypes and the two lowest density fractions were used in the tests, since they displayed the most pronounced change in petrographic composition of coal grains. All these samples have low ash content to avoid the contribution of hydrophilic minerals to the surface properties of the coal particles.

In wettability tests, particles were separated according to their critical surface tension of wettability. The mean value of the critical surface tension of wettability, $\overline{\gamma}_c$, was estimated from the wettability distributions for each of the samples. For samples enriched in vitrinite, the average value of γ_{cw}, is always lower than that for samples high in inertinite. Since, each of the samples still represents an assembly of particles of varying

surface tensions, the minimum, γ_{cmin}, and maximum, γ_{cmax}, values of the critical surface tension of wettability are observed. These values are the same for the two lowest density fractions, and for all the lithotypes and they may indicate the range of wettability for these particles.

Wettability distribution is almost independent of the size of floating particles. Film flotation test is found to be less selective than the small-scale flotation test, due to different hydrodynamic conditions.

9.3 Floatability distributions of various coal particles

In the floatability tests, which were carried out as small-scale flotation tests (P/S cell), particles were separated according to their critical surface tension of floatability, γ_{cf}. The floatability and non-floatability ranges were again characterized by the values of γ_{cf}^{min}, and γ_{cf}^{max}. These ranges, however, are different for each sample and much narrower, than the ranges in critical surface tension of wettability, especially for samples of varying petrographic composition.

Floatability distributions are found to be independent of the liberated mineral matter content. Only when the mineral matter occurred as unliberated from the composite coal grains it effected the floatability distributions.

The yield-ash relationships of flotation products are independent of mineral matter content for the two lightest density

fractions. For the composite samples the yield-ash relationships are only independent of the mineral matter in the range between maximum and minimum of floatability.

Floatability distributions of the particles from different density fractions are found to differ significantly in shape. This indicates that these fractions contained particles of different surface properties. Microscopic analyses confirmed variation in petrographic composition of coal grains in the studied density fractions.

In general, as observed under the microscope, samples enriched in free vitrinite have their maximum floatability at 10 % methanol concentration (54 dyne/cm). This value is in good agreement with the γ_c values for vitrain samples reported elsewhere (Eissler, 1962). Samples, where coal particles are of more composite nature (vitrinite with inertinite), have the maximum floatability shifted towards low-floatability regions (low-methanol concentration). The pseudovitrinite grains are found to have their maximum floatability at 20 % methanol concentration (45 dyne/cm) that is at high-floatability regions indicating the highest hydrophobicity. This is found to be in an agreement with the greater values of contact angle measured on this maceral, as reported in the literature (Arnold and Aplan, 1989).

A comparison of the wettability and floatability distributions confirms, that flotation response of particles cannot be fully predicted from wettability characteristics. Small-scale flotation is shown to be more selective in separating particles

into fractions of equal critical surface tensions. The floatability distributions as obtained from the small-scale flotation are more dependant on the size of floating particles.

CHAPTER 10

RECOMMENDATIONS

The present study is believed to be the first one to derive critical surface tension values of macerals by techniques different than contact angle.

Natural concentrates of macerals were used to assess the relationship between wettability and petrographic composition of coal. Due to insufficient quantities of the lithotypes (natural maceral concentrates), detailed studies of floatability of these samples were limited. Therefore the following recomendations are proposed:

- larger quantities of lithotypes will be rquired to study their response to the small-scale flotation in methanol solutions;

- more comprehensive microscopic analysis of flotation products should be applied to assess quantitevely recovery of various coal grains in flotation in methanol solutions;

- the selective flotation of macerals should be studied using their estimated values of critical surface tension of floatability;

- the clay peptizing effect in high methanol concentrations should be investigated in greater detail.

The segregation of coal petrographic components during the commercial flotation process is noteworthy, however, practical application may not always be feasible. A comprehensive study is needed to investigate the rate of flotation of different petrographic components in relation to their critical surface tension of floatability.

REFERENCES

Adamson, A.W., 1967, Physical Chemistry of Surfaces, Interscience, New York.

Alpern, B., Lemos de Sousa, M.J., and Flores, D., 1989, A progress report on the Alpern Coal Classification; International Journal of Coal Geology, 13, pp. 1-19.

American Standards for Testing Materials, ASTM D 2013 - 72,

American Standards for Testing Materials, ASTM D 2798 - 72, (reaproved 1976)

American Standards for Testing Materials, ASTM D 2799 - 72 (reproved 1976)

American Standards for Testing Materials, ASTM D 2797 - 75,

American Standards for Testing Materials, ASTM D 3888 - 77,

Ammosov, I.I, Ergmin, I.V., Sukhenko, S.F., and Oshurkova, L.S., 1957, Calculation of coking charges on the basis of petrographic characteristics of coals; Koks and Khimia, 12, pp.9-12.

Anfruns, J.P., and Kitchener, J.A., 1977, Trans. IMM, Sec. C, 86, C9.

Aplan, F.F., 1983, Estimating the floatability of Western coal; in Gold, Silver, Uranium and Coal: Geology, Mining, Extraction and the Environment, AIME, M.C. Fuerstenau and B.R. Palmer eds., New York, p.380.

Aplan, F.F., 1989, How the nature of raw coal influences its cleaning; Industrial Practice of Fine Coal Processing, chapter 13, pp.99-111.

Arnold, B.J., and Aplan, F.F., 1989, The hydrophobicity of coal macerals; Fuel, 68, pp.651-658.

Barysznikow, F.A., 1940, Flotation of some Kuzbass coals; Klassen, W.I, Coal flotation, Flotacja wegla, (in Polish) transl. by J.Laskowski, p.217-224.

Benedict, L.G., Thompson, R.R., Shigo, J.J., and Aikman, R.P. 1968, Pseudovitrinite in Appalachian coking coals; Fuel, 47, pp.125-143.

Benedict, L.G., Thompson, R.R., 1973, Coal and coke petrography and coke reactivity; presented at Geological Society of America, Pennsylvania, March, 1973.

Berkowitz, N., 1979, Chemical properties; in An introduction to coal technology; Academic Press, New York, pp.95-130.

Blom, L.L., Edelhausen and van Krevelen, 1957, Chemical structure and properties of coal - XVIII - oxygen groups in coal related products, Fuel, 36, pp.135-153.

Brady, G.A., and Gauger, A.W., 1940, Properties of coal surfaces, Ind. Eng. Chem., 32, p.1599.

Brown, H.R., Taylor, G.H., and Cook, A.C., 1964, Prediction of coke strength from the rank and petrographic composition of Australian coals; Fuel,43, pp.43-54.

Brown, D.J., 1962, Coal Flotation; in Froth Flotation 50th Anniversary Volume, D.W. Fuerstenau, ed., AIME, New York.

Bujnowska, B., 1985a, Floatability of petrographic constituents of coals of various coalification degree; Proc.; International Conference on Coal Science, Sydney, Australia, publ. by Pergamon Press, pp.541-543.

Bujnowska, B., 1985b, Studies on floatability of petrographic constituents of subbituminous coal; Coal Preparation,1, pp.169-188.

Bustamante, H., and Warren, L.J., 1983, Relation between the relative density of composite coaly grains and their flotation recovery; International Journal of Mineral Processing, 10, pp.1-17.

Bustin, R.M., 1982, The effect of sharing on the quality of some coals in the Southeastern Canadian Cordillera, CIM, Bulletin, 75, pp.76-83.

Bustin, R.M., Cameron, A.R., Grieve, D.A., and Kalkreuth, W.D., 1983, Coal Petrology: Its principles, methods and applications; Geological Association of Canada Short Course, May 8-10, 1983.

Campbell, J.A.L., and Sun, S.C., 1970, Bituminous coal electro-kinetics, Trans. SME/AIME, 247, pp. 11-114.

Cassie, A.B.D., and Baxter, S., 1944, Trans. Faraday Soc., 40, p.546.

Cassie, A.B.D., 1948, Contact angles; Discuss. Faraday Soc.,3, pp.11-16.

Chandra, D., 1962, Reflectance and microstructures of weathered coals; Fuel, 41, pp.185-193.

Chapman, W.R., 1922, Differential froth flotation applied to coal;

Fuel, 4, p.52.

Choi, Ch., Bloomquist, C.A.A., and Dyrkacz, G.R., 1989, Adsorption of surfactants on coals and macerals; Energy and Fuels, 3, pp.38-42.

Cook, A.C. 1981, What are we trying to separate?; Separation Science and Technology, 16, (10), pp.154-1569.

Crelling, J.C., Schrader, R.H., and Benedict, L.G., 1979, Effects of weathered coal on coking properties and coke quality; Fuel, 58 pp.542-546.

Cudmore, J.F., Denney, B., McDonald, A., and Ng, N., 1986, Use of petrographic analysis in coal preparation practice; in Proc. of Australian Coal Industry Research Laboratories, symposium on Improving the froth flotation of coal, pp.135-155.

Davis, A., Spackman, W. and Given, P.H., 1976, The influence of the properties of coals on their conversion into clean fuels; Energy Sources, 3(1), pp. 55-81.

Davis, A., 1978, The reflectance of coal; Analytical Methods for Coal and Coke, I, C.Karr, ed., Academic Press, New York, pp. 27-81.

Dieminowa, O.A., 1957, Selective separation of hard coal components from Kuzbass; Klassen, W.I, Coal flotation, Flotacja wegla, (in Polish), transl. by J.Laskowski, Wyd. Slask, pp.217-224.

Diessel, C.F.K., 1965a, An appraisal of coal facies based on maceral characteristics; Australian Coal Geology, 4, part 2, pp. 474-482.

Diessel, C.F.K., 1965b, Correlation of macro- and micropetrography of some New South Wales Coals; Proc. of 8th Commonwealth Mining and Metalurgical Congress, 6, pp.669-677.

Drozd, R. 1985, The Bullmoose mine project: Coal in Canada; T.H. Patching, ed., CIM, Special Volume 31 pp. 263-268.

Dupre, A., 1869, Theorie mechanique de la chaleur; Gautjer-Villars, Paris, p.386.

Dyrkacz, G.R., Bloomquist, C.A.A., and Horwitz, E.P., 1981, Laboratory scale separation of coal macerals; Separation and Technology, 16 (10), pp.1571-1588.

Dyrkacz, G.R., Bloomquist, C.A.A., and Ruscic, L., 1984a, Chemical variation in coal macerals separated by density gradient centrifugation; Fuel, 63 , pp.1166-1172.

Dyrkacz, G.R., Bloomquist, C.A.A., and Ruscic, L., and Horwitz, E.P., 1984b, Variations in properties of coal macerals elucidated by density gradient separation; American Chemical Society, Chemistry and characterization of coal macerals, Washington, D.C., pp.65-77.

Eissler, R.L. and Van Holde, K.E., 1962, Wettability of coal, graphite, and naphthalene as measured by contact angles; Illinois State Geological Survey Circular, 333, pp.1-20.

Elyashevitch, M.G., 1941, Krayevye ugly smatchivanya kak kritierii flotacyonnoy sposobnosti ugley; Klassen, W.I, Coal flotation, Flotacja wegla, (in Polish), transl. by J.Laskowski, Wyd. Slask.

Falcon, R.M.S, 1978, Coal in South Africa, part 2, The application of petrography to the characterization of coal; Minerals Science Engineering, 10, no.1, pp. 28-53.

Falcon, L.M, and Falcon, R.M.S., 1983, The application of coal petrography to certain beneficiation techniques on South African Coal; Geological Society of South Africa, Special Publication 7, pp. 137-148.

Falcon, L.M., and Falcon, R.M.S., 1987, The petrographic composition of Southern African coals in relation to friability, hardness, and abrasive indices; Journal of South African Institute of Mining and Metallurgy, 87, no. 10, pp. 323-336.

Finch, J.A., and Smith, G.W., 1975, Bubble-solid attachment as a function of bubble surface tension; Canadian Metallurgical Quarterly, 14 (1), pp.47-51.

Finkelman, R.B., 1982, Mineral Matter in Coal: Origin,Characterization for Coal-Processing Technologies; in Coal Science, vol.2; M.L. Gorbaty, J.W Larsen, and I.Wender, eds., Academic Press, p.5.

Fowkes, F.M., 1963, Dispersion force contribution to surface and interfacial tensions, contact angles, and heats of immersion. Advances in Chemistry Series, 43, Contact angle, wettability and adhesion, pp.99-111.

Fox, H.W., and Zisman, W.A, 1950, The spreading of liquids on low-energy surfaces. Polytetrafluoroethylene; J. Colloid Interface Sci., 5, pp.514-531.

Fuerstenau, D.W., Rosenbaum, J.M., and Laskowski, J., 1983, Effect of surface functional groups on the flotation of coal; Colloids and Surfaces, 8, pp.153-174.

Fuerstenau, D.W., Williams, M.C., Urbina, R.H., 1985, Assessing the effect of oxidation on the wettability and flotation response of coal; Proc.:International Conference on Coal Science, Pergamon:

Sydney, Australia, pp.517-520.

Fuerstenau, W., Yang, G.C.C., and Laskowski, J., 1986, Oxidation phenomena in coal flotation. Part 1. Correlation between oxygen functional group concentration, immersion wettability and salt flotation response; Coal Preparation, 2, pp.1-22.

Fuerstenau, D.W., Narayan, K.S., Herrera-Urbina, R., and Diao, J.L., 1987a, Assessing the effect of oxidation on the wettability and flotation response of coal; Conference on Coal Science, J.A. Moulijn, ed., Elsvier, Amsterdam, pp.475-478.

Fuerstenau, D.W., Yang, G.C. and Chander, S., 1987b, Characterization of coal interfacial behavior through flow microcalorimetry; American Chemical Society: Structure and Properties of Low Rank Coals, Surface Chemistry of Coals, Preprints of papers presented at Denver, Colorado, April 5-10, 1987.

Fuerstenau, D.W., and Williams M.C., 1987, Characterization of the Lyophobicity of Particles by Film Flotation; Colloids and Surfaces, 2, pp.87-91.

Fuerstenau, D.W., Diao, J.L., Narayan, K.S., and Herrera-Urbina, R.H., 1988a, Assessment of film flotation efficacy for the characterization of solid surfaces; Interfacial Phenomena in Biotechnology and Materials Processing, Y.A. Attia, B.M. Moudgil and S. Chander, eds., Elsvier, Amsterdam.

Fuerstenau, D.W., Williams, M.C., Narayan, K.S., Diao, J.L., and Urbina, R.H., 1988b, Assessing the wettability and degree of oxidation of coal by film flotation; Journal of Energy and Fuels, 2, pp.237-241.

Fuerstenau, D.W., Rosenbaum, J.M., and You, Y.S., 1988c, Electrokinetic behavior of coal; Journal of Energy and Fuels, 2, pp.241-245.

Garshva, S., Contreras, S., and Goldfarb, J., 1978, Hydrophobic characterization of powder; Colloid and Polymer Science, 256, pp.241-250.

Gaudin, A.M., 1957, Flotation, second edit., McGraw Hill, New York.

Gaudin, A.M., Miaw, H.L., and Spedden, H.H., 1957, Native floatability and crystal structure; Proc. Second Intern. Congr. Surface Activity, 3, pp.202-219.

Gibbs, J.W., 1928, The Collected Works of J.W. Gibbs; vol.1. Longmans-Green, New York.

Given, P.H., 1960, The distribution of hydrogen in coals and its

relation to coal structure; Fuel, 39, pp.147-153.

Given, P.H., 1984, An essay on the organic geochemistry of coal; in Coal Science, vol.3, M.L. Gorbaty, J.W. Larsen, and I. Wender, eds., Academic Press, New York, London.

Glanville, J.O., and Wightman J.P, 1980, Fuel, 58, p.557.

Good, R.J., and Girifalco, L.A., 1960, A theory for estimation of surface and interfacial energies. III. Estimation of surface energies of solid from contact angle data; Journal of Physical Chemistry, 64, pp.561-565.

Good, W.R., 1973, A comparison of contact angle interpretations; J. Coll. Interface Sci., 41,(1), pp.63-71.

Gorbaty, M.L., Larsen, J.W., and Wender, I., 1984, Coal Science, vol.2., Academic Press, New York, London.

Gray, R.J., Rhodes, A.H., and King, D.T., 1976, Detection of oxidized coal and the effect of oxidation on the technological properties; Trans. of SME/AIME, 260, pp.334-341.

Gray, D., 1978, Inherent mineral matter in coal and its effect upon hydrogenation, Fuel, 57, pp. 213-216.

Gray, R.J., Goscinski, J.S., and Shoenberger, R.W., 1978, Selection of coals for coke making; presented at AIME meeting, October 3, 1978.

Gray, R.J., and Lowenhaupt, D.E., 1989, Aging and weathering; Sample Selection, Aging, and Reactivity of Coal, R. Klein and R. Wellek, John Wiley and Sons, eds., New York.

Griffiths, P.R., Fuller, M.P., Hamadeh, I.M., and Lowenhaupt, D.E., 1982, Fuel, 61 , pp.529-536.

Gutierrez-Rodriguez, J.A., Purcell, R.J., and Aplan, F.F., 1984, Estimating the hydrophobicity of coal; Colloids and Surfaces, 12, pp.1-25.

Harkins, W.D., 1952, The Physical Chemistry of Surface Films; Reinhold Publ. Corp., New York.

He, Y.B., and Laskowski, J.S., 1991, Contact angle measurement on fine coal particles, Coal Preparation, in press.

Hevia Rodriguez, V. and Prado, G. 1961, Precision de los analysis de macerales realizados en el Instituto Nacional del Carbon; Bol. Inform. Inst.Nac.Carbon, 52, pp.1-19.

Hornsby, D.T.B., 1981, The floatability of coal and other inherent-

ly hydrophobic solids in relation to the surface tension of aqueous methanol solutions; Ph.D. thesis, The University of British Columbia, Vancouver, B.C., Canada.

Hornsby, D.T., and Leja, J., 1980, Critical Surface tension and the selective separation of inherently hydrophobic solids; Colloids and Surfaces, 1, pp.425-429.

Hornsby, D.T., and Leja, J., 1983, Critical surface tension of floatability; Colloids and Surfaces, 7, pp.339-349.

Horsley, R.M., and Smith, H.G., 1951, Principles of coal flotation; Fuel, 30, pp.54-63.

Hower, J.C., Frankie, K.A., and Wild, G.D., and Trinkle, E.J., 1984, Coal microlithotype response to froth flotation in selected Western Kentucky coals; Fuel Processing Technology,9, pp.1-20.

Hower, J.C., Trinkle, E.J., and Wild, G.D., 1986, Maceral partitioning through beneficiation of Illinois basin coals; Coal Preparation, 2, pp. 149-164.

Hower, J.C., Graese, A.M., and Klapheke, J.G., 1987, Influence of microlithotype composition on Hardgrove Grindability Index for selected Kentucky Coals; International Journal of Coal Geology, 7, pp.227-244.

Hower, J.C., 1988, Additivity of Hardgrove Grindability a case study; Journal of Coal Quality, 7, no.2, pp.68-70.

Hower, J.C., and Linberry, G.T., 1988, The interaction of coal lithology and coal cutting on the breakage characteristics of selected Kentucky coals; Journal of Coal Quality, 7, no.3, pp.88-95.

Hower, J.C., Esterle, J.S., Wild, G.D, and Pollock, J.D., 1990, Perspectives on coal lithotype analysis; Journal of Coal Quality, 9, no.2, pp.48-52.

Ignasiak, B.S., Szladow, A.J., and Montgomery, D.S., 1974, Oxidation studies on coking coal related to weathering. 3. The influence of acidic hydroxyl groups, created during oxidation, on the plasticity and dilatation of the weathered coking coal; Fuel, 53,(2).

Ignasiak, B.S., Gawlak, M., 1977, Polymeric structure of coal Fuel, 56 (2), pp. 216-222.

Ignasiak, B.S., Ignasiak, T.M., and Berkowitz, N., 1975, Advances in coal analysis, Reviews in Anal. Chem., II(3), pp.278-298.

Ihnatowicz, A., 1952, Studies of oxygen groups in bituminous coals,

Prace Glownego Instytutu Gornictwa, Komun., No. 125, (Polish text).

International Handbook of Coal Petrology, ICCP, 1963, second edition, Centre National de la Recherche Scientifique, Paris.

International Handbook of Coal Petrography, ICCP, 1971, supplement to the second edition, Centre National de la Recherche Scientifique, Paris.

Iskra, J., and Laskowski, J.S, 1967, New possibilities for investigating air-oxidation of coal surfaces at low temperatures; Fuel, 46, pp.5-12.

Jameson, G.J., Nam, S., and Moo Young, M., 1977, Physical factors affecting recovery rates in flotation, Miner. Sci. Eng., 9 (3), pp.103-118.

Jeremic, M.L., 1980, Coal strengths in the Rocky Mountains; World Coal, 6 (9), pp.40-43.

Johnson, R.E, 1959, Conflicts between Gibbsian thermodynamics and recent treatment of interfacial energies in solid-liquid-vapor systems; Journal Phys. Chem.,63, pp.1655-1658.

Jowett, A., 1980, Preparation of low ash coal for carbonization and conversion processes, Proc. Australas. Inst. Min. Metall., No. 275, pp.5-16.

Kalkreuth, W., Leckie, D.A. and Labonte, M., 1989, Gates formation (Lower Cretaceous) coals in Western Canada: A sedimentological and petrographical study; Contributions to Canadian Coal Geoscience; Geological Survey of Canada, Paper 89-8, pp.14-25.

Kelebek, S., 1987, Wetting behavior and related properties of aqueous methanol solutions; Colloids and Surfaces, 28, pp.219-232.

Kelebek, S., 1987, Wetting behavior, polar characteristics and flotation of inherently hydrophobic minerals; Trans. IMM, Sec.C, 96, pp.103-106.

Kelebek, S., and Smith, G.W., 1985, Selective flotation of inherently hydrophobic minerals by controlling the air-solution interfacial tension, Int. J. Miner. Process., 14, pp.275.

Keller, D.V., Jr., 1987, The contact angle of water on coal; Colloids and Surfaces, 22, pp.21-35.

Kitchener, J.A., 1960, Gravity, the contact angle and Young's equation; Proc. of the Third Internation Congress of Surface Activity, Cologne, pp. 426-432.

Klassen, W.I, 1953, Eliemienty tieorii flotacyi kammiennyh ugliey;

Ugletiechizdat, (Russian text).

Klassen, W.I, 1966, Flotation of petrographic components; Flotacja wegla, Coal flotation, (in Polish) transl. by J.Laskowski, Wyd. Slask.

Kroger, C., and Bade, E., 1961, Klassen, W.I, Coal flotation, Flotacja wegla, (in polish) transl. by J.Laskowski, Wyd. Slask, pp.217-224.

Lamberson, M.N., Kalkreuth, W., and Bustin, R.M. 1989, Petrology, sedimentology of Gates Formation coals, northeastern British Columbia: preliminary results; Contribution to Canadian Geoscience, Geological Survey of Canada, Paper 89-8, pp.88-95.

Lamberson, M.N., Bustin, R.M., Kalkreuth, W., and Pratt, K.C., 1990, Lithotype characteristics and variation in selected coal seams of the Gates Formation, northeastern British Columbia; Geological Fieldwork 1989, Paper 1990-1, British Columbia Geological Survey Branch, Min. of Energy, Mines and Petrol. Resources, pp.461-467.

Larsen, J.W., Kovac, J., 1978, Polymer structure of bituminous coals; in Organic Chemistry of Coal, J.W. Larsen ed., Washington D.C., American Chemical Society, Symposium Series, (71), pp.36-49.

Laskowski, J.S., 1964, Fizyko-chemiczne podstawy i niektore zagadnienia technologii procesu flotacji kopalin; Skrypty Uczelniane, Nr.104, Politechnika Slaska, Gliwice, (Polish text).

Laskowski, J.S., 1968, Vliyanye poviernostnyh svoystv ugley na ich flotiruyemost, Proc. of 8th Int. Mineral Processing Congress, Mekhanobr, Lenningrad, 1, pp.626-631.

Laskowski, J., and Kitchener, J.A., 1969, The hydrophilic-hydrophobic transition on silica; Journal of Colloid and Interface Science, vol.29, No. 4, April 1969, pp. 670-679.

Laskowski, J.S., 1974, Particle-bubble attachment in flotation; Miner. Sci. Eng., 6, pp.223-235.

Laskowski, J.S., 1986a, The relationship between floatability and hydrophobicity; Advances in Mineral Processing, P. Samosundaran, ed., chapter 11, pp.189-208.

Laskowski, J.S., 1986b, Flotation of difficult-to-float coals; Proc. of the 10th Inetrnational Coal Preparation Congress, Edmonton, CIM, 1, pp. 122-142.

Laskowski, J.S., 1987, Coal electrokinetics: the origin of charge at coal/water interface; ACS, Preprints of Papers Presented at Denver, Colorado, April 5-10, 1987, Structure and Properties of Low

Rank Coals, Surface Chemistry of Coals, pp.367-377.

Laskowski, J.S., and Parfitt, G.D., 1989, Electrokinetics of coal-water suspensions; Interfacial Phenomena in Coal Technology, ed. G.D. Botsaris, and Y.M. Glazman, eds., Marcel Dekker, Inc. New York, pp.279-327.

Laskowski, J.S., 1989, Thermodynamic and kinetic flotation criteria; Frothing in Flotation, J.S. Laskowski, ed., Gordon and Breach, N.Y., pp.25-42.

Laskowski, T., 1948, Problem of processing of fines in the polish coal industry; published for the National Science Foundation and the Department of the Interior, in Biuletyn Instytutu Naukowo-Badawczego Przemyslu Weglowego, no.23, pp.1-82.

Leja, J., 1983, Surface Chemistry of Froth Flotation; Plenum Press, New York and London.

Lowenhaupt, D.E., and Gray, R.J., 1980, The alkali-extraction test as reliable method of detecting oxidized metallurgical coal; International Journal of Coal Geology, 1, pp.63-73.

Lowry, H.H., 1963, Chemistry of Coal Utilization; Suppl. volume. John Wiley and sons, eds., New York, London.

Mackowsky, M.Th., 1982, Minerals and trace elements occurring in coal; Coal Petrology, third edition, E. Stach, M.-Th. Mackowsky, M. Teichmuller, G.H. Taylor, D. Chandra, and R. Teichmuller, eds., Gerbruder Borntraeger, Berlin-Stuttgart, pp.153-170.

Mackowsky, M.-Th., and Hoffmann, E., 1960, Coal preparation; Coal Petrology, third edition, E. Stach, M.-Th. Mackowsky, M. Teichmuller, G.H. Taylor, D. Chandra, and R. Teichmuller, eds., Gerbruder Borntraeger, Berlin-Stuttgart, pp.33-348.

Majer, L.M., Cukierman, L.J., 1934, Separation of fusain from the hard coal dust during the flotation; Klassen, W.I, Flotacja wegla, Coal flotation, (in Polish) transl. by J.Laskowski, Wyd. Slask, pp.217-224.

Marchioni, D.L., 1983, The detection of weathering in coal by petrographic, rheologic and chemical methods; International Journal of Coal Geology, 2 (3), pp.231-259.

Marchioni, D.L., 1980, Petrography and depositional environment of the Liddell Seam, Upper Hunter Valley, New South Wales, International Journal of Coal Geology, 1 pp.35-61.

Marchioni, D.L., The detection of weathering in coal by petrographic, rheologic and chemical methods; 1983, International Journal of Coal Geology, 2 (3), pp.231-259.

Marmur, A., Chen, W., and Zografi, G., 1986, Characterization of particles by the measurement of floatability; Journal of Colloid and Interface Science, 113, no.1, pp.114-120.

Meuzelaar, H.L.C., Hill, G.R., Yun, Y., Jakab, E., Winding, W., Urban, D., Yon, K.Y., Oestreich, J., and East, J., 1987, Weathering effects on the structure and reactivity of US coals; DOE, final report.

Miller, J.D., and Ye, Y., 1988, Selective flotation of fossil resin from Wasatch Plateau high-volatile bituminous coal; presented at the 117th AIME Annual Meeting Phoenix, Arizona.

Mineral Statistics, Mineral Policy Branch, Ministry of Energy, Mines and Petroleum Resources, April, 1991.

Neuman, A.W., and Good, R.J., 1972, Thermodynamics of contact angles. Heterogeneous solid surfaces; J. Colloid Interface Sci., 38, pp.341-358.

O'Gorman, J.V. and Walker, P.L., 1971, Mineral matter characteristics of some American coals; Fuel, 50 (2), pp.135-151.

Onlin, T.J., and Aplan, F.F., 1987, Use of oily collectors for the flotation in coals of various ranks; Proc. of Annual AIME Meeting, Denver.

Parekh, B.K, and Aplan, F.F., 1974, Wettability properties of minerals coated with surfactants; Proc. Chemical Institute of Canada, Flocculation and Dispersion Symp., pp.21.

Parekh, B.K., and Aplan, F.F., 1978, The critical surface tension of wetting of coal; Recent Developments in Separation Science, IV, CRC Press, West Palm Beach, Fl, pp.107-112.

Partridge, A.C., and Smith,G.W., 1971, Small-sample flotation testing: a new cell; Trans. Instn. Min. Metall. (sec.C), 80, pp.C199-C200.

Pugmuire, R.J., Woolfenden, W.R., Mayne, C.L., Karas, J., and Grant, D.M, 1984, Structural variations in coal macerals; Chemistry and Characterization of Coal Macerals, R.E. Winans and J.C. Crelling, eds., American Chemical Society, series 252, Washington, D.C., pp.79-99.

Ramesh, R., and Somasundaran, P., 1991, Surface site distributions on coal; Coal Preparation, 9, pp.1-2.

Rao, C.P., and Gluskoter, H.J., 1973, Occurrence and distribution of minerals in Illinois coals; Illinois State Geological Survey Circular, 476, p.56.

Reay, D., and Ratcliff, G.A., 1973, Removal of fine particles from water by dispersed air flotation: Effect of bubble size and particle size on collection efficiency; Can. J. Chem. Eng., 51, pp.178-185.

Raymond, A.C., and Murchison, G.D., 1991, Influence of exinitic macerals on the reflectance of vitrinite in Carboniferous sediments of the Midland Valley of Scotland; Fuel, 70, pp.155-161.

Rentel, K., 1987, The combined maceral-microlithotype analysis for the characterization of reactive inertinites; International Journal of Coal Geology, 9, pp.77-85.

Renton, J.J., 1978, Mineral Matter in Coal: Origin, Characterization for Coal-Processing Technologies; in Coal Science, vol.2, M.L. Gorbaty, J.W. Larsen, and I. Wender, Academic Press, p.5.

Roznowa, J.J., 1963, Floatability of petrographic components from the low-rank coals; Klassen, W.I, Flotacja wegla, Coal flotation, (in Polish), transl. by J.Laskowski, Wyd. Slask, pp.217-224.

Sarkar, G.G., and Ghose, S., Chaudhuri, S.G., Sakha, S., and Daschowdhury, 1984, Selectivity of coal macerals during flotation and oil agglomeration: a case study; Coal Preparation, 1, pp.39-52.

Schafer, H.N., 1970, Carboxyl groups and ion exchange in low-rank coals; Fuel, 49, pp.197-213.

Seylers classification; 1961, in W. Francis, Coal: its formation and composition; Edward Arnold, ed., London.

Shapiro, N., and Gray, R.J., 1964, The use of coal petrography in coke making; Journal of Institute of Fuel, XI, no.30, pp.234-242.

Silbernagel, B.G., Gebhard, L.A., Dyrkacz, G.R., and Bloomquist, C.A.A., 1984, Electron spin resonance of isolated coal macerals; in American Chemical Society, Chemistry and Characterization of Coal Macerals, Washington, D.C., pp.121-135.

Sobieraj, S. and Majka-Myrcha, B., 1980, A study of electrokinetics and floatability of Upper Silesia coals of different petrographic composition; Physicochemical Problems of Mineral Processing, Wroclaw, (in Polish), no.12, pp.165-174.

Stach, E., 1982, The microlithotypes of coal and their strength; Coal Petrology, third edition; E. Stach, M.-Th. Mackowsky, M. Teichmuller, G.H. Taylor, D. Chandra, and R. Teichmuller, eds., Gerbruder Borntraeger, Berlin-Stuttgart, pp.140-150.

Stach, E., Mackowsky, M.-Th., Teichmuller, M., Taylor, G.H., Chandra, D., and Teichmuller, R., 1982, Coal Petrology, third

edition; Gerbruder Borntraeger, Berlin-Stuttgart

Sun, S.C., 1954a, Hypothesis for different floatabilities of coals, carbons, and hydrocarbon minerals; Trans. AIME, 199, pp.67-75.

Sun, S.C., 1954b, Effects of oxidation of coals on their flotation properties; Trans. AIME, April 1954, pp.396-401.

Teichmuller, M., 1982, Origin of petrographic consistuents of coal; Coal Petrology, third edition; E. Stach, M.-Th. Mackowsky, M. Teichmuller, G.H. Taylor, D. Chandra, and R. Teichmuller, eds., Gerbruder Borntraeger, Berlin-Stuttgart, pp.219-295.

Teichmuller, M., and Teichmuller, R., 1982, Fundamentals of coal petrology; Coal Petrology, third edition; E. Stach, M.-Th. Mackowsky, M. Teichmuller, G.H. Taylor, D. Chandra, and R. Teichmuller, eds., Gerbruder Borntraeger, Berlin-Stuttgart, pp.5-82.

Tomlinson, H.S., and Fleming, M.G., 1963, Flotation rate studies; Proc. 6th Int. Mineral Processing Congress, A. Roberts, ed., Pergamon, Oxford, pp.563-579.

Trahar, W.J., and Warren, L.J., 1976, The floatability of very fine particles - a review; Int. Miner. Proces., 3, pp.103-131.

Tsai, S.C., 1982, Fundamentals of coal beneficiation and utilization, in Coal Science and Technology 2, Elsvier, New, York, p.17.

Tschapek, M., and Wasowski C., 1976, Adsorption of aliphatic alcohols by soil minerals as a method of evaluating their hydrophobic sites; Journal of Soil Science, 27, pp.175-182.

van Krevelen, D.W., 1961, Coal: typology - chemistry - physics - constitution; Elsvier, Amsterdam, Netherlands.

Walker, Jr., P.L., Petersen, E.E., and Wright, C.C., 1952, Surface active agent phenomena in dust abatment; Industrial and Eng. Chem., 44, no.10, p.2389.

Ward, C.R., 1984, Coal Geology and Coal Technology, Blackwell Scientific Publications, Melbourne, Australia.

Wen, W.W., 1977, Electrokinetic behavior and flotation of oxidized coal; Ph.D. Thesis, Pennsylvania State University.

Wenzel, R.N., 1936, Resistance of solid surfaces to wetting by water; Industrial Engng. Chem., 28, p.288.

Wenzel, R.N., 1949, Surface roughness and contact angle; J. Phys. and Colloid Chem., 53, pp.1466-1467.

Whitehurst, D.D., Mitchell, T.O., and Farcasiu, M., 1980, Coal Liquefaction; Academic Press, New York.

Widyani, E., and Wightman, J.P., 1982, Colloids and Surfaces, 4, p.209.

Winans R.E., and Crelling, J.C., 1984, Chemistry and characterization of coal macerals: overview, American Chemical Society, Chemistry and Characterization of Macerals, Washington, D.C., pp.1-19.

Winans, R.E., Hayatsu, R., Scott, R.G., and McBeth, R.L., 1984, Reactivity and characterization of coal macerals; American Chemical Society, Chemistry and Characterization of Coal Macerals, Washington, D.C., pp.137-156.

Wiser, W., 1975, Prepr. Amer. Chem. Soc. Div. Pertr. Chem., 7, (3), p.99.

Yarar, B., and Leja, 1982, Floatation of weathered coal fines from Western Canada; Technical Papers of 9th International Coal Preparation Congress, New Delhi, India, November 29 - December 4, pp. C5-1 - C5-16.

Yarar, B. and Kaoma,J., 1984, Estimation of the critical surface tension of wetting of hydrophobic solids by flotation; Colloids and Surfaces, 11, pp. 429-436.

Yarar, B. and Kaoma J., 1984, Critical surface tension of wetting of naturally hydrophobic solids; presented in 7th RM, ACS Meeting, Alberquerque, New Mexico.

Yarar, B., 1985, Gamma flotation: a new approach to flotation, using liquid-vapor surface tension control; Froth Flotation, Proc. of the 2nd Latin-merican Congress on Froth Flotation, Conception, Chile, 19-23 August 1985, pp.41-63.

Ye, Y., and Miller, J.D., 1988, Bubble/particle contact time in the analysis of coal flotation; Coal Preparation, 5, pp.147-166.

Yoon, R.H., and Luttrell, N.G.H., 1989, The effect of bubble size on the fine particle flotation; Frothing in Flotation, J.S. Laskowski, ed., Gordon and Breach, N.Y., pp.101-121.

Young, Th., 1805, An essay on the cohesion of fluids; Trans. Roy. Soc., 95, pp.65-87.

Zisman W.A. 1964, Relation of the equilibrium contact angle to liquid and solid constitution; American Chemical Society, Contact Angle, Wettability and Adhesion, Washington, D.C., vol.43, pp.1 - 51.

APPENDIX A PETROGRAPHIC DATA

A.1 Petrographic analyses

Maceral analyses of five lithotype samples, as described in section 7.3.1, are given in Table A.1 The vitrinite group was subdivided into telocollinite, pseudovitrinite, desmocollinite and vitrodetrinite. The inertinite group consisted of semifusinite, fusinite and other inerts. The reflectance values were included for all lithotypes except for fusain (fibrous). The fusain sample was mainly composed of fusinite particles with very few vitrinite suitable for taking reliable reflectance measurements.

Maceral composition of the density fractions are shown in Table A.2. In these analyses a total of 300 points was counted for each pellet representing coal sample. Results are reported on a mineral-matter-free basis. In these analyses vitrinite and pseudo-vitrinite represent vitrinite group macerals, inertinite group is divided into semifusinite, fusinite and inertodetrinite macerals. Inertodetrinite includes all other inerts found in the sample. In grain type analysis (Table A.3) grains were counted according to the set-up categories (see section 7.3.1).

Tables A.4 and A.5 include grain-type analysis of floats and rejects from flotation of density fractions derived from small-scale flotation.

	Bright volume %	Banded Bright volume %	Banded Dull volume %	Banded Coal volume %	Fibrous volume %
Telocollinite	32.00	24.0	16.00	23.00	27.0
Pseudovitrinite	10.00	7.0	9.00	0.00	5.0
Desmocollinite	28.00	35.0	30.00	30.00	12.0
Vitrodetrinite	0.00	0.0	1.00	1.00	0.0
Total Vitrinite	70.00	66.0	56.00	54.00	44.0
Semifusinite	11.00	10.0	22.00	21.00	29.0
Fusinite	10.00	16.0	11.00	11.00	21.0
Other Inerts	7.00	5.0	10.00	11.00	6.0
Total Inertinite	28.00	31.0	43.00	43.00	56.0
Total Liptinite	2.00	2.0	0.00	3.00	1.0
Inerts/Vitrinite	0.40	0.5	0.77	0.80	1.3
Ro mean	1.06	1.0	0.88	1.04	

Table A.1 Maceral analyses of five lithotype samples. (from point-counting technique)

	Density fraction <1.30	Density fraction 1.30-1.35	Density fraction 1.35-1.40	Density fraction 1.40-1.45	Density fraction 1.45-1.50	Density fraction >1.50
Vitrinite	95	80	70	69	70	80
Semifusinite	3	10	15	15	10	5
Fusinite	1	4	6	8	16	10
Inertodetrinite	1	6	9	8	4	5
Total Inertinite	5	20	30	31	30	20

Table A.2 Maceral composition of density fractions (from point-counting technique).

	Density fraction <1.30	Density fraction 1.30-1.35	Density fraction 1.35-1.40	Density fraction 1.40-1.45	Density fraction 1.45-1.50	Density fraction >1.50
Free vitrinite	60	46	29	26	25	49
Pseudovitrinite	23	6	2	2	1	0
Vitr>Inert	13	28	39	41	44	31
Total vitrinite	96	80	70	69	70	80
Inertod, Inert>Vitr	1	6	9	8	4	5
Fusinite	0	4	6	8	16	10
Semifusinite	3	10	15	15	10	5
Total inetrinite	4	20	30	31	30	20
*Oxidized vitrinite	3	4	3	3	4	3
*Vitrinite+MM	4	24	64	100	100	100

* on the basis of total vitrinite

Table A.3 Distribution of grains in density fractions. Description in terms of association with mineral matter and visible oxidation.

	Concentrate 5% meth. conc.	Rejects 5% meth. conc.	Concentrate 10% meth. conc.	Rejects 10% meth. conc.	Concentrate 20% meth. conc.	Rejects 20% meth. conc.	Concentrate 30% meth. conc.	Rejects 30% meth. conc.
Free vitrinite	59	53	81	71	69	71	77	29
Pseudovitrinite	13	19	8	12	16	9	9	1
Vitr>Inert	19	4	8	12	12	12	11	47
Total vitrinite	91	76	97	95	97	92	97	77
Inertod, Inert>Vitr	8	1	1	0	2	5	0	3
Fusinite	0	1	1	0	1	0	0	3
Semifusinite	1	2	1	3	0	3	3	17
Total inetrinite	8	4	3	3	3	8	3	23
*Oxidized vitrinite	3		2		7		2	10
*Vitrinite+MM	6	18	3	0	3		1	54

* on the basis of total vitrinite

Table A.4 Grain-type analysis of the floats and rejects for 1.30 specific gravity, at different methanol concentrations.

	Concentrate 5% meth. conc.	Rejects 5% meth. conc.	Concentrate 10% meth. conc.	Rejects 10% meth. conc.	Concentrate 20% meth. conc.	Rejects 20% meth. conc.	Concentrate 30% meth. conc.	Rejects 30% meth. conc.
Free vitrinite	32	32	35	23	30	47	66	29
Pseudovitrinite	1	1	0	2	2	1	4	1
Vitr>Inert	45	42	45	50	39	15	4	47
Total vitrinite	78	75	80	75	71	63	74	77
Inertod, Inert>Vitr	5	1	3	4	5	5	4	3
Fusinite	2	2	2	4	3	2	2	3
Semifusinite	15	22	15	17	21	30	20	17
Total inetrinite	22	25	20	25	29	37	26	23
*Oxidized vitrinite	3	10	1	12	3	15	4	10
*Vitrinite+MM	31	59	23	66	32	90	49	54

* on the basis of total vitrinite

Table A.5 Grain-type analysis of the floats and rejects for 1.30-1.35 specific gravity, at different methanol concentrations.

APPENDIX B SURFACE TENSION MEASUREMENT

B.1 Du Nouy ring method

The static surface tension of the methanol solutions was measured by the Du Nouy ring method (Adamson, 1967). In this method a platinum wire ring is immersed in the liquid solution and the force necessary to lift and detach a film of the liquid is measured. The force of detachment W is described as:

$$W = 2\pi R\,\gamma + 2\pi(R + 2r)\gamma + (\pi\,(R + 2r)^2 - \pi R^2)2\gamma \text{ and}$$

$$\gamma = W/2\pi\,(R + r)(1 + 2r)$$

The dimensions at the plane of breakage, R and r, are related to the dimensions of the ring, and the mass of the liquid lifted during the detachment (Figure B.1). The maximum weight W causing ring to separate is related to the surface tension through a correction factor F. The correction factor is calculated from the equation given below:

$$(F - a)^2 = (4b/\pi^2 * 1/R^2) * \gamma' / d_w + C$$

where

$a = 0.7250$

$b = 0.00090705$

$C = 0.04534 - 1.679\,(r/R)$

d_w - density of water

γ' - apparent surface tension

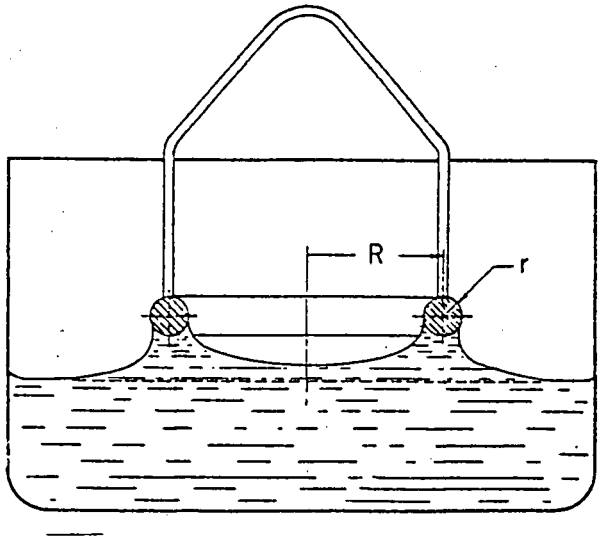

a

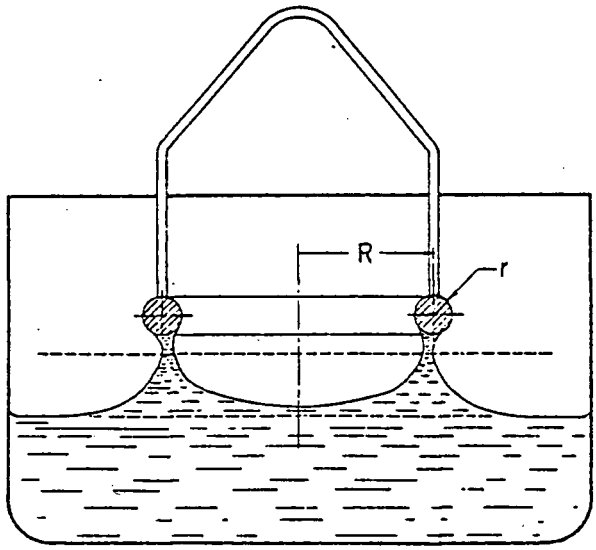

b

Figure B.1.1 Distention of surface film during surface tension measurement (a); condition of surface film at breaking point (b).

$$\gamma = \gamma' * F$$

Prior to the surface tension measurement, the calibration of the tensiometer was performed using known weights. The weights were placed on the ring and the dial rotated to keep the index level. The results were graphed as the dial values versus apparent surface tension γ' by using the relationship

$$\gamma' = Mg/2L$$

M is weight placed on ring, in grams

g is the gravity value cm/sec^2

L mean circumference of the ring

γ' apparent surface tension, dyne/cm, dial reading

For each measurement, 50 ml of prepared methanol solution is poured in a clean sample container and placed carefully on the leveled platform of the tensiometer. The platform is raised until the ring is immersed in the solution to a depth not exceeding 6 mm. Then the platform is lowered slowly, increasing the torque of the ring by keeping the pointer on the zero mark. Proceeding slowly with the adjustment, the dial reading at which the rupture of the solution film took place is recorded. From the calibration the apparent value of the surface tension is read, and using the

Concentration % Methanol	Tensiometer Reading (dyne/cm)	(F-A) ^ 2	Correction Factor	Actual value (dyne/cm)
0	74.1	0.0440	0.935	69.3
10	58.9	0.0378	0.920	54.2
20	49.6	0.0341	0.910	45.1
30	43.1	0.0314	0.902	38.9
50	36.1	0.0286	0.894	32.3
70	30.8	0.0265	0.888	27.3
100	24.5	0.0239	0.880	21.6

Surface Tension Measurements for methanol/water

Table B.1 The surface tension values for methanol solutions used in experiments.

The values of surface tension for the methanol solutions used in the experiments are given in Table B.1.

APPENDIX C OXIDATION DETECTION - PROCEDURES

C.1 Stain test for detection of oxidized particles

To detect oxidized coal particles a staining procedure was used. This technique was developed by Gray (Gray et al., 1976) for bituminous coals and successfully used by others Marchioni (1983). Marchioni, in his study of the detection of weathering in Western Canadian coals, concluded that staining with safrinin is the most sensitive parameter for detecting oxidized coal, even more sensitive than rheological tests. This technique involves immersing the polished coal pellet in a specially prepared staining solution. The solution for the test is prepared by mixing 2 grams of KOH in 50 ml of water and 1 gram of safrinin O (a red stain). The coal pellets are soaked for approximately 20 minutes, and then rinsed and blown dry with air for microscopic examination. Unweathered coal grains are unaffected by the etch stain, whereas oxidized areas are accentuated by preferential staining. Slightly oxidized, moderately oxidized, and highly oxidized coal particles become light green, yellow green and olive-green respectively. The number of oxidized grains was point-counted and included in the grain-type analysis of samples used in the flotation tests, as depicted in Figures 6.3.2.b, and Tables A.3, A.4 and A.5.

C.2 Alkali-extraction test for oxidized coal particles

In this test a small amount of representative coal sample is immersed in 100 ml of one normal NaOH solution and brought to a boil. When the coal is oxidized the humic acids are produced, and as result discoloration of the solution occurs. The discoloration usually increases with the increase in oxidation. After the solution is filtered, the transmission at 520 nm relative to a standard of one normal NaOH, representing 100 % light transmission, is measured. A coal with transmittance value less than 80 percent is considered to be oxidized. The detailed test procedure according to Gray (Lowenhaupt and Gray, 1980) is given below:

1. Weigh out 1.0 gram of coal (+/- 0.001) of - 60 mesh coal.
2. Transfer the coal to a 400 ml beaker containing boiling chips or glass beads.
3. Add 100 ml of NaOH solution and one drop tergitol to the coal.
4. Bring the solution to a boil for 2 to 3 minutes, stirring with a glass rod, then remove the beaker and allow the contents to cool to room temperature.
5. Filter the slurry on No. 40-42 filter paper into an Erlenmeyer flask. Transfer the filtrate into a graduated cylinder. There should be approximately 80 percent recovery. If not, the filtrate volume should be brought up to 80 ml using distilled water.
6. Set spectrophotometer to a wavelength of 520 nm.

7. Adjust the spectrophotometer to read zero percent transmittance, then fill cuvette with a blank solution and adjust reading to 100 percent transmittance.

8. Using the same cuvette as for the blank, test the transmittance of the coal alkali extract and report percent transmittance. The two percent repeatability should be allowed for the same operator in the same laboratory.

Table C.6 The transmittance values for composite sample and density fractions (%T, percent light transmitted).

Sample Description	Transmittance %
Composite (low-ash)	86.1
< 1.30	92.0
1.30 - 1.35	95.2
1.35 - 1.40	92.6
1.40 - 1.45	90.3
1.45 - 1.50	89.5
> 1.50	84.8

This procedure was followed when examining the degree of oxidation of composite and density fraction samples used in wettability-floatability study. The transmittance values for these samples are included in Table C.6. The transmittance value for the 1.30-1.35 specific gravity fraction appears to be greater than the one for the lowest density. All of the examined samples had transmittance values higher than 80 percent indicating an un-

oxidized surface.

C.3 A diffuse reflectance FTIR technique.

A Fourier Transform Infra Red (FTIR) technique is frequently used to detect oxidation in coal samples. An interesting infrared study on naturally weathered coal was reported by Griffiths (1982).

In a typical infrared spectra of coal there are three regions of major interest. The area between 2800 to 3200 wave numbers (cm^{-1}) represents the C-H aromatic and the aliphatic stretching mode, the 3200 to 3500 cm^{-1} corresponds to -OH stretching frequency, and 1700 cm^{-1} to the -CO stretching frequency. In addition, important information may be gathered from the observation of other frequencies, such as the region of 1100 to 1300 cm^{-1}, where phenolic and alcoholic -CO stretching is detected.

The FTIR spectra analysis of the cleaned (low-ash) composite, lowest density fraction (1.30 s.g.) and oxidized composite sample were obtained. The analyses were performed in the Department of Metallurgical Engineering, of University of Utah, thanks to professor Jan D. Miller. For the composite sample and 1.30 specific gravity fraction no significant difference (including both peak position and intensity) between spectra were detected. The spectra for these samples are enclosed in Figure C.1. On the other hand, the spectra of the samples labeled Bull A unoxidized (low-ash composite) and Bull A oxidized (composite oxidized at

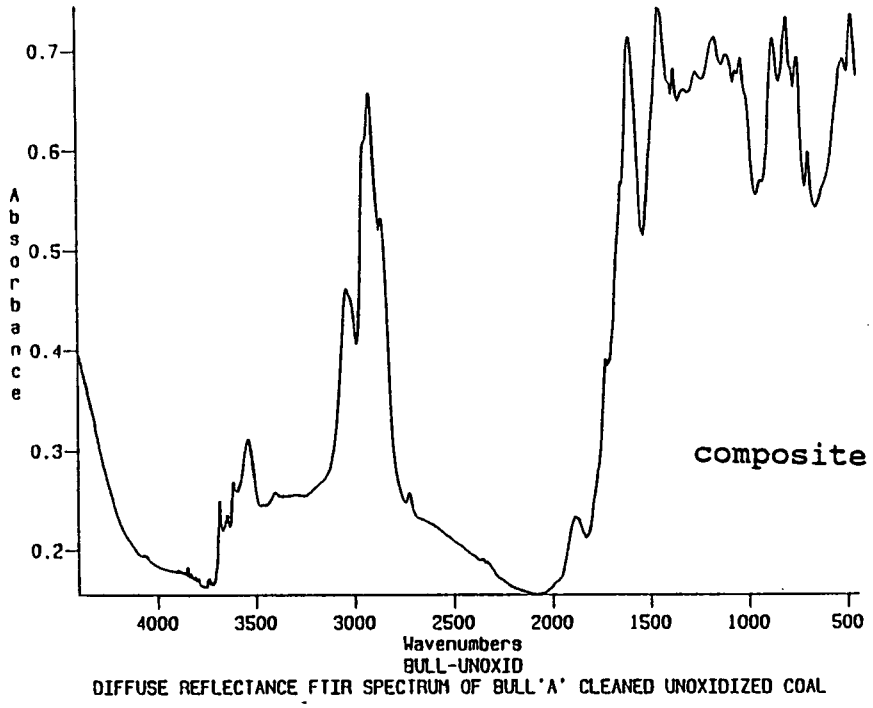

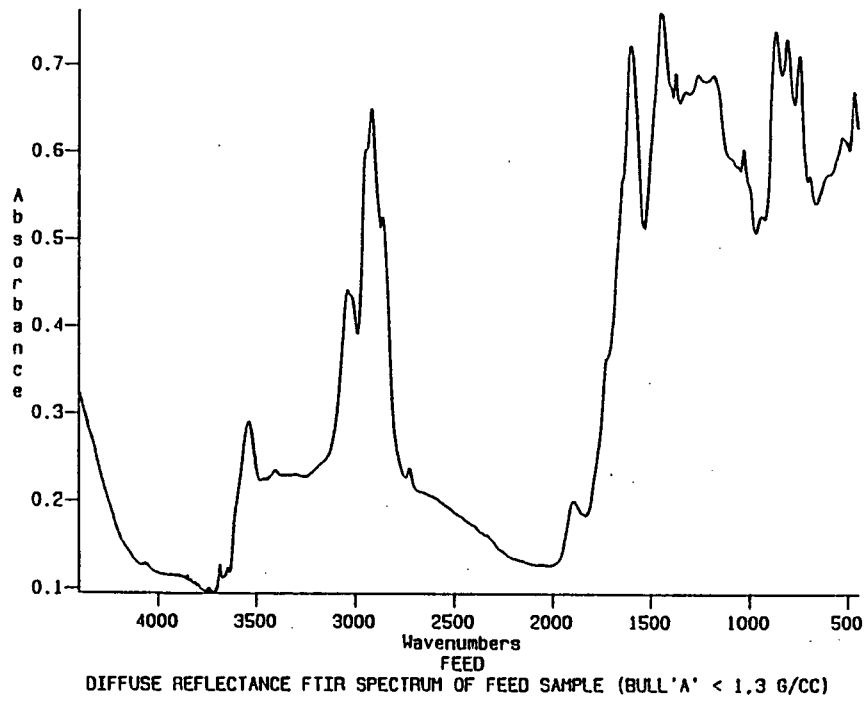

Figure C.1 The FTIR spectra for two samples; composite and 1.30 specific gravity fraction.

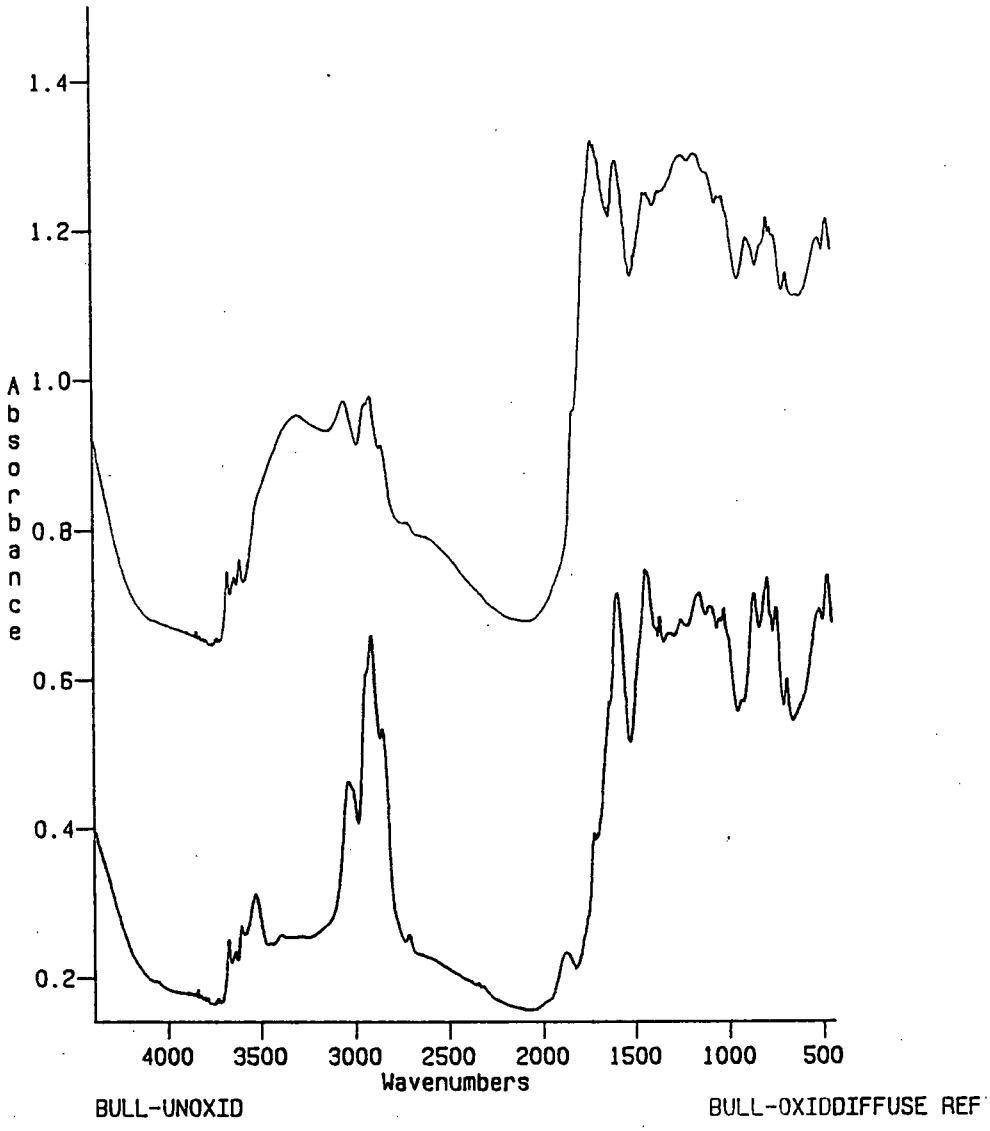

Figure C.2 The FTIR spectra of the samples labeled Bull A unoxidized (low-ash composite) and Bull A oxidized (at 200^{o}C).

200°C) differ significantly (Figure C.2). The important points to note for the oxidized sample are:

1. A significant increase in the -OH stretching frequency at 3200 to 3500 cm^{-1}.
2. A significant increase in the -CO stretching frequency at 1700 cm^{-1}.
3. A decrease in aromatic hydrogen (out of phase vibration) at 780 to 900 cm^{-1}.
4. An increase in other oxygen functionality in the frequency region 1100 to 1300 cm^{-1}.

The spectral data were collected under the following conditions:

Spectrometer: Bio-Rad FTS-40
Temperature: 25°C
Sampling Technique: DRIFT
Spectral Conditions: 256 scans, 4 cm^{-1} resolution.

The samples examined were considered to have fresh unoxidized surfaces with the exception of the sample labeled as oxidized.

APPENDIX D STATISTICAL ANALYSIS

The ash contents of the floats and rejects with the corresponding yield (wt%), from each small-scale flotation test, were used to back-calculate the ash content of the feed coal sample. These data are given in Appendix E. The mean calculated ash contents are compared with the measured feed ash (from the proximate analysis). The calculated ash contents of the feed data are assumed to be a normally distributed, therefore the confidence intervals are calculated for the two composite samples and three density fractions (Table D.1)

.

Table D.1 Comparison of the calculated feed ash values with the measured ash values. Testing the confidence interval for feed ash content data.

Sample	Hi-ash	Lo-ash	<1.30	1.30-1.35	1.35-1.40
Measured ash	28.34	16.03	3.01	7.87	14.89
Mean calc. ash	28.53	16.06	2.82	7.94	14.90
n_i	15	6	5	6	6
S_i	0.636	0.496	0.144	0.183	0.049
95% confidence interval	$\pm$0.36	$\pm$0.57	$\pm$0.20	$\pm$0.19	$\pm$0.051

where n_i - number of ash values
S_i - standard deviation

APPENDIX E SMALL-SCALE FLOTATION TESTS

The following tables (Table E.1, E.2, E.3 and E.4) list the flotation test results as derived from small-scale tests (P/S). The cumulative yield and cumulative ash content of floats and rejects from each flotation run are recorded according to the test conditions. The mean cumulative yields were calculated whenever replicate data was available. From the ash content of floats and rejects the ash content of the feed sample was back-calculated. All tests were carried out with the+149-212 µm size fraction.

Table E.1 Small-scale flotation results (from tests with P/S cell). The yield vs flotation time and yield vs conditioning time, for the high-ash composite sample.

Bullmoose A (-212+149um), high-ash
Yield vs flotation time

Methanol conc.	Time min	Yield conc.		Ash % conc.	Ash % rejects	Feed ash calc'd
		Run 1	Run 2			
2	0.5	73.53	67.5	18.45	58.02	28.92
2	1	78.87	77.6	19.01	61.46	27.97
2	2	81.18	79.21	20.22	61.69	28.02
2	3	81.44	82.04	20.89	62.66	28.64
2	4	84.06	83.18	22.91	61.4	29.05

Bullmoose A (-212+149um), high-ash
Yield vs conditioning time

Methanol conc.	Condit time	Yield conc.	Yield conc.	Yield conc.	Ash % conc.	Ash % rejects	Feed ash calc'd
		Run 1	Run 2	Run 3			
2	0	85.8	84.6	83.9	21.82	63.47	27.73
2	3	86.61	85.8	86.3	22.36	66.54	28.28
2	5	86.76	86.8	86.8	22.43	63.56	27.88
2	10	87.09	87.51	87.9	22.88	63.85	28.17

Table E.2 Small-scale flotation results (from tests with P/S cell). The yield vs surface tension, for high and low-ash composite sample.

Bullmoose A (-212+149um), high-ash
Yields vs surface tension

Methanol conc.	Yield conc. Run 1	Yield conc. Run 2	Ash % conc.	Ash % rejects	Feed ash calc'd	Inc.yld	Inc.ash
2	80.4	81.2	19.08	71.37	29.33	1.05	24.03
5	81.2	78.3	18.67	70.09	28.34	12.55	0.93
10	67.5	66.9	14.32	56.41	27.99	35.3	0.32
20	31.82	31.98	12.66	35.88	28.49	8.61	0.7
30	23.75	22.83	15.27	33.62	29.26	23.29	15.27
40	23.37	21.56	34.21		29.92		

Bullmoose A (-212+149um), low-ash
Yields vs surface tension

Methanol conc.	Yield conc. Run 1	Run 2	Ash % conc.	Ash % rejects	Feed ash calc'd	Incr.yld	Icr.ash
2	93.23	95.12	14.55	35.28	15.95	1.1	10.95
5	92.74	93.41	13.2	46.64	15.63	12.17	0.81
10	81.69	80.12	12.44	36.99	16.94	50.47	0.17
20	30.96	29.91	12.25	18.17	16.34	30.44	12.25
30	30.01	29.09	10.9	17.86	15.77		
40	29.81	29.06	11.03	17.76	15.75		

Table E.3 Small-scale flotation results (from tests with P/S cell). The yield vs surface tension for the density fractions.

Bullmouse A (-212+149um), <1.3 s.g.
P/S small scale flotation.
Yields vs surface tension

Methanol conc.	Yield conc.	Ash % conc.	Ash % rej.	Feed ash calc'd	Incr. yld	Incr.ash
2	96.83	2.43			2.25	1.24
5	94.58	2.41	10.54	2.85	21.27	0.07
10	73.31	2.82	3.07	2.89	32.45	0.021
20	40.86	2.55	2.6	2.58	11.27	0.11
30	29.59	2.68	2.86	2.81	29.59	2.68
40	32.67	2.62	3.12	2.96		

Bullmouse A (-212+149um), 1.3-1.35 s.g.
P/S small scale flotation.
Yields vs surface tension

Methanol conc.	Yield conc.	Ash % conc.	Ash % rej.	Feed ash calc'd	Incr.yld	Incr.ash
2	93.32	7.69	11.28	7.93	7.87	0.72
5	85.45	7.76	9.32	7.99	51.14	0.1
10	34.31	7.71	8.33	8.11	6.46	0.7
20	27.85	7.54	7.97	7.85	27.85	7.54
30	27.45	7.62	7.97	7.87		
40	25.4	7.69	7.98	7.91		

Table E.4 Small-scale flotation results (from tests with P/S cell). The yield vs surface tension for the density fractions (continuation).

Bullmouse A (-212+149um), 1.35-1.40 s.g.
P/S small scale flotation
Yield vs surface tension

Methanol conc.	Yield conc.	Ash % conc.	Ash % rej.	Feed ash% calc'd	Incr.yield	Incr.ash
2	58.52	14.64	15.35	14.93	14.09	0.75
5	44.43	14.77	14.86	14.82	9.3	0.46
10	35.13	15.33	14.78	14.94	6.05	0.38
20	29.08	15.14	14.8	14.92	4.91	0.23
30	24.17	18.57	13.69	14.87	24.17	18.57
40	22.95	18.46	13.89	14.94		

Bullmoose seam A (-212+149um), density fractions
P/S small-scale flotation
Yield vs surface tension

Methanol conc.	1.4-1.45 Yield conc.	1.45-1.5 Yield conc.	>1.50 Yield conc.
2	27.13	24.67	12.61
5	25.25	23.03	11.02
10	20.05	23.09	10.96
20	20.04	23	10.43
30	20.88	22.9	9.89

APPENDIX F FILM FLOTATION TESTS

Tables F.1, E.2, and E.3 list film flotation test results. The cumulative yield and cumulative ash content of floats and rejects from the flotation runs are given. The mean cumulative yields were calculated whenever replicate data was available. All tests were carried out with the 149-212 μm size fraction and following the film flotation procedure as described in section 7.1.

Table F.1 Film flotation results of the two composite samples and the density fractions.

Bullmoose A (-212+149um), composite samples
Film flotation

	Low-ash				High-ash
Methanol conc.	Yield conc.	Ash % conc.	Ash % rejects	Feed ash calc'd	Yield conc.
2	73.58	14.47	21.97	16.07	58.48
5	71.66	14.29	22.27	16.55	53.31
10	45.5	14.71	20.6	17.92	31.68
15	28.81	13.11	18.71	17.09	16.21
20	14.43	10.92	17.25	16.33	11.23
30	8.42	10.67	17.15	16.69	7.49

Film Flotation of density fractions

Methanol conc.	<1.30 Yield conc.	1.30-1.35 Yield conc.	1.35-1.40 Yield conc.	1.40-1.45 Yield conc.	>1.50 Yield conc.
2	69.7	55.01	19.31	10.1	6.27
5	64.54	49.51	11.95	9.66	3.87
10	43.66	15.05	10	8.29	2.84
15	22.22	12.31	8.33	5	1.69
20	10.65	8.04	4.83	3.35	
30	5.74	2.56	2.87		

Table F.2 Film flotation results of lithotypes samples.

	Film Flotation Bright - Vitrain			Film Flotation Banded Coal	
Methanol conc.	Yield conc.	Yield conc.	Ash % conc.	Yield conc.	Ash % conc.
	Run 1	Run 2			
2	98.62	94.76	3.65	86.94	7.03
5	95.19	93.74	3.74	85.17	7.25
10	92.71	93.43	3.5	51.44	6.78
15	45.12	43.11	3.49	34.5	6.46
20	42.78	41.72	4.01	18.19	6.54
30	29.51	29.62	3.86	7.59	3.15

	Film Flotation Banded Bright		Film Flotation Fibrous - Fusain	
Methanol conc.	Yield conc.	Ash % conc.	Yield conc.	Ash % conc.
2	95.47	4.56	18.71	3.56
5	92.35	4.12	16.32	3.87
10	87.52	3.94	4.29	4.01
20	35.18	3.58	1.99	3.45
30	20.54	3.57		

Table F.3 Film flotation results of lithotypes samples (continuation).

Film Flotation
Banded Dull

Methanol conc.	Yield conc. Run 1	Yield conc. Run 2	Ash % conc.
2	92.04	91.84	5.54
5	91.56	89.31	5.06
10	42.71	41.34	5.19
20	23.75	24.37	5.12
30	15.31	16.76	3.19

APPENDIX G GENERAL

The following Table G.1 contains washability data on the -212 + 149 μm size fraction of the Bulmoose seam A composite coal sample, as obtained form sink-and-float analysis.

Table G.1 Washability data of composite (- 212 + 149 µm) Bullmoose seam A.

	Wt % floats	Ash % floats	Cum. wt %, floats	Cum. ash %, floats	Cum. wt %, rejects	Cum. ash %, rejects
+1.30	32.71	3.01	32.71	3.01	100.00	28.72
1.30-1.35	14.08	7.87	46.79	4.47	67.29	41.21
1.35-1.40	7.32	14.89	54.11	5.88	53.21	50.03
1.40-1.45	5.15	20.89	59.26	7.19	45.89	55.64
1.45-1.50	2.94	25.24	62.20	8.04	40.74	60.03
+1.50	37.80	62.74	100.00	28.72	37.80	62.74